

Mineralogy and Geochemistry of Upper
Cretaceous Clay Mineral Assemblages from
The Star Lake-Torreón Coal Fields,
San Juan Basin, New Mexico

by

Alan Barnett Carmichael

Submitted in Partial Fulfillment of the
Requirements for the Degree of Master of Science

New Mexico Institute of Mining and Technology

Socorro, New Mexico

May, 1982

CONTENTS

	Contents.....	i
	Listings of Figures, Tables, and Plates.....	iv
	Abstract.....	vi
	Acknowledgments.....	ix
I	Introduction.....	1
II	Location and Geography.....	2
III	Previous Work.....	4
IV	General Depositional Setting.....	6
V	Regional Stratigraphy.....	7
	The Satan Tongue of the Mancos Shale.....	10
	The Menefee Formation.....	10
	The Cleary Coal Member.....	11
	The Upper Coal Member.....	12
	The Fruitland Formation.....	13
VI	Structural Geology.....	24
VII	Sample Locations.....	25
VIII	Sample Collection, Preparation and Analysis.....	26
	Shales.....	26
	Coal Ashing.....	28
	Chemical Analysis by X-ray Fluorescence.....	29
IX	Problems in Clay Fraction Analyses.....	31
X	Reproducibility.....	35
XI	X-ray Chart Interpretation.....	36
	Whole Rock.....	36

	Ironstone Concretions.....	37
	Quantification of Whole Rock Percents.....	38
	Clay Minerals.....	40
	Smectite.....	40
	Illite.....	43
	Kaolinite.....	44
	Chlorite.....	44
	Mixed-Layer Illite-Smectite.....	45
	Relative Clay Mineral Abundances....	47
XII	Results and Conclusions.....	49
	Clay Mineral Assemblages.....	52
	Relative Particle Sizes.....	54
	Stratigraphic Variations in Clay Mineralogy.	55
	Lithologic Variations in Clay Mineralogy....	59
	Coal Ash Mineralogy.....	61
	Chemistry of Some Relatively Pure Smectites.	68
	Lateral Clay Studies (Upper Menefee).....	74
	Summary of Results.....	78
XIII	References Cited.....	81
XIV	Appendixes.....	A1
	1 -Procedure for Calculation of Relative	
	Abundances of Clays.....	A1
	2A-Clay Data for Computer Analysis.....	A2
	2B-Relative Abundances of Clay Minerals.....	A6
	2C-Whole Rock Data for Computer Analysis....	A11

2D-Whole Rock Percents.....	A13
3A-Chemical Compositions-Weight Percents of Oxide Constituents.....	A15
3B-Chemical Compositions-Mole Percents of Oxide Constituents.....	A18
4 -Coal Ash Results.....	A20
5A-Smectite + Mixed-Layer Illite-Smectite + Illite (001) D-Spacings.....	A21
5B-Percent Expandable Layers in Mixed- Layer Illite-Smectite.....	A24
5C-Low Intensity Clay Peaks.....	A26
6A-Average Mineralogic Compositions for Carbonaceous vs. Non-Carbonaceous Strata.	A27
6B-Formational Averages for Clay Minerals...	A28
6C-Average Clay Mineralogy for Various Clay Fractions.....	A29
6D-Average Mineralogic Compositions of Samples Taken Above and Below Coals.....	A30
7 -Recasting a Clay Analysis.....	A31
8 -Whiteprint of Stratigraphy vs. Clay Mineralogy for Selected Coal-Bearing Upper Cretaceous Strata	Sleeve

Plates

1) Cleary Coal Member of the Menefee Formation.....	15
2) " " " " "	15
3) " " " " "	16
4) Upper Coal-Bearing Member of the Menefee.....	17
5) " " " " " " "	17
6) " " " " " " "	18
7) " " " " " " "	18
8) " " " " " " "	19
9) La Ventana Sandstone and Adjacent Upper Menefee...	20
10) Fruitland Formation.....	21
11) " "	21
12) " "	22
13) " "	22
14) " "	23

ABSTRACT

The great diversity of Upper Cretaceous clay-bearing strata in the Star Lake-Torreón area of the San Juan Basin, N.M. provides a unique opportunity to study variations in clay mineralogy, both vertically and laterally. This investigation's primary concern was clay mineral variations in paludal environments. Clays and coals from four coal-bearing intervals were sampled in order to compare and contrast the clay mineralogy above, below and within the coals. Coal-bearing segments studied include the deltaic deposits of the upper coal-bearing member of the Menefee Formation, interdeltic deposits of the Cleary Coal Member, transitional (marine to terrestrial) paludal deposits of the Upper Mancos Shale, and coastal swamp to alluvial-plain deposits of the Fruitland Formation.

Provenance, mechanical sorting during transport, flocculation properties, environments of deposition, and diagenetic alteration all influence the observed variations in clay mineralogy.

One hundred three shales and mudstones were analyzed for whole rock and clay mineralogy through x-ray diffraction, supplemented by chemical analysis using x-ray fluorescence (XRF). The Menefee and Upper Mancos samples contained high relative abundances of random mixed-layer illite-smectite, with lesser amounts of kaolinite, smectite, illite, and chlorite (locally) in decreasing order of

abundance. The Fruitland samples contain dominantly smectite with lesser quantities of random mixed-layer illite-smectite, and locally illite and kaolinite. Two types of smectite, including sodium and calcium varieties, are present. Chemical analyses reveal sodium smectites with large concentrations of octahedral iron and magnesium, some interlayer calcium and minor potassium substitution, and high interlayer charges in the Mancos and Menefee. Otherwise similar Fruitland smectites usually contained substantially more interlayer calcium.

Eight coals were analyzed for ash content and mineralogy by employing a low temperature asher to preserve the clay mineralogy. Coal ash samples invariably show large kaolinite content relative to adjacent shales and mudstones. This can be attributed to detrital clay recrystallization in the acidic coal swamp depositional environment, and/or to diagenetic dissolution and precipitation prior to and/or after lithification. Authigenic kaolinite in cross-cutting coal cleats document some post-lithification crystallization of kaolinite. In Menefee samples the relative abundance of kaolinite in the clay assemblage steadily increased with decreasing ash content; conversely, the relative abundance of other clay, particularly mixed-layer illite-smectite decreased with decreasing ash content.

Clay mineral group averages by formation were compared between carbonaceous and barren strata. The carbonaceous strata contain more kaolinite and less illite

and K-feldspar than barren strata. Clay mineral group averages for shales found above and below coals reveal that shales under the coals contain more kaolinite and less illite and K-feldspar than shales above the coals. Kaolinite enriched in carbonaceous beds and in strata directly underlying coals reflect the acidic coal swamp depositional environment.

A variety of clay fractions (<8, <2, <1, <0.5, <0.25, and <0.1 micron), separated by formation from representative samples, show that clay mineralogy is a function of particle size. The general order of Menefee and Mancos clay particle sizes, from largest to smallest, was kaolinite, chlorite, illite, smectite, and random mixed-layer illite-smectite.

Lateral studies of upper Menefee shales reveal increasing illite and decreasing kaolinite contents below coal pinchouts, illustrating that illite to kaolinite alteration is most pronounced below coals. The shale overlying the coal increased in kaolinite and quartz with concomitant decrease in mixed-layer clay content with coal pinchout, and most likely reflects variation in mechanical sorting of detrital sediments.

ACKNOWLEDGMENTS

I wish to thank my principal adviser, Marc W. Bodine, Jr., for his guidance, suggestions and financial support of this project (under State Mining and Mineral Resource Institute grant #G510577). Thanks are also due to my other committee members, Drs. George S. Austin of the New Mexico Bureau of Mines and Mineral Resources and David B. Johnson of the Geoscience Department, who critically read this manuscript.

I would also like to thank David E. Tabet for conducting the initial field reconnaissance. Thanks are extended to Dr. Philip R. Kyle of the Geoscience Department for his help in the chemical analysis of my samples by x-ray fluorescence.

Stanley Krukowski, my co-worker on this project, also deserves thanks for his suggestions, comments, and company during the course of the field and lab work. I am also grateful to Larry Queen for his help in sample preparation and Ralph Durkee for writing the PASCAL computer program used to reduce the clay data.

The objective of this thesis was to relate mineralogic and chemical variations of clay assemblages to lithology, stratigraphy, environments of deposition, coal ashing properties, and provenance in Upper Cretaceous coal-bearing strata in the Star Lake-Torreon area of the San Juan Basin, New Mexico. It was hypothesized that variations in detrital influx, mechanical sorting of clays by particle size, the chemical environment of deposition, and diagenetic changes all play important roles in determining the clay assemblages observed. Barren and carbonaceous shales and mudstones interbedded with sandstones, siltstones, and coals from such depositional environments as nearshore marine, deltaic, fluvial, paludal, and coastal alluvial-plain provide an ideal opportunity for clay studies. Previous studies supply the necessary stratigraphic, environmental and petrographic framework to properly evaluate environments of deposition in the area.

Four coal-bearing segments are included: the upper and lower coal-bearing horizons of the Menefee Formation, the Upper Mancos Shale, and the Fruitland Formation. Coal environments range from fresh-water deltaic, through interdeltic, to brackish-water environments.

Clay-bearing units were systematically sampled and analyzed along selected stratigraphic intervals to determine clay mineralogy and geochemistry. Analysis of whole rock and

clay fractions was accomplished by x-ray diffraction and supplemented by chemical analysis by XRF.

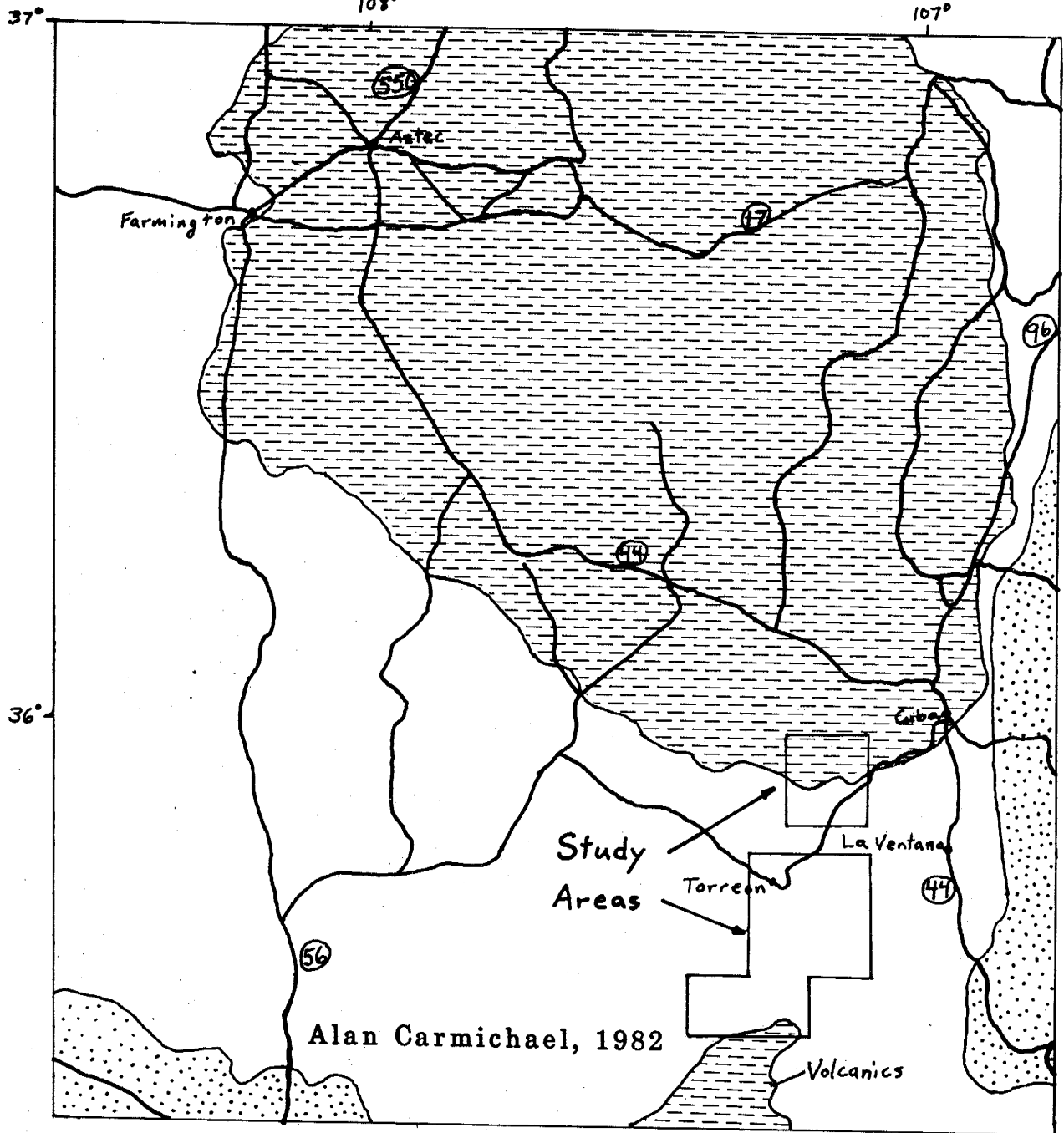
II

LOCATION AND GEOGRAPHY

Most of the study area was mapped by Tabet and Frost (1979) while the northern portion, containing Fruitland and Kirtland strata, was mapped by Hinds (1966) (Figure 1). The areas, covering about 200 square miles, are located in the southeastern part of the San Juan Basin. Sample localities are within the bounds of four maps, totaling seven and a half quadrangles, within the following townships and ranges:

- (1) T20N, R4W (eastern 2.7 sections), R3W (western 4.5 sections) T19N (northern 2.7 sections), R3&4W, (Hinds, 1966),
- (2) T18N, R3W, R4W (Tabet and Frost, 1979),
- (3) T17N, R3W, R4W (" " " "),
- (4) T16N, R4W, R5W (" " " ").

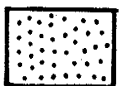
The field area consists of a series of arroyos, washes, mesas, and outwash plains. The Nacimiento Uplift, about 20 miles to the east, forms the basin's eastern boundary. The southwestern portion of the area lies on the edge of the Chaco Slope which eventually gives way to the Zuni Uplift to the southwest. The Mt. Taylor-Mesa Chivato volcanic touches the southernmost portion of the field area.



Rocks younger than Kirtland



Mancos Shale, Mesaverde Group,
Lewis Shale, Pictured Cliffs Sandstone,
Fruitland and Kirtland



Rocks older than Mancos Shale

Figure 1 - Index map of field area

III

PREVIOUS WORK

Holmes (1877) first recognized three divisions of the Mesaverde Formation, consisting of an upper escarpment sandstone, a middle coal-bearing shale, and a lower escarpment sandstone. Collier (1919) named them the Cliff House Sandstone, the Menefee Formation and the Point Lookout Sandstone and raised the Mesaverde Formation to group status. Schrader (1906) described eastern San Juan coal districts, and delineated Upper Cretaceous formations including: the Dakota Sandstone, the Mancos Shale, the Mesaverde Formation, the Lewis Shale, and the Laramie Formation; the latter subsequently renamed the Fruitland Formation (Bauer, 1916). Gardner (1909, 1910) traced and mapped the western coal-bearing units of the Mesaverde and Laramie and wrote a more detailed description of the geology and geography of the basin. Sears (1934) lithologically described and named the Satan Tongue of the Mancos Shale (Cross and Whitman, 1899) between two tongues of the Hosta Sandstone. Hunt (1936), working in the Mesaverde, and Dane (1936), working in the La Ventana Sandstone, Kirtland Shale, and Fruitland Formation, detailed the geology and coal deposits of the southeastern basin. Shomaker and others (1971), Beaumont and Shomaker (1974), and Shomaker and Whyte (1977) discuss the areas' coal resources.

Detailed stratigraphic studies were done by Sears, Hunt, and Hendricks (1941) and Pike (1947), who contributed

to the concept of transgressions and regressions being caused by imbalance between sediment influx and subsidence in order to explain the complex intertonguing, thickening, and thinning of strata found throughout the basin. Beaumont and others (1956) introduced the name Cleary Coal Member for the upper beds of the Gibson Coal Member of the Menefee. Hollenshead and Pritchard (1961) determined the geometry of the Mesaverde sandstones by recognizing a series of thick sand benches seaward of major coal deposits and locating vertical and lateral positions of Cliff House and Point Lookout shorelines. Fassett and Hinds (1971) established bentonite marker beds by electric log subsurface mapping and related thick coal deposits to stable strand lines. Shomaker and others (1971), and Fassett and Hinds (1971) recognized thick coal lenses trending parallel to old shorelines. Tabet and Frost (1979) mapped the field area, located coals, and provided the framework for this investigation.

Sabins (1964) defined stratigraphic and petrographic criteria for distinguishing sandstones resulting from transgressions and regressions. Mannhard (1976) contributed detailed sedimentological and paleoenvironmental analyses of the upper Menefee, Cliff House (La Ventana Tongue) Sandstone and Lower Lewis Shale and established the deltaic nature of the La Ventana and surrounding upper Menefee strata. Shetiwy (1978) determined paleoenvironments for the Point Lookout Sandstone, the underlying Mancos, and overlying Menefee from petrographic and outcrop investigations.

Siemers and Wadell (1977) discussed and defined humate deposits, the stratigraphy of the upper Menefee deposits (near Cuba, New Mexico), and environments of deposition within the deltaic deposits of the La Ventana.

IV

GENERAL DEPOSITIONAL SETTING

Time-stratigraphic relations indicate that a shallow seaway existed to the northeast during Cretaceous time. Clastics were supplied across an area of low relief on the southwest. Relative sea level was rising and/or the trough containing the ephemeral sea was subsiding, which resulted in deposition of over 6500 feet of sediments. Pronounced stratigraphic rises existed between the landward (southwest) and seaward (northeast) extents of shoreline sands (Molenaar, 1977). Two major transgressions and regressions, brought about by varying rates of trough subsidence and/or sediment influx, occurred in the area; coastal deposition dominated during regressions. Extensive, thick, transition zones between shales and overlying sandstones suggest that slowed subsidence resulted in coastal sands being deposited conformably on older offshore muds (Sears and others, 1941).

Wedges of deltaic and interdeltaic deposits, some influenced by longshore currents, produced straight shorelines and thick shoreface or coastal-barrier sands. Depositional environments include marine and non-marine facies. This study includes non-marine facies,







encompassing lower delta or coastal-plain facies and upper delta-plain or alluvial-plain facies. The lower delta or coastal-plain facies consists of paludal carbonaceous shale, coal, lacustrine sandstone, and fluvial channel sandstones with associated levee and splay deposits (Molenaar, 1977). Thick coal deposits often appear landward of thick sandstones where shorelines stood still and coastline buildups occurred (Fassett, 1977). Upper delta plain or alluvial-plain facies consist of predominately flood plain or interchannel shales and fluvial-channel sandstones (Molenaar, 1977).

V

REGIONAL STRATIGRAPHY

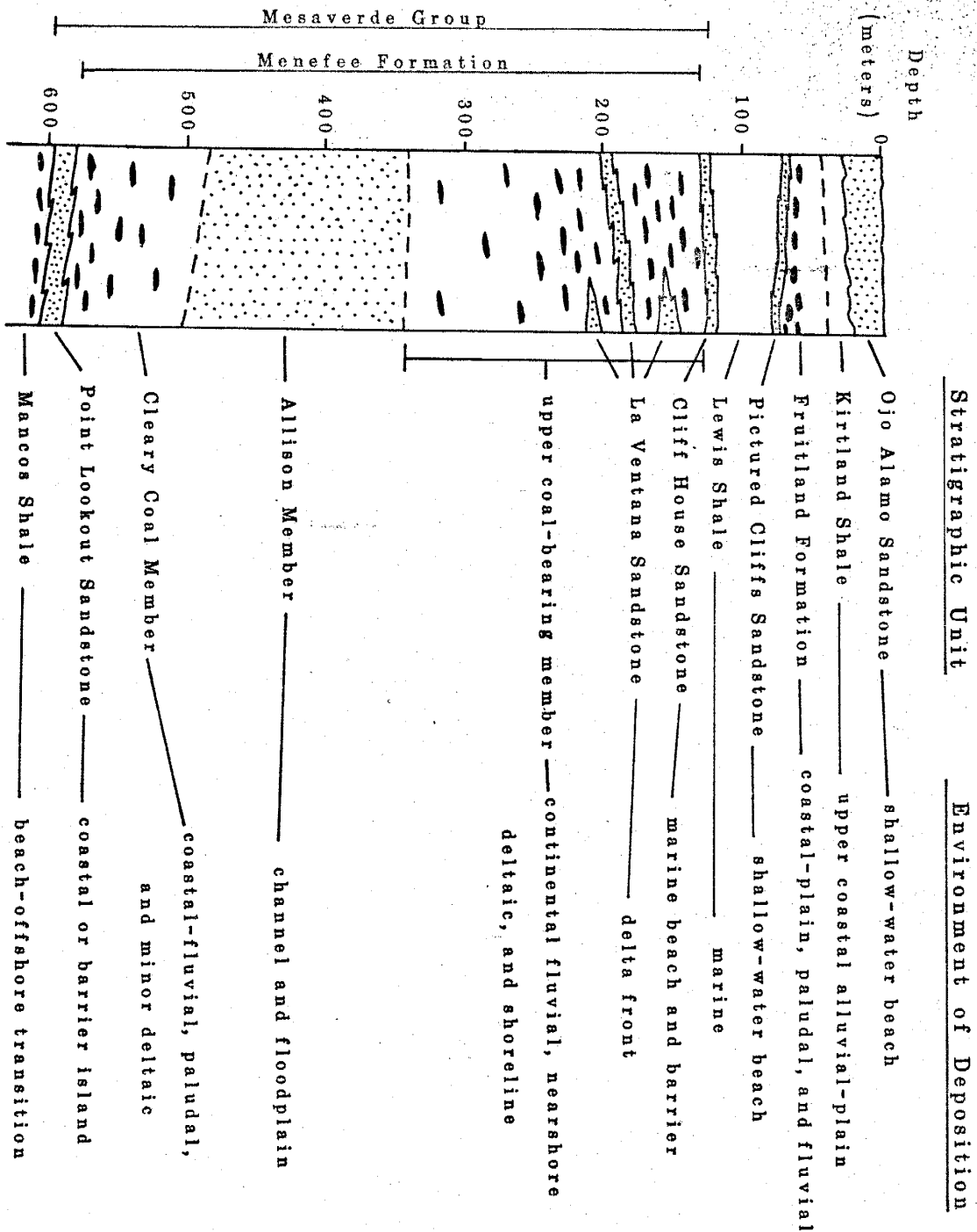
Stratigraphic units in the area include both marine and continental Upper Cretaceous sediments. Strata consist mainly of shales, sandstones, and coals with minor igneous intrusives. The igneous rocks are not discussed in this report. Formations include the marine Mancos Shale, the Point Lookout Sandstone, the continental Menefee Formation, the deltaic La Ventana Sandstone, the Cliff House Sandstone, the marine Lewis Shale, the Pictured Cliffs Sandstone (not exposed in the area), the continental Fruitland Formation, and the Kirtland Shale. Formations sampled are listed below in ascending order, from oldest to youngest. Regional stratigraphic relations and environments of deposition are shown in Figure 2.

Key and References by Formation

	Shale
	Sandstone
	Coal Seams
	Gradational contact
	Interfingering contact
	Unconformable contact

Formation	References
Mancos Shale	Hunt (1936), Sears and others (1941), Molenaar (1977), Tabet and Frost (1979), Shetiwy (1978)
Point Lookout Ss.	Hollenshead and Pritchard (1961), Sabins (1964), Shetiwy (1978)
Menefee Formation	Hunt (1936), Sears (1941), Mannhard (1976), Molenaar (1977), Siemers and Wadell (1977), Shetiwy (1978), Tabet and Frost (1979) Fush-Parker (1977)
Cliff House and La Ventana Ss.	Hollenshead and Pritchard (1961), Mannhard (1976), Fassett (1977), Molenaar (1977), Tabet and Frost (1979)
Lewis Shale	Fassett and Hinds (1971), Molenaar (1977), Tabet and Frost (1979)
Pictured Cliffs Ss.	Fassett and Hinds (1971)
Fruitland Formation	Fassett and Hinds (1971), Molenaar (1977), Lindsay and others (1981)
Kirtland Shale	Same references as Fruitland
Ojo Alamo Sandstone	Fassett and Hinds (1971)

Figure 2 - Regional Stratigraphic Section



Satan Tongue of the Mancos Shale

The Satan Tongue (Sears, 1934) of the Upper Mancos Shale (Plate 15), exposed in southeastern parts of Torreon Wash, represents a transgression of regional significance (Tabet and Frost, 1979). Although the bulk of the Tongue is marine, the uppermost part of the Satan Tongue (with which this study is concerned) is dominantly terrestrial, consisting of fine-grained silty sandstones interbedded with carbonaceous shales, barren mudstones, and coals, although Shetiwy (1978) believes that this facies represents a beach-offshore transition zone.

Menefee Formation

The continental clastic Menefee Formation is a wedge of sediments consisting of three members: the Cleary Coal Member, the Allison (sandstone) Member, and the upper (unnamed) coal-bearing member. The coal-barren Allison Member was not sampled. Contacts between members intertongue and are gradational. The upper coal-bearing member contains intertongues of the La Ventana Sandstone near the top (Tabet and Frost, 1979). "The Menefee represents nonmarine-paludal to alluvial-plain deposition landward from the Point Lookout and Cliff House shorelines." Coals usually occur just landward of shorelines where coastal swamps predominated

(Molenaar, 1977).

Lithologic units reflect a non-marine coastal-swamp complex consisting of intercalated:

- (1) barren to slightly carbonaceous light gray mudstones,
- (2) gray to brown carbonaceous (some coaly) shales,
- (3) thin tabular splay and levee siltstones and sandstones,
- (4) lenticular fluvial channel sandstones,
- (5) massive to bedded black to brownish black coals (some with amber and/or pyrite).

Tabet and Frost (1979) and Mannhard (1976) indicate that Menefee deposits are fresh water rather than brackish water through such evidence as the absence of brackish water invertebrate fossils, the presence of channel sandstones associated with coals, tree-dominated fresh-water pollen distributions, and low sulfur coals.

Source rocks for the Menefee and La Ventana strata, as indicated by the clay mineralogy and sandstone framework composition, include mature sandstones, illitic shales, dolomites, cherty carbonates, granitic plutonics, felsic volcanics, volcanic ash, and low rank metamorphics (phyllites and quartz-mica schists) (Mannhard, 1976).

The Cleary Coal Member

The Cleary Coal Member resulted from coastal swamp sedimentation and consists of thick (200-300 feet) paludal deposits. Coal beds are common in the lower half where

organic debris accumulated. "Occasional lenticular channel sandstone deposits and related splay and levee sandstone deposits make up a minor portion of the Cleary member." Ironstone concretions are found associated with carbonaceous shales and mudstones. Plant debris are abundant along bedding planes, but no macroinvertebrate fossils are present (Tabet and Frost, 1979). Where samples from the Cleary were collected (Plates 1-3), beds seemed to exhibit more lateral continuity and fewer channel sandstones and siltstones than in an adjacent deltaic area (half mile to the east), suggesting an interdeltatic environment (Tabet, oral communication, 1980).

The Upper Coal Member

The upper coal-bearing member (Plates 4-8) is lithologically similar to the Cleary Coal Member. Most coal beds occur in the upper portion between sandstone tongues of La Ventana (Plate 9) (Tabet and Frost, 1979). The Upper Menefee represents continental fluvial, nearshore deltaic, and shoreline deposits (Siemers and Wadell, 1977). Most field samples of the upper coal member were taken below the La Ventana Sandstone, representing predominantly fluvial-deltaic environments (Mannhard, 1976). Krukowski (in prep.) sampled the La Ventana Sandstone.

Fush-Parker (1977) believes that all Menefee and La Ventana strata in the area formed in a deltaic environment;

he infers a southeast source from cross-stratifications of La Ventana Sandstone and finds it predominantly fluvial, unlike the marine Cliff House sandstone.

The Fruitland Formation

The Fruitland Formation represents lower coastal-plain deposition of swamp, river, flood-plain, and lake sediments shoreward of the Pictured Cliffs Sandstone. Thin coal beds (2-3 feet) indicate little vertical accumulation of vegetal matter, a steady rate of regression, and small unconnected swamps (Fassett and Hinds, 1971). The Fruitland is absent in the eastern basin and thin in my area (100-150 feet vs. 300-350 feet elsewhere), due to either erosion or lack of deposition (Molenaar, 1977). Lindsay (spoken communication, 1982) believes the Fruitland source area was to the northwest, which explains southeastward thinning. The lower contact with the Pictured Cliffs Sandstone is not exposed in the field. The upper contact with the Kirtland Shale was arbitrarily placed at the uppermost carbonaceous shale (Molenaar, 1977).

The Fruitland Formation consists of interbedded sandstone, siltstone, mudstone, carbonaceous shale, coal, and ironstone concretions, nearly all of which are laterally discontinuous within several hundred feet. The Fruitland outcrops abound in fresh-water swamp fossil assemblages (Tabet and Frost, 1979), consisting of silicified tree parts

(often upright stumps), coprolites, and vertebrate bones (see Lindsay and others, 1981, or Fassett and Hinds, 1971). The Fruitland (Plates 10-14) contrasts with Mancos Shale and Menefee Formation outcrops, with its brighter and wider color ranges and round weathered mounds of sediment.

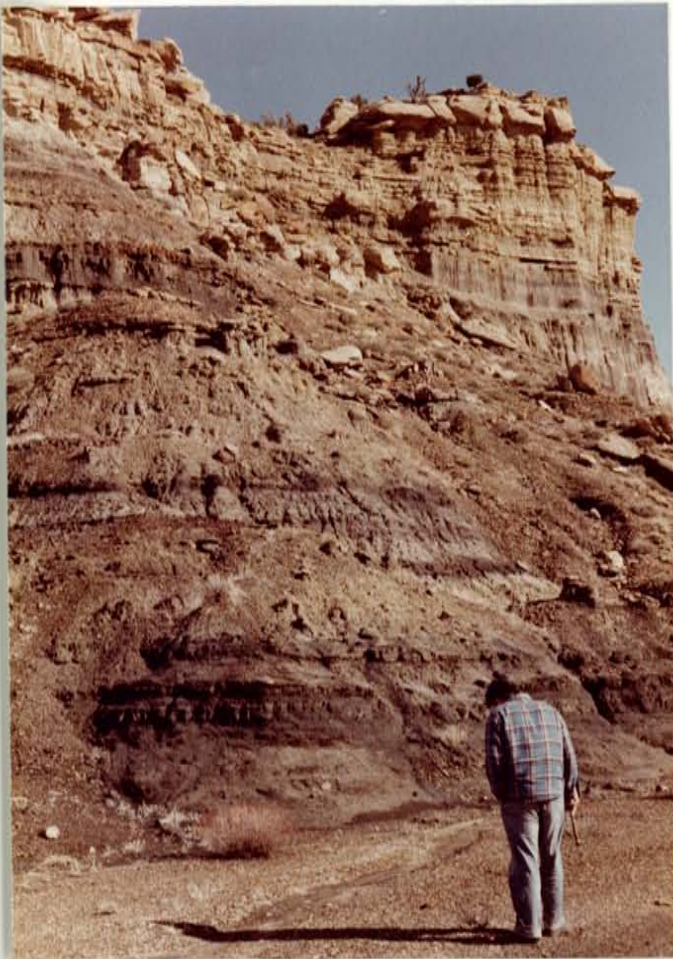


Plate 1: Photo of outcrop of the Cleary Coal Member of the Menefee Formation. Sandy member at top is the Allison Member of the Menefee.

T17N, R4W, sec. 34, NE 1/4

Plate 2: Photo of the Cleary Coal Member taken below an old coal mine where clays AC-CM-(56-63) were sampled. T17N, R4W, sec. 34, NE 1/4

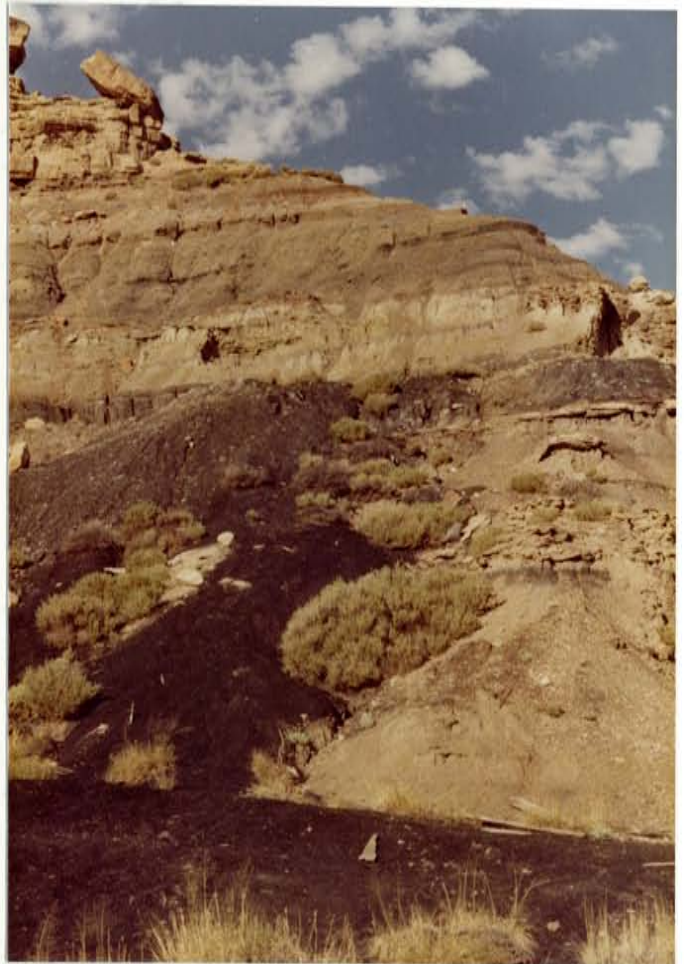




Plate 3: Outcrop of Cleary Coal Member, below Allison Member (sandstone) at top.

T17N, R4W, sec. 34, NE 1/4



Plate 4: Photo of upper Menefee strata taken near station IV of lateral clay study (p. 74) along cliffside of plate 9. T18N, R4W, sec. 15, NW 1/4

Plate 5: Photo of an outcrop of upper Menefee strata in the Torreon Wash channel.

T18N, R4W, sec. 15, NW 1/4



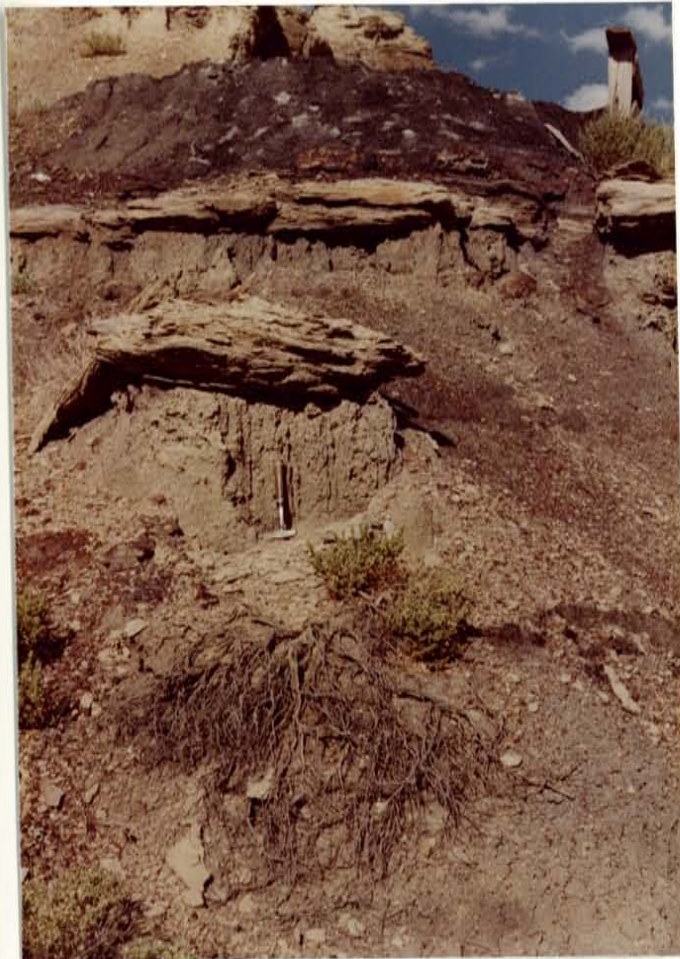


Plate 6: Outcrop of upper
Menefee strata occurring at
station IV.

T18N, R4W, sec. 15, NW 1/4

Plate 7: Photo of upper
Menefee outcropping below
Plate 6.



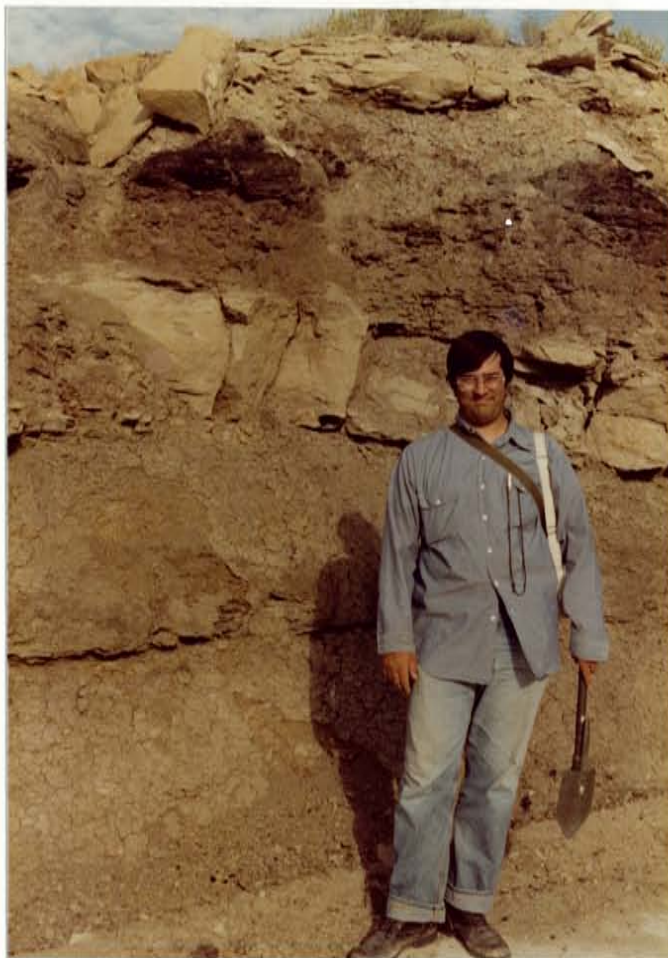


Plate 8: Outcrop of the lower part of the upper Menefee
where samples AC-UM-(64-67) were collected.
T18N, R3W, sec. 34, NW 1/4

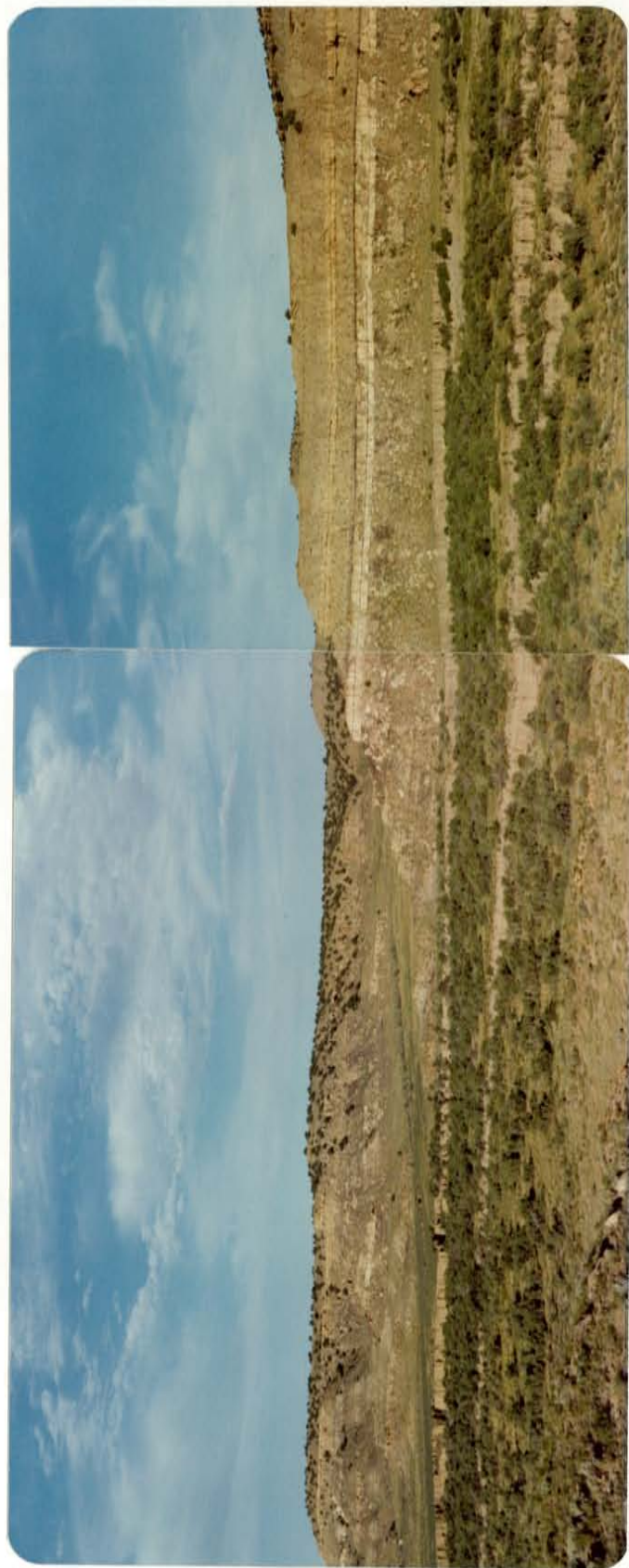


Plate 9: Outcrops of upper Menefee (Kmu), La Ventana tongue of the Cliff House Sandstone (Klv), and Lewis Shale (Kl), where clays were sampled for lateral study (pg. 74).
T18N, R4W, sec. 10 & 15



Plate 10&11: Typical shales and sandstones of the Fruitland Formation deposited in coastal-plain, paludal, and fluvial environments.



Plate 12: Photo looking north toward Eagle Mesa
showing Fruitland and Kirtland shales.



Plate 13: Photo still closer to Eagle Mesa. Kirtland
strata may or may not be present below
the Ojo Alamo Sandstone at top.



Plate 14: Fruitland Formation clay sample area south of Eagle Mesa. T19N, R4W, sec. 2, SE 1/4

VI

STRUCTURAL GEOLOGY

The San Juan Basin, which covers over 10,000 square miles, is structurally unique in the western U.S., since it is only moderately deformed. It is a roughly circular, stratigraphically asymmetrical, Colorado Plateau basin consisting of thick (up to 14,000 feet) sediments. In the central basin, Tertiary rocks are exposed, giving way to Upper Cretaceous and older rocks toward the margins.

Deformation occurs along monoclines. The Hogback Monocline, the Defiance Monocline, the Chaco Slope (grading into the Zuni Uplift), and the Nacimiento Uplift (a near linear 60-mile fault zone, 6-10 miles wide) define the Basin's northern, western, southern, and eastern boundaries, respectively. Radial folds, due to differential subsidence, plunge toward the center of the basin and occur along most of the perimeter (Woodward and Callender, 1977).

Strata in the area dip gently (2-5 degrees) to the northwest, except where disturbed by primary depositional slopes or faults. Linear, northeast-trending normal faults and basaltic dikes with small displacements (measured in a few tens of feet) are present. Greater displacements, of up to 150 feet, occur in southern faults, which splay out to the north. Minor folds occur as gentle north-plunging anticlinal flexures in T17N, R3W and T16N, R5W, and around some faults as a result of drag (Tabet and Frost, 1979).

VII

SAMPLE LOCATIONS

Sample locations are given in Table 1 by township, range, and quarter section. For the core samples the formations exposed at the surface may or may not represent the formations which were sampled in the subsurface.

TABLE 1 SAMPLE LOCATIONS

SAMPLE #'S	FORMATIONS	TOWNSHIP&RANGE	SECTION
AC-TW-1	UPPER MENEFEE	T18N,R4W	16-NE 1/4
AC-TW-(3-29)	UPPER MENEFEE	T18N,R4W	15-NW 1/4
AC-TW-(32-40)	UPPER MENEFEE	T18N,R4W	10-SW 1/4
AC-CM-(56-63)	CLEARY	T17N,R4W	34-NE 1/4
AC-UM-(64-67)	UPPER MENEFEE	T18N,R3W	34-NW 1/4
AC-FR-(71-82)	FRUITLAND	T19N,R4W	2-SE 1/4
CORE #1	UPPER MENEFEE	T18N,R3W	20-SW 1/4
CORE #2	UPPER MENEFEE	T18N,R4W	18-NE 1/4
CORE #3	CLEARY, MANCOS	T17N,R3W	29-NE 1/4
CORE #4	CLEARY, MANCOS	T17N,R4W	27-NW 1/4
CORE #5	CLEARY, MANCOS	T16N,R4W	5-NW 1/4

VIII SAMPLE COLLECTION, PREPARATION, AND ANALYSIS

Shales

Two groups of samples were collected, one from surface outcrops, and the second from six cores available from Tabet and Frost's (1979) study. Mudstones (rocks without fissility) and shales were collected from a variety of coal-bearing strata, including the Cleary and upper members of the Menefee Formation, the Mancos Shale, and the Fruitland Formation. This study was restricted to coal-bearing horizons and immediately adjacent strata.

Approximately 75 grams of each sample was crushed into particles less than 0.25 cm by using a hammer and metal plate. Twenty-five gram splits were retained for chemical and whole rock analysis. The remaining 50 grams was put into a 500 ml beaker with 400 ml of distilled water and magnetically stirred for five hours or more. If material remained in suspension 45 minutes after stirring, disaggregation was considered complete. If the sample was not disaggregated, ultrasonic disruption and additional stirring were employed.

Matrix material, such as carbonates, sulfates, and organics, can interfere with disaggregation in some samples. These matrix materials were removed by mixing the sample with a 0.5N EDTA solution in a 1000 ml flask and boiling for

four hours (Bodine and Fernalid, 1973). The sample was then transferred to 500 ml centrifuge bottles which were placed in a Sorvell high speed refrigerated centrifuge at 8800 rpm for 60 minutes. By sequential centrifuging, decanting, and washing all EDTA solution was removed from the sample.

After the sample was disaggregated, it was then separated into size fractions using estimated spherical settling velocities as determined by Stoke's law. For the <8 micron fraction a freshly stirred sample was put in an evaporation dish at room temperature; after 11 minutes the clay material in suspension was decanted to a depth of 5 centimeters. For the <2 micron fraction, the sample was stirred, allowed to settle for about 45 minutes at room temperature, and pipetted from a depth of approximately 1 centimeter onto the slides. A Sorvell high speed refrigerated centrifuge for the <0.5, <0.25 and <0.1 micron fraction separations, and a International model SBR centrifuge for the <1 micron fraction separations, were employed. Three diffraction mounts sedimented on glass slides were prepared for each sample by pipetting approximately 3ml of clay fraction solution onto each and air-drying. One slide was left untreated after air drying, the second was saturated with ethylene glycol vapors in a closed vessel for five hours, and the third was heated to 350 degrees centigrade for five hours and analyzed, then reheated to 550 degrees centigrade and analyzed.

The slides were x-rayed using a Phillips Norelco

diffractometer, a Tennelec TC 941 high voltage bias supply, a Tennelec TC 590 ratemeter, and a Bristol Dynamaster recorder. The counts were adjusted so that the most intense peak stayed on the scale, and all four charts were run at the same rate, since differing counts per second were not easily convertible when dealing with peak areas.

Diffraction analyses were conducted at 20 milliamps and 40 kilovolts, slit settings of 1-4-1 degrees, a chart rate of 1 inch per minute, and a scan rate of 2 degrees per minute.

Twenty five grams of each whole rock sample was prepared by thorough hand grinding with an agate mortar and pestle, and sieving to <200 mesh. Two-gram pressed pellets were made, at 21 tons pressure, and then x-rayed.

Coal Ashing

To obtain clay concentrates from coals and carbon-rich shales a low temperature asher (LTA/504 MP4), model #248012, manufactured by LFE Corporation, Waltham, Mass. was used. By using a low temperature asher, clay mineralogy is preserved in the ash, rather than being destroyed as in conventional ashing which uses higher temperatures (about 800-1000 degrees centigrade). With the low-temperature technique ashing occurs at <190 degrees centigrade and is suitable for analysis of clay residues (Gluskoter, 1967).

Coal samples obtained from the cores and very

carbonaceous shales (or humates) collected from outcrop were prepared for ashing by hammer and sieve; particle sizes ranged from about 0.6 to 0.85 mm. Ashing was considered complete if the sample lost less than 0.1 percent of its' initial weight in ten hours.

Chemical Analysis by X-ray Fluorescence (XRF)

Samples were fused into pellets using the method of Norrish and Hutton (1969). A fully automated Rigaku XRF setup performed the analysis (see Jenkins, 1976, for theory). Counts were converted to oxide percents (Appendix 3) for various elements. Instrumental conditions are listed in Table 2.

Loss on ignition (representing organics, unbound and bound water, and additional volatiles) was determined by taking the difference in the sample weights of 1 gram samples before and after heating to 1000 degrees centigrade for an hour.

TABLE 2

INSTRUMENTAL CONDITIONS FOR XRF

ELEMENT	2 THETA ANGLE	COUNTING TIME (SEC)	SCAN RATE (2 THETA/MIN)	CRYSTAL
SI	144.53	40	2	RX4
AL	37.98	80	4	TAP
FE	57.49	20	1	LIF3
K	136.75	20	1	LIF3
NA	55.24	200	1	RX4
CA	113.18	20	1	LIF3
MG	45.32	80	4	TAP
MN	63.00	20	1	LIF3
TI	86.19	20	1	LIF3
P	140.97	20	1	GE

IX PROBLEMS IN CLAY FRACTION ANALYSES

Results are called relative abundances instead of percents because Torreon clay groups cannot be separated and mixed in known proportions to obtain calibration curves. Pure samples of San Juan clays, other than smectites, are not available, and clays from other areas should not be used to approximate the San Juan samples. Any clay analysis has to be taken with a grain of salt because many variables come into play, the precise nature and relative importance of which are largely unknown. Variables include mass absorption coefficients of individual minerals, orientation of grains, thickness of the mounts, weight of clay sample x-rayed, evenness of mixture spread, differences in crystal perfection, polytypism, hydration, chemical composition, and many others (Carroll, 1970). However, results should be comparable relative to each other because analytic methods were consistently employed, the clay assemblages were similar, and samples were obtained from the same area.

Additional analytic errors when obtaining peak areas and heights were introduced by:

(1) Broad gypsum peaks at $2\theta = 11.6$ add intensity and area to the kaolinite peak at $2\theta = 12.3-12.4$. By excluding gypsum peaks on the kaolinite tracings and height measurements by visual inspection errors were minimized.

(2) A broad glycolated (001)₁₀/(002)₁₇ random mixed-layer

illite-smectite peak at $2\theta = 8.8-10.2$ can interfere with the illite (001) peak at $2\theta = 8.8-9.0$. The (001)₁₀/(002)₁₇ peak was excluded from the illite peak visually, so some error was introduced.

(3) Successive scans of the same slides show that cps can vary as much as 10 percent for individual peaks; however, relative clay abundances determined by computer vary (at most) plus or minus 4 parts in 100, revealing that peak areas were more reliably reproduced than peak heights.

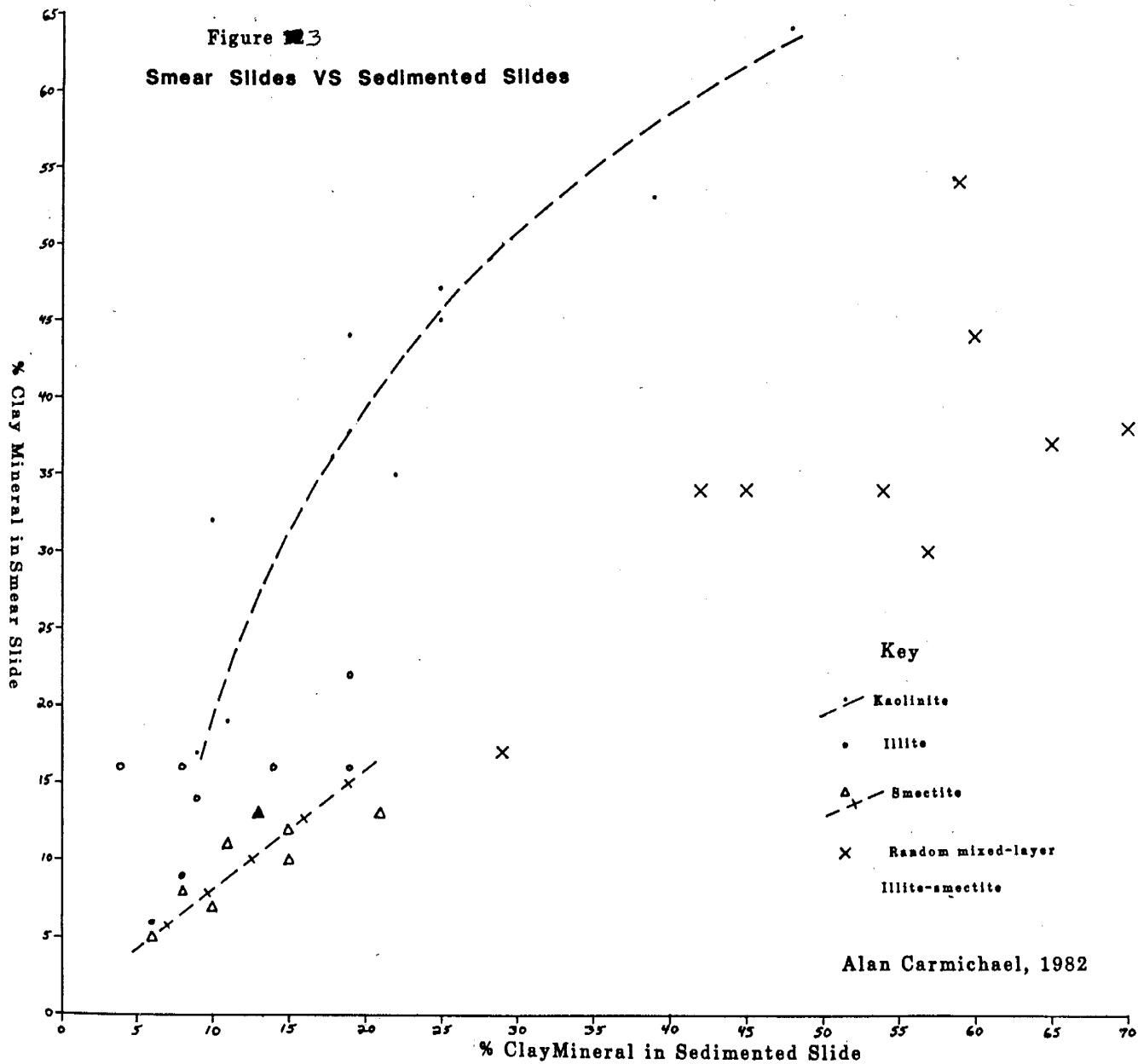
(4) The assumption that smectites have higher ratios of (001) glycol peak heights to 350 degree peak heights than random mixed-layer material, and that these ratios relate linearly to amounts of smectites vs. mixed layers present is questionable. This method's ability to discriminate between smectites and mixed layers may introduce serious errors.

(5) An arbitrary base line must be drawn on the charts as a starting point to measure peak heights and areas.

Although sedimented slides provide a rapid means of data collection, their use has been criticized by Gibbs (1965 and 1968) and many others. The larger particles, especially kaolinite, settle more rapidly and are concentrated at the bottom of the slide. Subsequent x-raying yields low concentrations of the larger particles, since x-rays reaching and leaving the bottom layer are less intense due to absorption by the overlying layers.

Using a smear technique, nine clay fraction analyses were duplicated to quantify clay species concentration

Figure 3
Smear Slides VS Sedimented Slides



Alan Carmichael, 1982

variations between sedimented and smear slides. Scotch tape was wrapped around each side of the slides and pasty clay material was placed in the middle. Then a slide was pulled across the top to producing an oriented clay slide not affected by differential settling. Figure 3 shows the relation between amounts of kaolinite and smectite in the smear vs. sedimented slides. Relationships for illite and mixed layers are not well defined. Kaolinite and illite, concentrated in the larger fractions, appear in smaller relative abundances in the sedimented slides, while smectite and mixed layers, concentrated in the smaller fractions, usually have larger relative abundances in the smear slides.

Regarding sedimented slides, Kinter and Diamond (1956) state, "the degree of particle orientation varies widely in specimens of different clays, often being little better than that of 'random' specimens." However, evidence revealing orientation problems was not found in this study. All clay fraction traces show good orientation as evidenced by strong (001) reflections and the absence of any prominent non-basal reflections (Figures 4-7).

Many investigators allow one or two hours for glycol treatments, but for some Torreon samples (particularly smaller fractions), up to five hours exposure was necessary to maximize 17A peak height. Clay mineral chemistry reveals that most samples have relatively high interlayer charges, a possible cause of longer expansion time. Heat-treated samples required up to five hours before peak shifts ceased.

REPRODUCIBILITY

Reproducibility experiments were carried out (samples marked RS, R, and SR in Appendix 2B). Several samples of AC-TW-58 and AC-FR-76 ("RS"-Appendix 2B) were analyzed by the same methods using shales taken several inches apart from the same bed. Sample AC-FR-76 (bentonite) was 100 percent smectite in both analyses. Relative abundances of clay minerals were variable (plus or minus 3 parts in 100) for AC-TW-58, but do not exceed normal analytic error ranges. However, samples collected from the same bed one or two feet apart (TW-C3-106.6 and TW-C3-107.3, TW-C3-117.9 and TW-C3-120.1, TW-C3-149.2 and TW-C3-150.4) sometimes showed large differences in clay mineralogy (up to plus or minus 12 parts in 100).

Samples marked R were duplicate analyses of the same sample using two separately prepared series of slides, while those marked SR were duplicate analyses of the same slide. Results reveal that relative abundances of clay minerals were reproducible within plus or minus 4 parts in 100 if the same starting material was used.

XI

X-RAY DIFFRACTION INTERPRETATION

Whole Rock

For non-clay minerals, routinely identified by their most intense peaks (Table 3), the <200 mesh whole rock pellet x-ray charts were used. In some cases (such as with low albite, quartz, and microcline), less intense peaks were resolvable when the minerals were present in large enough concentrations. For feldspars various additional peaks (Fellows and Spears, 1978) to those in Table 3 were:

- (1) low albite (201) at 2 theta = 22.0
- (2) low albite (131,130) at 2 theta = 24.2
- (3) microcline (131) at 2 theta = 30.3

TABLE 3 PEAKS USED IN WHOLE ROCK IDENTIFICATION

MINERALS	MOST INTENSE	PEAK POSITION	INTENSITY FACTORS
	PEAK (hkl)	2 THETA, Cuk	(CPS PER 100%)
QUARTZ	(101)	26.6	2000
ALBITE	(002), (040)	27.8-30.0	1000
MICROCLINE	(220), (002), (040)	27.4-27.6	1000
ORTHOCLASE	(220)	27.0	1000
CALCITE	(220)	29.4	1000
CALCITE*	(220)	29.6-30.0	500
GYPSUM	(020)	11.6	1500

*-MIXED MG OR MN SUBSTITUTION

Ironstone Concretions

Several ironstone concretions (Tabet and Frost, 1979) from the upper coal-bearing member of the Menefee Formation were pelletized and x-rayed. Weathered surfaces appearing light orange in color consisted of goethite, hematite, quartz, illite, and kaolinite. Fresh surfaces contained calcite in addition to the minerals mentioned above, while quartz was no longer detected. The ratios of hematite-to-goethite peak heights increased from 0.32 in weathered samples to 1.14 in fresh samples, due to hydration of hematite forming goethite on weathered surfaces. Clay minerals were less abundant and crystalline on weathered surfaces compared to fresh ones, as evidenced by peak broadening and a drop in counts per second from weathered to fresh samples. Kaolinite and illite peaks decrease from 350 to 70 and 125 to 30 counts per second, respectively. No siderite was found in any of the ironstone concretions examined from the Menefee. A small amount of albite and microcline was found in one of the ironstone concretions.

Quantification of Whole Rock Percents

Pure quartz was obtained from a fine grained sandstone lacking feldspar (TW-C3-224.8) by centrifuging the clay away. The resulting quartz was then ground to <200 mesh, pelletized and x-rayed five separate times. On our equipment the 100 percent quartz sample yielded 17,000 cps (plus or minus 175) on the most intense (101) quartz peak. By dividing the (101) quartz peak height from the whole rock pellet by 17,000 and multiplying by 100 percent, the percent quartz in the whole rock was obtained. Using ratios of intensity factors from Schultz's (1964) study (Table 3), approximate percents of other minerals were obtained. The formula used was: percent mineral = $(\text{cps}/17,000) \times 100$ percent. A computer program aided in whole rock data reduction.

Total clay percent was calculated by subtracting the sum of percents for individual non-clay minerals from 100 percent. Whole rock clay percents may be high, since amorphous material, unbound water, and organic material were included. The combined effect of the last two factors ranges up to 20 percent, as evidenced by loss on ignition.

Quartz standards were prepared to test the validity of assuming that a linear relation existed between counts of quartz (101) peaks and percent quartz in the sample. Pure clay (AC-FR-73) and quartz standards were weighed (plus or

minus 1/10,000 gram), mixed (yielding approximately 10, 20, 25, 30, 40, 50, and 70 percent quartz by weight), pelletized, and x-rayed in triplicate at 25,000 cps. The 10, 20, and 25 percent quartz standards were also x-rayed at 5000 cps, since this was the level used for samples containing up to 25 percent quartz (Table 4). Calculated vs. known percents of quartz generally show agreement (plus or minus 1.5 percent), and never disagree by more than plus or minus 3 percent.

TABLE 4 CALCULATED VS KNOWN PERCENT QUARTZ

% QUARTZ IN STANDARD	CPS	CALCULATED % QUARTZ			AVE. CALCULATED % QUARTZ
		RUN# 1	RUN# 2	RUN# 3	
9.97	5000	10.44	10.74	11.18	10.78
"	25000	8.82	8.82	8.38	8.67
20.03	5000	23.38	23.82	21.76	22.99
"	25000	19.12	20.59	18.09	19.27
25.01	5000	26.47	23.53	25.59	25.20
"	25000	26.47	25.00	26.47	25.98
29.96	25000	28.97	30.15	31.62	30.25
40.02	25000	39.71	38.97	42.12	40.27
50.02	25000	52.94	50.00	51.47	51.47
69.96	25000	70.58	67.65	69.12	69.12
100.00	25000	100.74	99.56	98.97	
			100.15*	100.44*	99.97

* Additional Quartz runs (total of five runs)

Clay Minerals

Using treated and untreated mounts of clay-size material sedimented on glass slides, clay mineral groups were routinely identified by their (001) d-spacings determined by x-ray diffraction. These groups were classified as smectite, illite, kaolinite, chlorite, or random mixed-layer illite-smectite.

Discussions of individual clay minerals are given on the following pages. Examples of x-ray charts are included in Figures 4-7.

Smectite

Smectite group clay minerals are characterized by expansion of the (001) peak to 17 angstroms (A) upon glycolation (Carroll, 1970). The most prevalent smectite was the one interlayer water Na+1 variety; there were a large number of samples with (001) d-spacings between 12.1-12.5A. Less commonly, a two interlayer water Ca+2 variety (d=14.0-14.5A) and occasionally a mixture of the Na+1 and Ca+2 varieties (d=12.5-14.0A) occur. Appendix 5A lists the d-spacing of untreated samples' (001) peaks, which represent a composite of smectite, illite, and mixed-layer.

Some untreated samples (Appendix 5C, Group 2) show broad, low-intensity traces, whose d-spacing ranges from

Figures 4-7 Examples of clay mineral x-ray diffraction charts

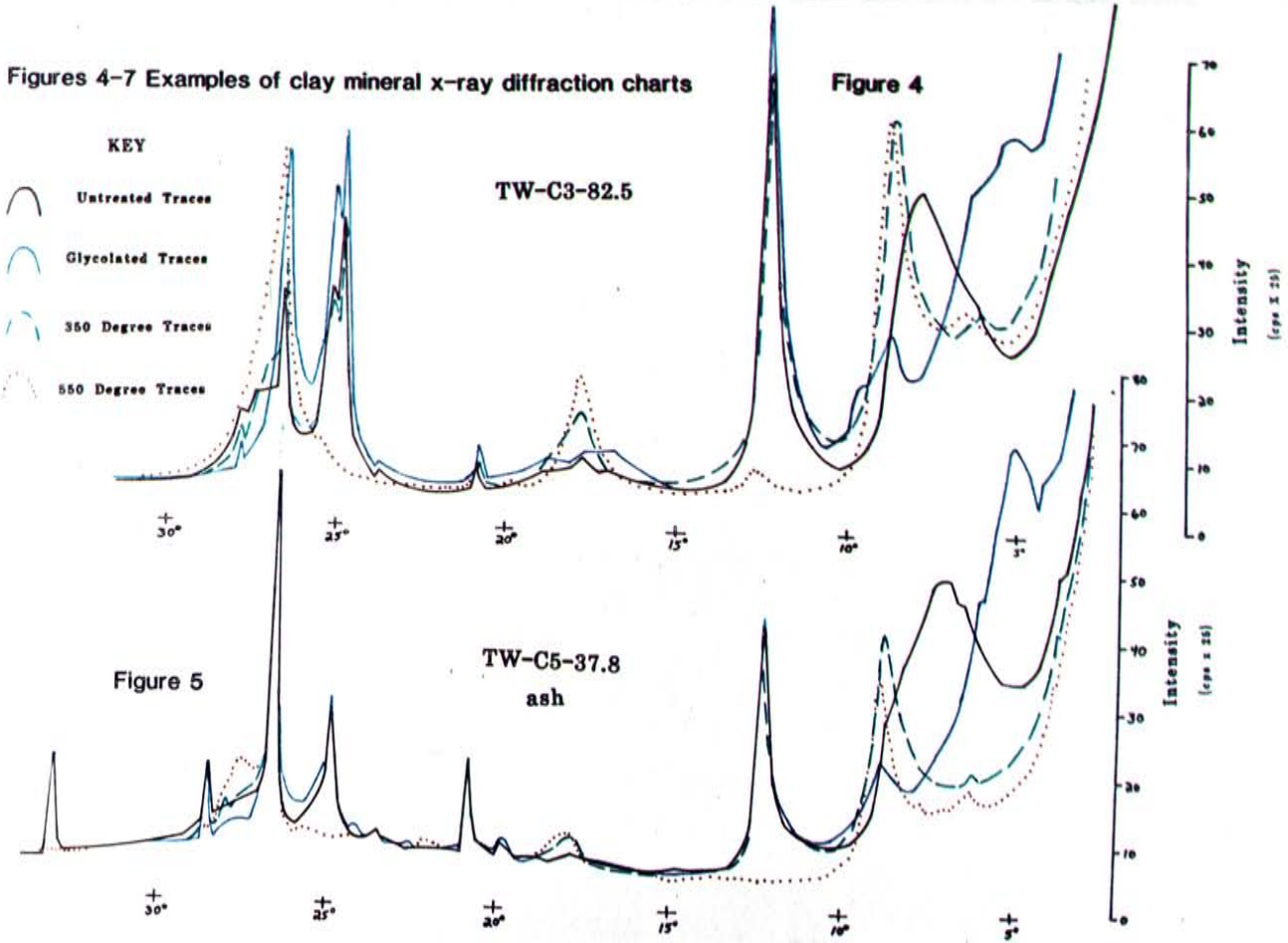
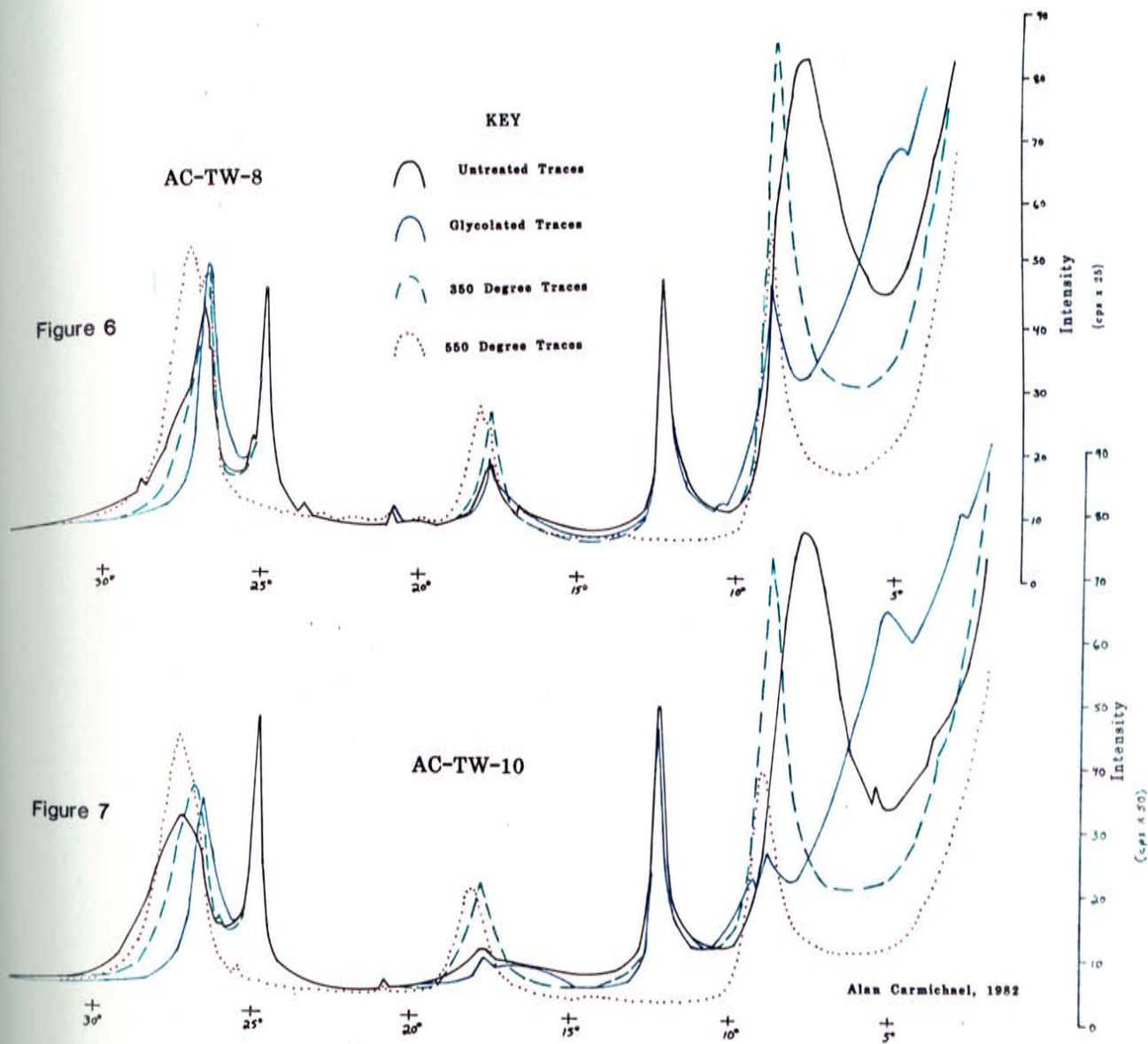


Figure 6



16.07 to 19.21A. Upon glycolation d-spacing for these peaks either expanded or remained the same. Destruction of organics on heating was evidenced by the disappearance of the 17A smectite peaks which were incorporated into the 10A peak. These samples are interpreted as smectites with organic interlayers. Czarnecka and Gillot (1980) found that bitumens were adsorbed into smectite interlayers (particularly calcium varieties), yielding d-spacings of up to 17A.

Illite

Illite was identified by a peak at about 10A that did not shift on glycolation; illite's high interlayer charge ($K(+1) > 0.7$ per half unit cell) prevents penetration of ethylene glycol into interlayers. Illite is best resolved on charts of glycol-treated samples, since the smectite (001) peak shifts to 17A, while the illite peak stays at 10A (Carroll, 1970). On the charts of untreated samples, the illite (001) peak was observed as a broad shoulder on the low angle side of the (001) smectite peak.

Illites and smectites are defined here on the basis of expansion properties on glycolation, but may be mineral end members of the smectite-illite mixed-layer series. They may represent mixed layers of mica (illite) and smectite that x-ray diffraction does not have the ability to resolve (Hower and Mowatt, 1966), instead of discrete minerals.

Kaolinite

The presence of kaolinite group minerals (referred to as kaolinite hereafter) was determined by a series of basal x-ray reflections at 7.2, 3.6 and 2.4A. All but the most well crystallized kaolinite is destroyed when heated to 550 degrees centigrade (Carroll, 1970). This treatment destroyed all kaolinite present in every sample analyzed.

Most kaolinite peaks of shales and mudstones in the range of <8 to >0.25 microns seem to be somewhat sharp, indicating that they are moderately well crystallized (Schultz, 1964). Charts of several sandstone and coal ash samples possess sharp peaks, implying that well-crystallized kaolinite of authigenic rather than detrital origin exists (Mannhard, 1976, and Gluskoter, 1967).

Chlorite

In most samples chlorite was not detectable. Frequently only the 14A reflection appears as a broad hump on the (001) peaks of 550 degree heat-treated samples, since heat treatment increased the crystallinity to within detectable limits. Expansion of the (001) peak was not observed on the traces of glycol treated samples. In five heat-treated (550 degrees centigrade) samples, the (002) peak was detected as a broad peak at about 7A (Figure 4). The (004) peak at 3.5A appears only in two coal ash samples

(TW-C3-108.4 and TW-C4-172.8). A combination of low concentration and poor crystallinity explains the absence of this peak in all other samples.

Chlorite (001) d-spacings occur within the entire range of spacing found for this mineral (13.81 to 14.79A).

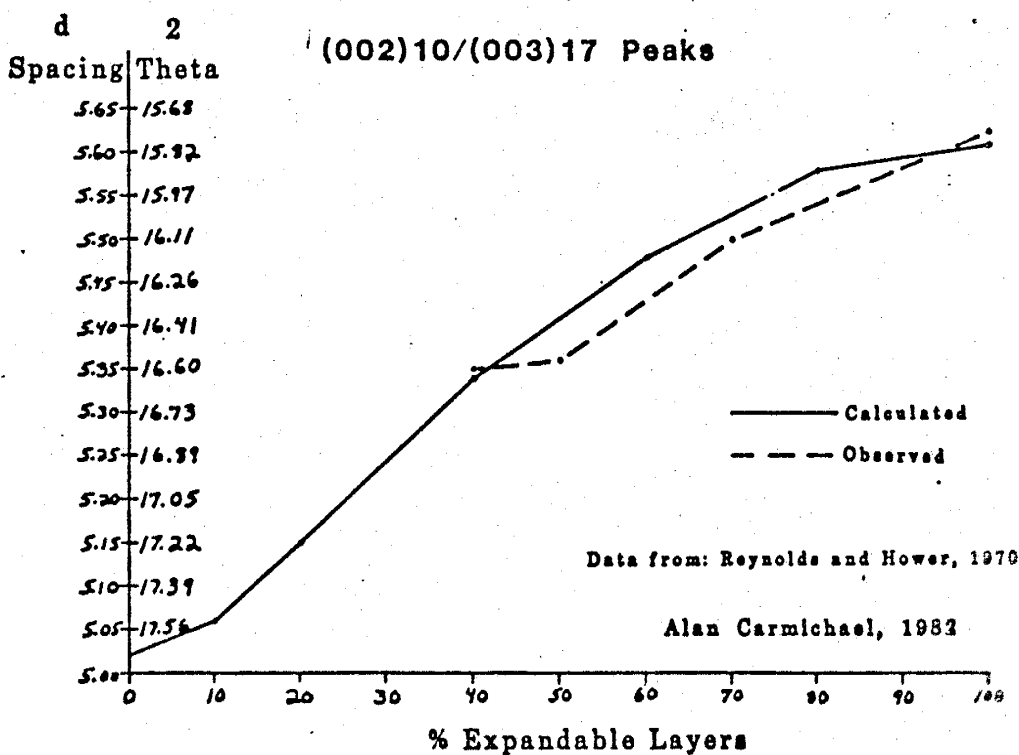
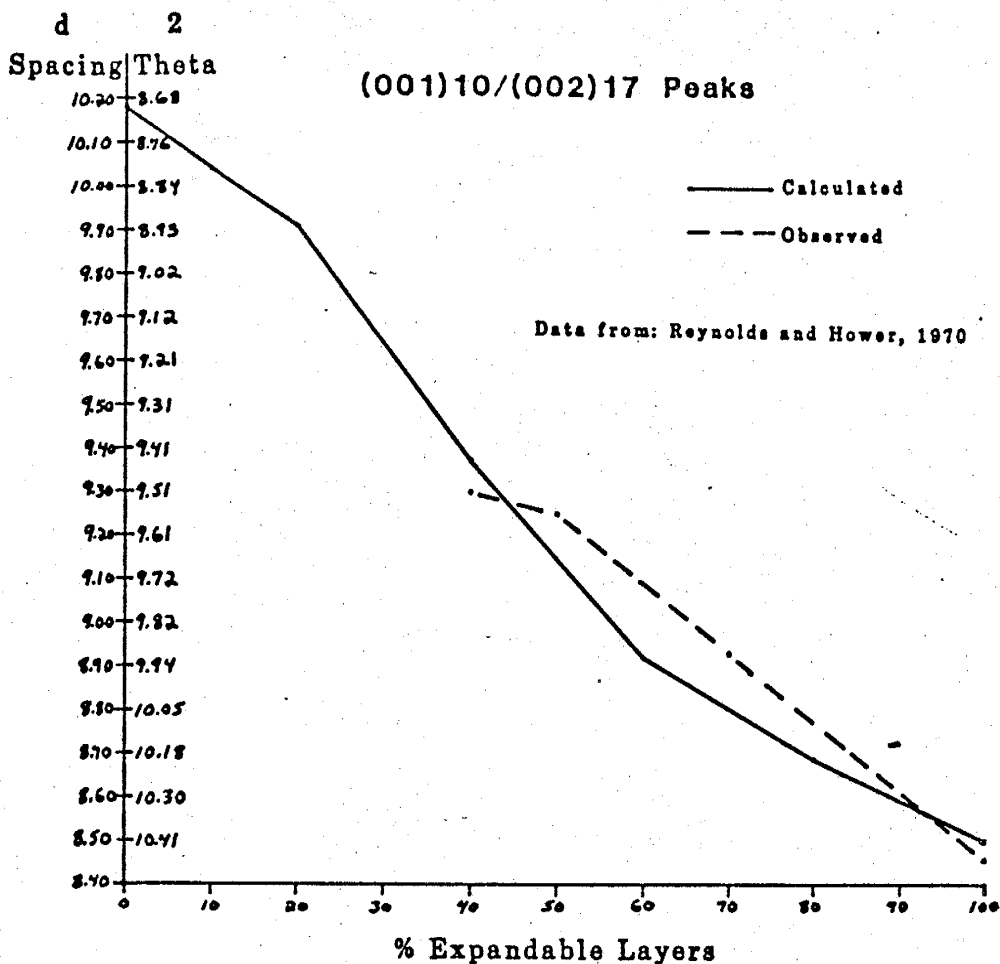
Mixed-Layer Illite-Smectite

Mixed-layer clays in San Juan samples are mainly random mixed-layer illite-smectite as supported by:

- (1) non-integral basal reflections (Weaver, 1956),
- (2) broad, poorly developed (001)10/(001)17 reflections (Hower, 1974),
- (3) the presence of (001)10/(002)17 glycol peaks (Mills and Zwarich, 1972).

Percent expandable layers in mixed layers can be approximated by positions of (001)10/(002)17 glycol traces. For San Juan samples, these values are variable. Using data from Reynolds and Hower (1970) I plotted Figure 8, showing percent expandable layers vs. (001)10/(002)17 peak positions. There were considerable errors in analyses due to measuring 2 theta, interferences by the illite (001) peak, linear extrapolation between graph points, the assumption that my samples were similar to those used to construct the graph, and errors in the graph points themselves; so values should be considered approximate (plus

Calculated 2 Theta and d Spacing VS % Expandable Layers
for Glycolated Random Mixed-Layer Illite-Smectite



or minus 5-10 percent). Percent expandable layers vs. (002)10/(003)17 glycol peak positions were graphed (Figure 8), when resolvable, to check values obtained from the more intense (001)10/(002)17 peak (see Appendix 5B); these values agree to plus or minus 10 percent.

Some broad, low intensity shoulders and peaks are often barely resolvable. Present at about 22-27A, 27-35A, and 20-22A on the traces of a few untreated, glycolated, and 350 degree heat-treated charts, respectively (Appendix 5C, Group 1), these were interpreted as regular mixed-layer clays.

Relative Clay Mineral Abundances

For semi-quantitative analysis of clay minerals, (001) reflections provided the main interpretative tool. The method used was that of Schultz (1964) (Appendix 1) with the following modifications:

- (1) samples were prepared by air drying clay-water suspensions on a glass microscope slide instead of the porous tile technique of Kinter and Diamond (1956);
- (2) the heated slides were treated at 350 and 550 degrees centigrade instead of 300 and 550;
- (3) total clay was calculated by subtracting out the non-clay minerals from the whole rock analysis rather than by using whole rock non-basal clay reflections;
- (4) peak areas were obtained by weighing tracings of peaks

to the nearest 1/10,000 of a gram;

(5) a PASCAL computer program aided in computations.

XII

RESULTS AND CONCLUSIONS

Variations in clay mineralogy with environments of deposition, stratigraphy, and lithology can result from four factors: variations in detrital influx influenced by provenance and transporting agencies; physical sorting of clays by particle size resulting from differential settling and/or flocculation; chemical changes in the depositional environment; and diagenetic (all physical and chemical processes acting on sediments from time of deposition, excluding weathering) changes.

Whether clay assemblages were in equilibrium with their depositional and diagenetic environments or changed their properties, in a recognizable way, in response to their environments is a major concern of this report. Authigenic (formed in place) "...clay minerals reflect the material and energies of their genetic reactions, but clay rocks, i.e., mudstones, reflect also -possibly dominantly- the energies of the medium controlling their deposition..." (Keller, 1970). If a clay found here did not form here, then "...it may be entirely invalid to infer or attempt to infer, the environment of the site of deposition from the characteristics of the clay mineral which, in truth, reflect only the first environment of its site of genesis." When a distinction cannot be made between clay minerals "formed here" and those "found here", "...almost any or all kinds of

clay minerals may occur in any major depositional environments..." (Keller, 1970). Obviously, care should be taken when using clay mineralogy to interpret environments of deposition, and should only be used in conjunction with additional environmental indicators.

Some geochemical constraints on the formation of clays include temperature, pressure, pH, Eh, concentrations of metallic ions, and concentrations of alumina and silica (as ions, polymorphs, complexed soluble compounds, etc.). Time is also an important constraint affecting the alteration of clays. For instance, the smectite-to-illite conversion proceeds rapidly given ideal geochemical conditions (particularly adequate potassium), but may take millions of years otherwise (Keller, 1970).

If clay assemblages are used for environmental indicators, it must be shown that changes in clay mineral assemblages are not the result of depth-dependent diagenesis. Hower and others (1976) documented depth-dependence of clay and whole rock mineralogy in Gulf Coast sediments. With increasing depth (from 2000-3500m), illite and regular mixed layer contents increased, while smectite and potassium feldspar contents decreased. Other workers (Heling, 1978; Shutor, 1969; Burst, 1969) have found similar relations, with variations in depth of occurrence dependent on the geothermal gradient. Sediments of the study area are restricted to a relatively narrow, conformable stratigraphic interval, with maximum burial

depths of 1300m for the Upper Mancos Formation. The virtual absence of regular mixed layers and large (50 percent or more) illite concentrations, and presence of abundant smectite and potassium feldspars in the <1 micron fractions also indicate that strata was not deeply buried.

Evidence has accumulated against chemical alteration of clays at or near the depositional interface. Gibbs (1977) studied 150 Atlantic Ocean bottom samples near the Amazon River, ranging up to 1400 km from the shelf, and concluded "...the dominant mechanism responsible for the laterally changing composition of the clay minerals" was "...physical sorting of sediments by size." Whitehouse and McCarter (1958) stored kaolinite and illite in sea water for five years with no detectable changes. MacKenzie and Garrels (1966) estimate that only 7 percent of ocean sediments are authigenic material. Helgeson and MacKenzie (1970) calculate that reaction rims on detrital minerals are very thin before burial. Rhoton and Smeck (1981) found no significant changes in basal spacings of predominantly illitic soil clays for 217 days in the Auglaize River, Ohio, and concluded that "...mineralogic differences between soils in the watershed and sediments in the drainage system cannot be attributed to mineralogic transformation during residence in the drainage system." However, Keller (1970) states that, "...clay may be a stable or equilibrium product of the reaction, or alternatively, the clay may be a metastable form controlled by the reaction rate." Thus, alterations

may involve geologic periods and be accomplished only on diagenesis. Whether environments of deposition and diagenetic environment are independent controlling factors presents a potential problem. However, environments of deposition usually appear to control chemical environments of diagenesis, particularly in clay assemblages within and surrounding coals.

The results and conclusions are split into seven sections. The first section discusses the general clay mineralogic variations and some factors responsible for them. The second is concerned with relative particle sizes as determined from the clay fraction splits. The third section discusses stratigraphy vs. clay mineralogy using the whiteprint (Appendix 8). The fourth section relates clay mineralogy to lithology (carbonaceous vs. barren mudstones and shales). The fifth section concerns coal ash results. The sixth section discusses chemistry of some relatively pure smectites. The last section concerns a lateral clay study performed in the upper Menefee Formation below the La Ventana Sandstone.

Clay Mineral Assemblages

Based on peak areas and heights, Menefee and Mancos Formation clay fraction samples generally show high relative abundances of mixed-layer illite-smectite, followed by kaolinite, smectite, illite, and locally chlorite (in

order of decreasing relative abundance). Upper Menefee strata are an exception, showing relatively greater illite than smectite concentrations. The Fruitland Formation is dominantly composed of smectite, with some random mixed layers present in most samples. Kaolinite, illite, and chlorite may be present in small quantities.

Large differences between the clay mineralogy of the Fruitland and Menefee Formation samples may be caused by various factors, such as changes in distance to source, lower stream gradients, environments of deposition (and diagenesis), hydrothermal alteration, and/or provenance. Deposition of smaller clay fractions, favoring smectite and random mixed layers, could result from increased distance to the source and lower stream gradients, but not to the point of excluding other clays such as illite and kaolinite. Fruitland environments of deposition were probably not sufficiently different from those of the Menefee to account for the extreme contrast in clay mineralogy. No evidence of igneous intrusions, contact metamorphism or major disturbance of bedding, which should accompany hydrothermal alteration exists. The only plausible explanation by process of elimination appears to be a change in provenance. If the direction of sediment supply changed to the northwest (Lindsay, oral communication, 1982), a volcanic ash source might be expected, since the Laramide orogeny was occurring in Colorado during latest Cretaceous times. Virtually pure Fruitland smectites, showing compositional differences

(increased interlayer calcium) from the Menefee smectite-bearing clays, may indicate a volcanic ash source for the Fruitland. However, this finding is preliminary and further study is recommended.

Clay mineralogy and chemical analysis reveal that exchange of calcium and sodium occurred locally within smectite interlayers. Calcium smectites often cluster (TW-C3-10.4-TW-C3-21.7, TW-C2-115.5-TW-C2-122.3) and/or appear together with sodium smectites. Smectite compositions could reflect cation exchange with any of the following: the transporting fluids, the environment of deposition, the diagenetic environment and/or the near-surface weathering environment. Thus, smectites are not reliable indicators of environments of deposition.

Relative Particle Sizes

Average clay mineralogy for various Torreon clay fractions (Appendix 6C) shows that clay mineralogy is a function of particle size. Kaolinite and chlorite show tendencies to be concentrated in the <8 micron fraction and decrease gradually as fractions become smaller. Illite shows a gradual decrease in relative abundance as particle size decreases, except for Upper Mancos samples which prefer the <0.5 and <0.25 micron fractions. Smectite increases from <8 to <1 micron fractions and from <1 to <0.1 micron fractions, but shows no significant preferences between <2

microns and <0.25 micron fraction ranges.

Mixed layers generally increase with decreasing particle size. Mancos Shale samples in the <0.5 and <0.25 micron fractions were exceptions, with the <0.5 fraction decreasing and the <0.25 fraction remaining constant. The lower mixed-layer values for the <0.5 micron fraction were attributed to increase in illite, which prefers the <0.5 micron fraction.

Average clay mineral particle size distributions for both members of the Menefee, deduced from clay mineralogy of various size fractions, from largest to smallest were:

- 1) kaolinite,
- 2) chlorite,
- 3) illite and smectite (both approximately the same),
- 4) mixed-layer illite-smectite.

Two <0.25 micron fractions, and one <0.1 micron fraction were prepared from the Fruitland Formation. Averages of the two samples reveal that from the <1 micron to the <0.25 micron fraction kaolinite and chlorite values remained unchanged, while illite decreased and mixed layers increased. The <0.1 micron fraction shows little difference from the <0.25 micron fraction.

Stratigraphic Variations in Clay Mineralogy

The following discussion relates to Appendix 8, which illustrates vertical stratigraphic variations vs.

clay mineralogy. Appendix 6D gives average mineralogic compositions above and below coals.

Concentrations of illite that are larger than in surrounding strata often occur directly below sandstones. These relatively large concentrations of illite persist down-section until coals or carbonaceous strata occur, and indicate a transition from marine to terrestrial environments (Brown and others, 1977). In the marine environment illite is stable, since high potassium-to-hydrogen concentrations exist. As brackish water conditions give way to fresh water shoreward, potassium-to-sodium and potassium-to-magnesium ratios decrease and smectite or chlorite becomes stable (Weaver and Pollard, 1973). Illite to kaolinite conversion could occur if the potassium-to-hydrogen ratio is sufficiently low, if the dissolved silica species approach saturation with respect to quartz (Keller, 1970), or if sodium, iron, and magnesium content is insufficient for smectite and chlorite formation.

One alternative explanation to chemical alteration in the environment of deposition for variations in clay mineral assemblages would be differential flocculation, influenced by salinity and varying settling rates for kaolinite, illite, and smectite. Edzwald and O'Melia (1975) have shown that in Recent sediments of the Palimo River Estuary, North Carolina, kaolinite and illite distributions can be explained by "considering the combined

effects of flocculation rates and settling." Since illite undergoes particle aggregation at a slower rate than kaolinite and montmorillonite, and aggregates faster when salinity increases, preferential deposition of illite would occur in estuaries, while kaolinite would be preferentially deposited upstream in fresh water.

Examples of both smectite-to-illite, and illite-to-kaolinite reactions as illustrated by vertical mineralogic changes were observed. In several samples below sandstones (TW-C1-153.4 and TW-C5-95.8), high illite and low smectite content relative to surrounding shales probably indicates conversion of smectite to illite in a potassium-rich brackish water environment, while abundant kaolinite and low illite content in other samples (TW-C3-64.2, TW-C5-38.6, and TW-C5-128.1) reveal a fresh water, lower pH, potassium-deficient aqueous environment.

Smectite to illite conversion reactions and chemical results may imply a dual source yielding two distinct types of smectite. Keller (1970) states that smectites derived from degraded mica or illite return to illite or chlorite in sea water (and presumably any potassium or magnesium-rich fluids) by taking up potassium or magnesium, but smectite derived from framework silicates or volcanic ash is relatively stable at or near the marine depositional interface. The smectites contained in some samples (TW-C1-153.4) have converted to illite and others (TW-C5-19.2) have not.

Except for core 1 (which is carbonaceous throughout and shows no trend), kaolinite increases from directly above to directly below coals. This is due to the presence of underclays, which usually display increased kaolinite content. Numerous opinions exist concerning the origin of underclays. They have been interpreted as fossil soils, transported sediments (with or without subsequent diagenetic alterations), or strata formed in place resulting from poor drainage and weathering (Parham, 1965). Slickensided, homogenous, kaolinite-rich underclays, lacking old soil profiles, but similar in clay mineral content to many San Juan samples, have been reported in Illinois and suggest a detrital origin, which resulted from flocculated clay masses with kaolinite acting as a nucleus (O'Brien, 1964). Subsequent diagenetic alteration of illite to kaolinite was probable, since many carbonaceous shales also show kaolinite increases below coals.

Illite generally decreases from above to below coals (Appendix 6D). Smectite increases below coals in the Menefee Formation, but shows the opposite trend in the Mancos Shale and Fruitland Formation samples. Mixed layers increased slightly below Menefee coals, but decrease sharply below coals of the Upper Mancos Shale. Changes in clay mineral assemblages from above to below coals reflect depositional and diagenetic environments, mainly below coals, which vary considerably, as discussed in the coal ash section.

Reactions generally do not proceed to completion, as illustrated by shales containing clay assemblages rather than one (or several) stable type(s) of clay; i.e., illite and kaolinite would not be expected to be found together if reactions were complete. Restricted pore-water circulation and rapid burial account for incomplete reactions. Large amounts of ferric iron (hematite) in ironstone concretions associated with carbonaceous strata were surprising, since ferrous iron would be expected in a reducing environment. "Restricted pore-water circulation (low porosity) obviously would favour the preservation of ferric iron from reduction..." (Curtis and Spears, 1971).

Lithologic Variations in Clay Mineralogy

Lithologies were subdivided visually on the basis of organic content as determined by color, carbonaceous plant material, and coal fragments. Mineralogy for three general groups, including carbonaceous, intermediate, and barren strata, were averaged for each formation (Appendix 6A).

Average whole rock and clay fraction (<1 and <2 micron) mineralogy, by formation or member, was used to calculate average percent mineralogic changes from carbonaceous to barren (plus intermediate) strata (Table 5). The formula employed was: $((\text{Carb}-\text{Bar})/\text{Bar}) * 100\%$, where Carb = mineral content averages for carbonaceous strata, and Bar = weighted mineral content averages for intermediate plus

barren strata.

TABLE 5 ENRICHMENT/DEPLETION* OF MINERALS IN
CARBONACEOUS SHALES RELATIVE TO BARREN SHALES

FORMATION	N	QTZ	FELD	KAOL	ILL	SMCT	MIXED
UPPER MENELEE	15-19	-5	-55	15	-20	10	0
CLEARY	12-17	20	-40	15	-25	-10	20
MANCOS	11-14	0	-40	40	-15	35	-25

* POSITIVE AND NEGATIVE VALUES REPRESENT ENRICHMENT AND DEPLETION, RESPECTIVELY, EXPRESSED TO NEAREST FIVE PERCENT N (X-Y) = THE NUMBER OF SAMPLES, WHERE:

X = CARBONACEOUS SAMPLES Y = BARREN SAMPLES

Whole rock results show that quartz content increased in carbonaceous strata of the Cleary Member of the Menefee, but quartz content did not vary significantly between carbonaceous and barren strata in other formations. Feldspar, unstable in acidic swamp environments, breaks down to form either illite or smectite (depending on metallic ion concentrations) (Weaver and Pollard, 1973).

Clay fraction results indicate substantial differences in clay mineralogy between carbonaceous and barren strata. Factors influencing percent increases or

decreases include sorting of sediments by size and chemical environments of deposition and diagenesis. Variations in detrital influx probably occur, but did not extensively affect lithologic comparisons; values represent averages, and it is unlikely that provenance or transportation mechanisms were significantly different in contemporaneous strata. Illite to kaolinite alteration (especially in the Mancos) in carbonaceous strata, as illustrated by kaolinite increase and illite decrease, was significant. Smectite increases and feldspar decreases for the Mancos and upper Menefee indicate that sodium feldspar converts to sodium smectite in carbonaceous strata. Smectite decrease and mixed-layer increase in the Cleary, accompanied by increases in average percent expandable mixed layers (Appendix 5B), may reveal episodes in which smectite species were converting to mixed layers.

Coal Ash Mineralogy

Coal ash samples invariably show relatively large kaolinite contents. Kaolinite reflections in coal ash samples are very sharp and intense relative to those in shales and appear similar to authigenic kaolinite reflections commonly found for sandstones (Mannhard, 1976). Kaolinite in some coals, which tended to have low ash contents (TW-C1-165.0, TW-C3-63.5, and TW-C3-108.4), was definitely authigenic. Authigenic kaolinite has also been

reported by Gluskoter (1967) in Illinois coal ash. A whitish clayey material was observed filling desiccation cracks and cleats (not parallel to bedding) in some Torreon coals. Ash from these coals upon analysis yielded almost pure kaolinite. Oxygen isotope studies for authigenic kaolinite, occurring as cleat fillings in Illinois coals, reveal that temperatures of formation for kaolinite were 24-30 degrees centigrade, suggesting formation "at or near the surface perhaps in fairly recent geologic time." (Shieh and Suter, 1979). Two coal ash samples (TW-C3-50.9 and TW-C1-59.0) contain abundant kaolinite, but show no change in illite (relative to surrounding shales). These findings suggest that much authigenic kaolinite resulted from precipitation after coal lithification, rather than in situ illite-to-kaolinite conversion.

San Juan coal ash samples with variable clay mineralogy reveal that chemical environments of coal deposition range widely. The presence of illite in some samples, but not others, indicates a range of potassium-to-hydrogen ratios including both illite and kaolinite stability fields. The presence of chlorite in five of eight samples was surprising, since chlorite was believed to be unstable in fresh-water coal swamp environments (Gluskoter, 1967). Relatively high iron (pyrite was present in two samples) and magnesium contents occur in some environments. It was impossible to quantify how much kaolinite resulted from illite alteration, but since this

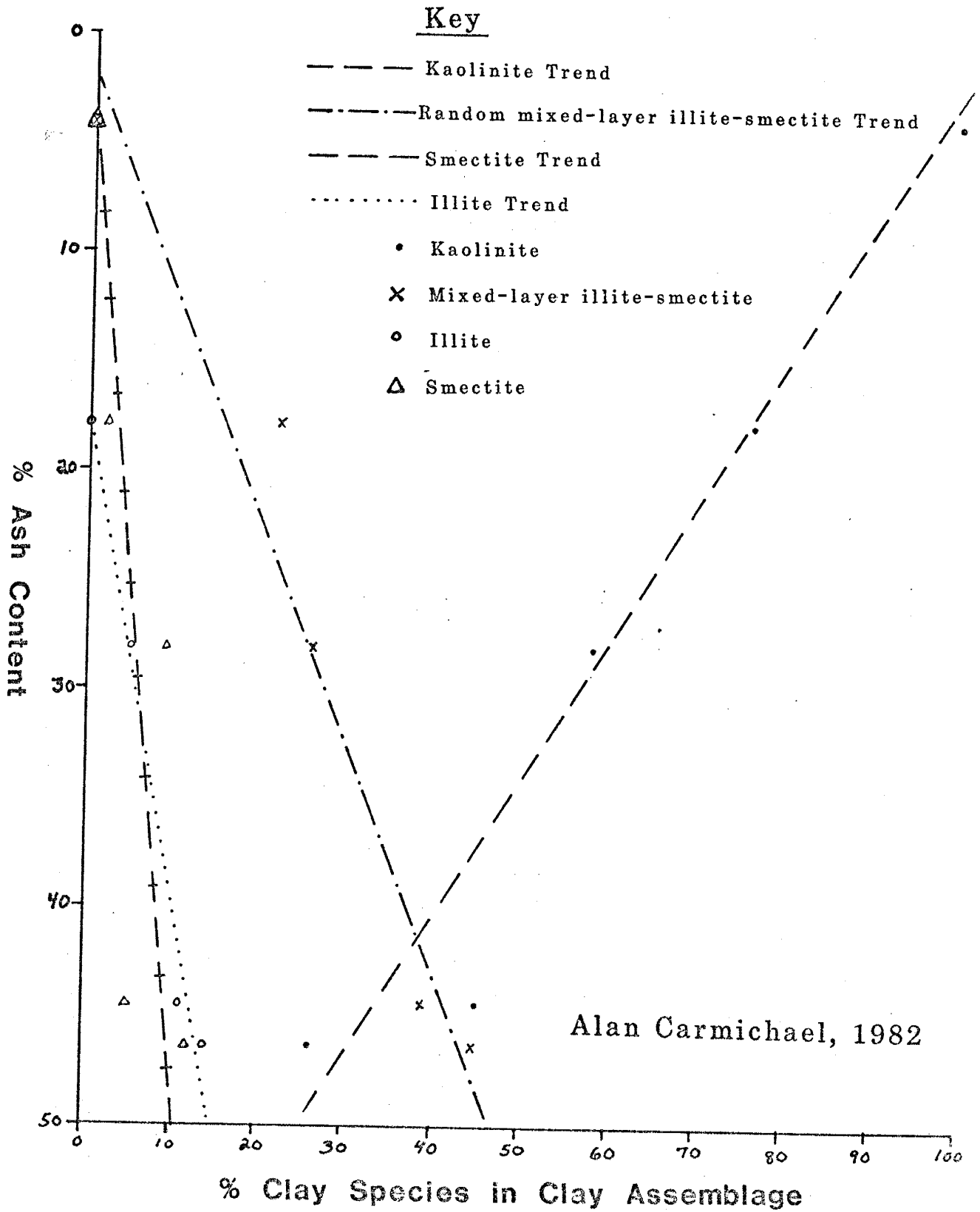
reaction was noted in the carbonaceous shales, it was very likely to proceed in the coals. However, thin dirt partings in French coal seams contained 90 percent or more illite. "These results certainly do not support the hypothesis of kaolinization of illite in the swamp environment." (Bouroz, 1964, as reported in Curtis and Spears, 1971).

Clay mineralogy shows a correlation to the ash content of coal for Menefee Formation samples. Percent ash content vs. relative abundance of individual clay species was plotted (Figure 9). For kaolinite, four out of five samples fall on virtually a straight line. The fifth sample (TW-C1-59.0) contained organics after 90 hours of ashing, and had these been considered the sample would have fallen on line. The linear relation between ash content and clay mineralogy can be explained by the presence of both detrital and authigenic clay minerals. As the ash content decreases the percentage of detrital clays decreases linearly, but the percentage of authigenic clays remains nearly constant. This relation gives a straight line with a positive slope for kaolinite, since virtually all the authigenic material is kaolinite (with the possible exception of some chlorite). The detrital clays yield a straight line with a negative slope showing the opposite trend of the authigenic clays.

Pyrite and microcline occurred together in two Menefee Formation coals (TW-C1-59.0 and TW-C5-37.8), both of which contained large quantities of ash. Small euhedral

Figure 9

% ASH CONTENT vs. % CLAY SPECIES
FOR MENELEE COALS



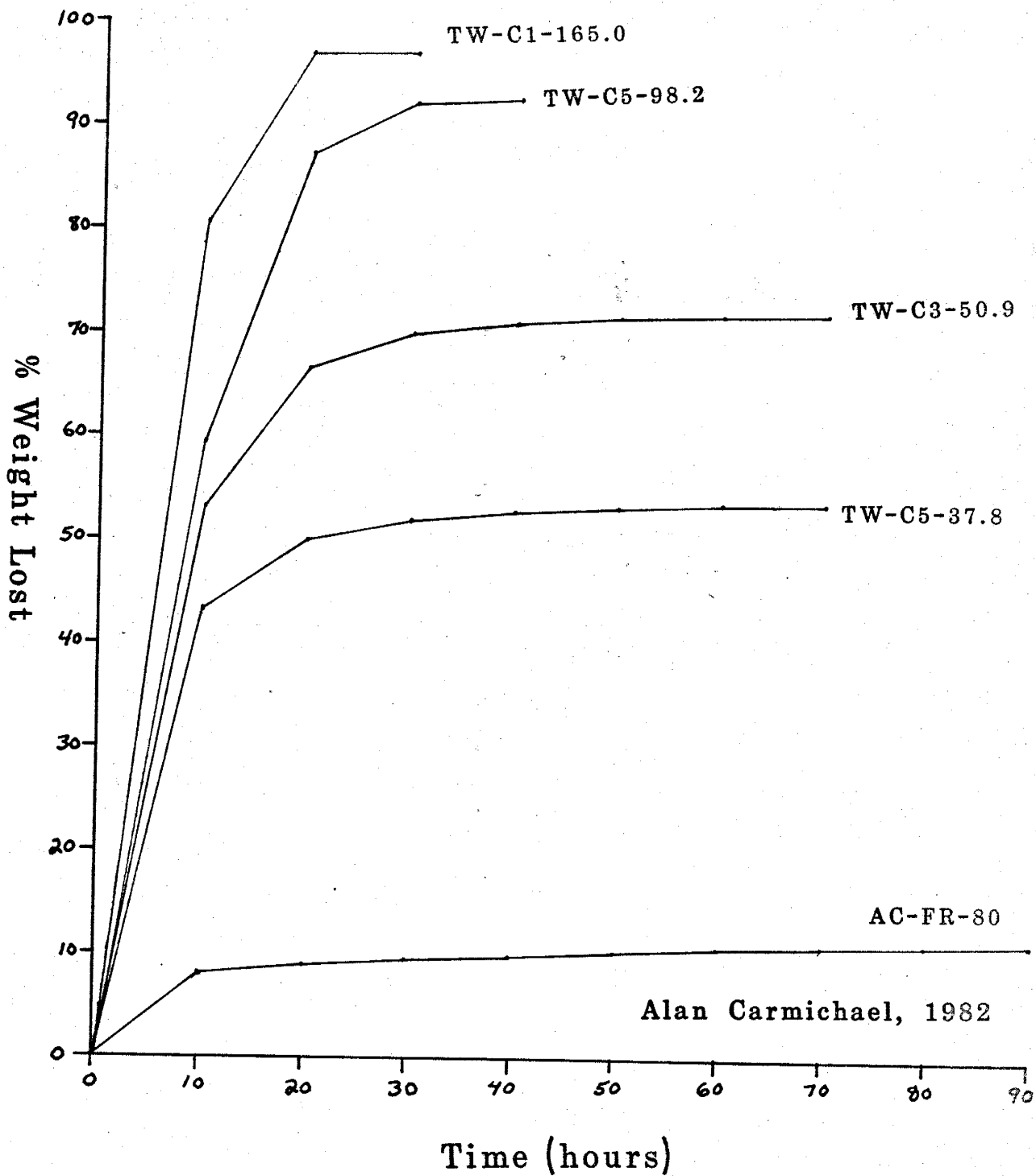
pyrite crystals forming along bedding planes indicate a reducing environment of deposition. Sulfur contents of coals were low (Tabet and Frost, 1979) and probably limited the amount of pyrite precipitation that could occur. Quartz was detected in all samples, but was unrelated to ash content. Counts per second for non-clay minerals are listed in Table 6.

Coals of the Mancos Shale (TW-C4-172.8, TW-C3-108.4, and TW-C5-98.2) all had high losses on ashing (92 percent or more) and similar clay mineralogy. Mancos coal ashes were high in kaolinite content relative to shales, but not as high as Menefee coals with equivalent weight losses. All Mancos ashes contained kaolinite, mixed layers, chlorite, and smectite. Average relative abundances were: chlorite = 3, kaolinite = 54, illite = 3, smectite = 15, and mixed-layer illite-smectite = 25.

Differences between coal ashes of the Mancos Shale and Menefee Formation probably reflect environments of deposition. Mancos coals possibly were deposited in brackish water marshes instead of fresh-water swamps as in the Menefee, so kaolinization was partly inhibited by greater concentrations of metallic ions. This would be expected in an intermediate transition zone between continental and marine strata.

A relationship between time ashed and percent weight loss was noticed (Figure 10), with smaller weight losses requiring more time to ash. One might expect the opposite

Figure 10 - %Weight Lost vs Time Ashed



relation to occur; however, the ash content retards the escape of volatiles, particularly when interlayer organics occur in smectites and/or mixed layers. A carbonaceous shale sample (TW-C3-57.4) showed substantial increase in mixed layers and some increase in smectite after removal of organics by EDTA. Before addition of EDTA the larger organic-rich mixed layers settled out, but upon removal of the organics more mixed layers remained in the clay fraction.

When several extremely carbonaceous shales (AC-TW-1, and AC-FR-80) were ashed, they had unusually high contents of mixed layers compared to the surrounding strata. Sample AC-TW-2, a mixture of peat and shale, ("humate" of Siemers and Wadell, 1977) was considerably less dense and more organic rich than "normal" shales and contained many organics after ashing, which were removed with EDTA. Analysis yielded relatively high kaolinite and illite values and relatively low mixed-layer and smectite values.

TABLE 6 NON-CLAY MINERALS OF THE COAL ASH SAMPLES
(EXCLUDING CARBONACEOUS SHALES)

SAMPLE NUMBER	TOTAL LOSS (PERCENT)	QUARTZ (CPS)	MICROCLINE (CPS)	PYRITE (CPS)
TW-C1-59.0	55.61	1300	250	1100
TW-C1-165.0	96.95	1350		
TW-C3-50.9	71.95	1650		

TW-C3-63.5	82.19	3950		
TW-C3-108.4	96.02	1000		
TW-C4-172.8	94.15	900		
TW-C5-98.2	92.66	2550		
TW-C5-37.8	53.67	1325	225	375

Chemistry of Some Relatively Pure Smectites

Recast chemical analysis (see Appendix 7 for procedure) of a relatively pure sodium smectite (AC-FR-76) from the Fruitland Formation, in terms of its structural formula, shows a total interlayer charge of 0.738 (Table 7), with calcium and potassium substituting for interlayer sodium. Magnesium and possibly ferrous iron substitute for aluminum in the octahedral layer to create a charge deficiency of 0.280. Ferric iron substitutes for aluminum in the octahedral layer, but does not affect the charge balance. Small amounts of titanium and manganese occur in the octahedral layer. Some substitution of aluminum for silica, evident in the tetrahedral layer, creates a charge deficiency of 0.340. Total (TOT) charge is -0.604, and total interlayer charge is 0.738, giving an excess positive charge of 0.134. This result is probably due to ferrous iron substitution in the octahedral position, which, if considered, would increase octahedral charge deficiency and balance interlayer charge excesses. Whole rock analysis yields 1 percent quartz, with the remaining portion composed

of almost pure smectite, indicating a bentonite layer.

Sample AC-FR-73 shows a higher amount of tetrahedral aluminum substitution (0.531) than AC-FR-76, lower octahedral magnesium (0.183), higher octahedral iron (0.345), and higher interlayer sodium (0.719). The overall effect is higher interlayer and TOT charges. The charges for this sample do not balance either, with an excess of 0.132. Again, this imbalance is probably due to ferrous iron substitution in the octahedral layer.

Recast analysis of sample TW-C5-19.2 (<0.25 micron fraction) shows extensive substitution in both the octahedral and tetrahedral layers, which attracts a large amount of interlayer cations. Octahedral charge seems to be due exclusively to magnesium(+2) substitution. Ferric iron also substitutes in the octahedral layer. Sodium(+1) is the dominant interlayer cation, with some potassium(+1) and calcium(+2) present. Layer and interlayer charges balance perfectly, although they are both relatively high (-0.804 and 0.804), because the sample is a mix of smectite and random mixed-layer illite-smectite.

TABLE 7 RECAST CLAY ANALSES

RECAST CLAY ANALYSIS OF SAMPLE TW-C5-19.2 <0.25

TETRAHEDRAL

SI = 3.558

LAYER CHARGE

AL = .442

TOTAL TET. = 4.000

TETRAHEDRAL = -0.442

OCTAHEDRAL

OCTAHEDRAL = -0.362

TI = .012

TOTAL TOT = -0.804

AL = 1.455

INTERLAYER = 0.804

FE = .160

DIFFERENCE = 0.000

MG = .374

MN = .000

TOTAL OCT. = 2.001

INTERLAYER

CA = .047

NA = .620

K = .090

TOTAL INT. = .757

EXPLANATION

1) First it is assumed based on x-ray diffraction data that the structure is smectite plus mixed-layer smectite-illite. This means that the resulting recast is a average structural formula for the two.

2) It is assumed that all of the silica goes into the tetrahedral site, which has four positions, with only 3.558 of them filled with silica. The remaining 0.442 sites are assumed to be filled with aluminum.

3) The remaining aluminum is assumed to fill 1.455 octahedral sites. Titanium, iron, magnesium, and manganese also go into octahedral sites.

4) Sodium, potassium, and calcium occupy the interlayers.

5) Charge deficiencies occur in the tetrahedral and octahedral sites and are compensated for by interlayer charges. The total net charge should be zero.

6) The next two samples were done the same way, except AC-TW-73 <1 is a relatively pure smectite. The TOT and the interlayer charges do not balance on these samples since some of the iron is in the +2 oxidation state in the octahedral layer. The charge difference should be roughly equivalent to the amount of Fe(+2) present.

RECAST CLAY ANALYSIS OF SAMPLE AC-FR-73 <1

TETRAHEDRAL

SI = 3.469

AL = .531

OCTAHEDRAL

TI = .023

AL = 1.403

FE = .345

MG = .183

MN = .002

INTERLAYER

CA = .044

NA = .719

K = .018

LAYER CHARGE

TOTAL TET. = 4.000

TOTAL OCT. = 1.956

TOTAL INT. = .781

TETRAHEDRAL = -0.531

OCTRAHEDRAL = -.0162

TOTAL TOT = -0.693

INTERLAYER = 0.825

DIFFERENCE* = 0.132

RECAST CLAY ANALYSIS OF SAMPLE AC-FR-76 <1

TETRAHEDRAL

SI = 3.660

AL = 0.340

OCTAHEDRAL

TI = 0.018

AL = 1.429

FE = 0.227

MG = 0.280

MN = 0.002

INTERLAYER

CA = 0.076

NA = 0.524

K = 0.062

TOTAL TET. = 4.000

TOTAL OCT. = 1.956

TOTAL INT. = 0.662

LAYER CHARGE

TETRAHEDRAL = -0.340

OCTAHEDRAL = -0.264

TOTAL TOT = -0.604

INTERLAYER = 0.738

DIFFERENCE* = 0.134

* - PROBABLY DUE TO
OCTAHEDRAL FE(+2)

Lateral Clay Studies (Upper Menefee)

A lateral clay study was completed for upper Menefee Formation mudstones and shales beneath the La Ventana Sandstone. The attempt was difficult because the majority of mudstones and shales in the vicinity are not laterally continuous for more than 50-100 feet. A few beds were found that continued for a quarter of a mile or more, and these were sampled. The cliff face along which samples were collected is pictured in plate 9, and a small map (Figure 11) is given showing sample locations.

Samples AC-TW-2, AC-TW-4, and AC-TW-8 were collected from the same bed at stations I, II, and III, respectively. These coaly brown carbonaceous shales were sampled directly above a coal bed. At station I the coal bed consists of about 20 feet of interbedded peats, carbonaceous shales, and humates with a lens of sandstone near the top. These layers grade laterally into a black bituminous coal at stations II and III, where a well developed sandstone bed intervenes between coal and overlying carbonaceous shales. Another laterally continuous bed, consisting of a coaly brown carbonaceous shale, was sampled below the coal bed and is represented by samples AC-TW-1, AC-TW-3, and AC-TW-10 at stations I, II, and III, respectively. The La Ventana and Cliff House Sandstones pinch out several hundred feet to the north, so the Lewis Shale lies directly on the sediments of

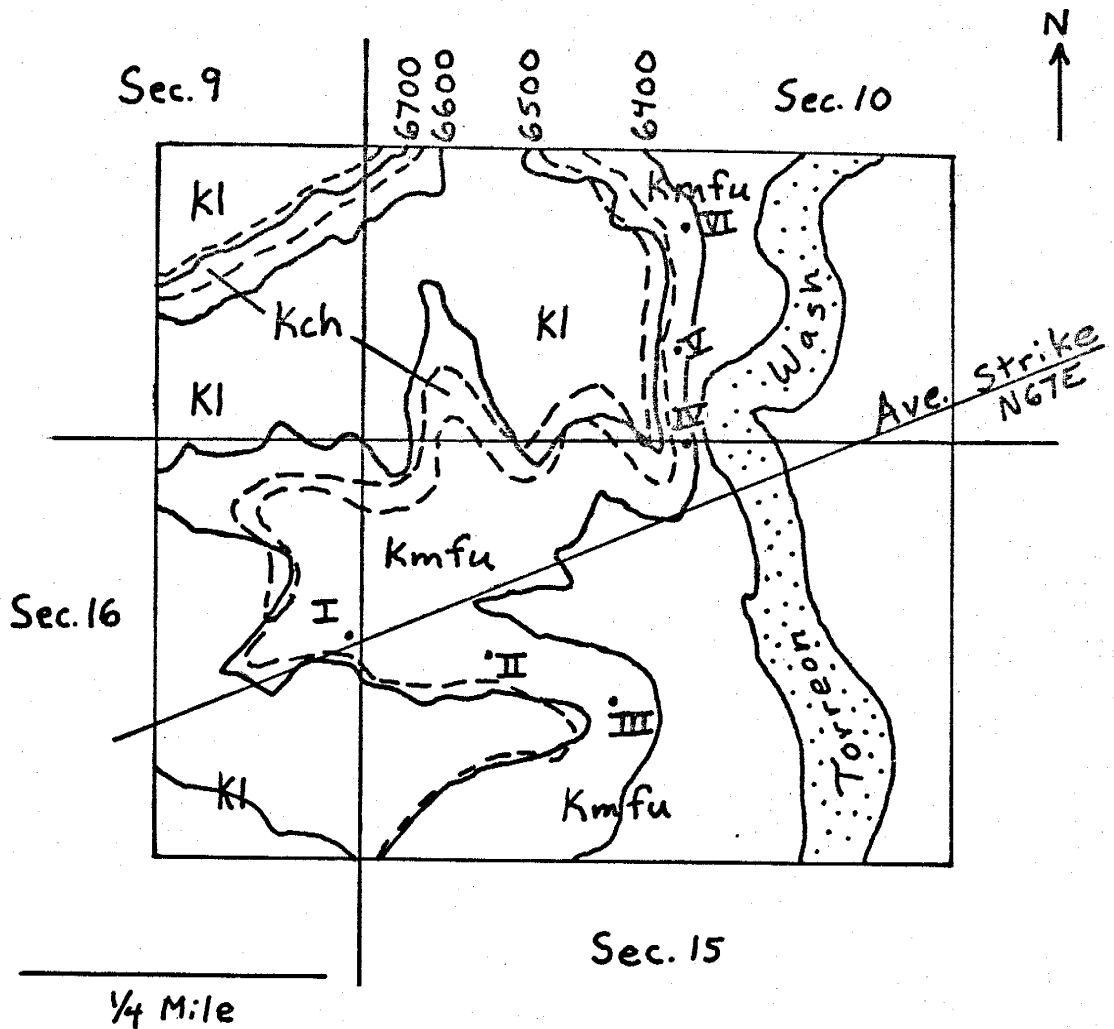


Figure 11 - Sample locations for lateral study

Legend

- | | | | |
|-------|-----------------------|------|------------------|
| --- | Formation Contacts | I-VI | Sample Locations |
| ~~~~~ | Contour Lines | | |
| KI | Lewis Shale | | |
| Kch | Cliff House Sandstone | | |
| Kmfu | Upper Menefee | | |

the upper Menefee Formation.

Stations II and III were used as controls to see how clay mineralogy changes as the coal pinches out at station I. Results for the bed above the coal show that kaolinite increases and mixed layers decrease where the coal pinches out. This was attributed to a slight (5 percent) increase in quartz content and indicates that mechanical sorting by grain size was the dominant factor above the coal. Results for the bed below the coal show that kaolinite decreased and mixed layers increased as the coal pinched out, in spite of an 11 percent increase in quartz content. As strata became less carbonaceous where the coal pinched out, the potassium-to-hydrogen ratio increased until kaolinization of illite was inhibited.

The next group of Menefee Formation samples was taken below the La Ventana Sandstone. Samples AC-TW-26 and AC-TW-32 were both sampled from the same bed at stations IV and V, respectively. The bed occurs about two feet below a black bituminous coal and consists of brown carbonaceous shale that gets siltier to the north. The only significant change in clay mineralogy was a slight increase in kaolinite and a slight decrease in mixed-layer material as the silt content increased. Two additional samples, taken at stations V and VI (AC-TW-34 and AC-TW-40) from silty gray shale to mudstone, also show an increase in kaolinite and a decrease in mixed layers as silt content increases. Results reveal that mechanical separation of clays, dependent on

particle size, energy regimes, and settling rates, was the dominant factor in determining lateral changes in clay mineralogy for shales and mudstones not directly below coals (or very carbonaceous).

Summary of Results

1) Dominant Menefee Formation and Mancos Shale clay assemblages in order of decreasing relative abundance include random mixed-layer illite-smectite, kaolinite, smectite, and illite, locally with chlorite. The Fruitland Formation, containing dominantly smectite and random mixed-layer illite-smectite, probably reflects a change in source to dominantly volcanic ash.

2) Sodium and/or calcium-rich smectites were present in all formations, but cannot be used as environmental indicators because cation exchange could occur at any stage in their genesis.

3) San Juan clay mineralogy is a function of particle size. Kaolinite, and chlorite were concentrated in the larger clay fraction (<8 microns); illite was abundant in the medium clay fractions (<2, <1, and <0.5 microns); and random mixed layers and smectite dominate the smaller fractions (<0.25 and <0.1 microns).

4) Stratigraphic studies show relatively large illite concentrations below sandstones, which persist down-section until interrupted by coals or carbonaceous strata and indicate illite stability in brackish waters. Kaolinite

increases and illite decreases in shales and mudstones from above to below coals reflected kaolinization of illite in reducing, acidic, fresh-water, swamp environments. Examples of both smectite-to-illite and illite-to-smectite reactions as illustrated by vertical mineralogic changes were observed.

5) Lithologic comparisons of average carbonaceous and barren strata reveal that feldspars and illite, unstable in the carbonaceous strata, converted to illite and/or smectite and kaolinite, respectively.

6) Coal ash samples invariably show relatively large kaolinite contents, due to detrital clay recrystallization and/or diagenetic dissolution and precipitation prior to and/or after lithification. Variable illite content reveals that the acidic coal swamp environment spans both illite and kaolinite stability fields. For Menefee samples, percent ash content correlates with percent clay species. Kaolinite increases and illite, smectite, and mixed layers decrease with decreasing ash content. Volatile loss was greater for coals with smaller ashing times, since organic removal in smectite and mixed-layer clays was difficult. Brackish-water Mancos coal ashes contained less kaolinite than fresh-water Menefee coals with similar ash contents, since kaolinization was inhibited by metallic ions.

7) Two recast chemical analyses of relatively pure smectites from the Fruitland and one from the Cleary reveal high interlayer charges (0.74-0.83 per 1/2 unit cell), extensive iron (0.16-0.35) and magnesium (0.18-0.37) substitution for aluminum in the octahedral layer, large amounts of aluminum (0.35-0.53) substitution for silica in the tetrahedral layer, and some calcium (.04-.08) and potassium (0.02-0.09) substitution for sodium in the interlayers.

8) Lateral clay studies in Upper Menefee carbonaceous shales revealed that as coal pinched out, kaolinite decreased and mixed layers (and quartz) increased below coal, while kaolinite (and quartz) increased and mixed layers decreased above coal. In shales underlying coals kaolinization of illite occurred, while in shales above coal mechanical sorting of sediments by size was the dominant factor in controlling clay mineral assemblages.

9) Provenance, mechanical sorting of clays during transport, flocculation properties, environments of deposition, and diagenetic changes all influence variations in clay mineralogy.

REFERENCES CITED

- Austin, G.S. and Leininger, R.K., 1976, The effect of heat-treating sedimented mixed-layer illite-smectite as related to quantitative clay mineral determination: *Jour. Sed. Pet.*, v. 46, p. 206-215.
- Bailey, S.W., 1972, Determination of chlorite compositions by x-ray spacing and intensities: *Clay and Clay Minerals*, v. 20, p. 381-388.
- Bauer, C.M., 1916, Stratigraphy of a part of the Chaco River Valley: U.S.G.S., Prof. Paper 98, p. 274.
- Bauer, C.M., and Reeside, J.B., Jr., 1921, Coal in the middle and eastern parts of San Juan County, New Mexico: U.S.G.S., Bull. 716, p. 34.
- Beaumont, E.C., Dane, C.H., and Sears, J.D., 1956, Revised nomenclature of Mesaverde Group in San Juan Basin: A.A.P.G., Bull., v. 40, p. 2149-2162.
- Beaumont, E.C., and Shomaker, J.W., 1974, Upper Cretaceous coal in the Cuba-La Ventana-Torreon area, eastern San Juan Basin, New Mexico: *New Mex. Geol. Soc., guidebook 25th field conf.*, p. 329-345.
- Bodine, M.W., Jr. and Fernald, T.H., 1973, EDTA dissolution of gypsum, anhydrite, and Ca-Mg carbonates: *Jour. Sed. Pet.*, v. 43, p. 1152-1156.
- Brown, G., ed., 1961, The x-ray identification and crystal structure of clay minerals: Mineralogical Society (Clay Minerals Group), London, 544 p.
- Brown, L.F., Jr., Bailey, S.W., Cline, L.M., and Lister, J.S., 1977, Clay mineralogy in relation to deltaic sedimentation patterns of Desmoinesian cyclothems in Iowa-Missouri: *Clays and Clay Minerals*, v. 25, p. 171-186.
- Burst, J.F., 1969, Diagenesis of Gulf Coast clayey sediments...: *Am. Ass. Pet. Geol.*, v. 53, p. 2013-2021.
- Butler, R.F., Lindsay, E.H., Jacobs, L.L., and Johnson, N.M., 1977, Magnetostratigraphy of the Cretaceous-Tertiary boundary in the San Juan Basin, New Mexico: *Nature*, v. 267, p. 318-323.
- Carroll, Dorothy, 1970, Clay minerals: a guide to their identification: G.S.A., Spec. Paper 126, 80 p.
- Collier, A.J., 1919, Coal south of Mancos, Montezuma

- County, Colorado: U.S.G.S., Bull. 691, p. 296.
- Cross, and Whitman, 1899, U.S. Geol. Sur. Atlas, Telluride Folio (no. 57), p. 4.
- Curtis, C.D., and Spears, D.A., 1971, Diagenetic development of kaolinite: Clays and Clay Minerals, v. 19, p. 219-227.
- Czarnecka, E., and Gillott, J.E., 1980, Formation and characterization of clay complexes with bitumen from Athabasca oil sand: Clays and Clay Min., v. 28, No. 3, p. 197-203.
- Dane, C.H., 1936, The La Ventana-Chacra Mesa coal field: U.S.G.S., Bull. 860-C, p. 81-161.
- Dutton, C.E., 1885, Mount Taylor and the Zuni Plateau: U.S.G.S., 6th Annual Rept., 1884-85, p. 105-198.
- Edzwald, James K., and O'Melia, Charles R., 1975, Clay distributions in Recent estuarine sediments, Clays and Clay Minerals, v. 23, p. 39-44.
- Fang, J.H., and Bloss, F.D., 1966, X-ray diffraction tables: Southern Ill. Univ. Press, Carbondale.
- Fassett, J.E., and Hinds, J.S., 1971, Geology and fuel resources of the Fruitland Formation and Kirtland Shale of the San Juan Basin, New Mexico and Colorado: U.S.G.S., Prof. Paper 676, 76 p.
- Fassett, J.E., 1977, Geology of the Point Lookout, Cliff House and Pictured Cliffs Sandstone of the San Juan Basin, New Mexico and Colorado: New Mex. Geol. Soc., Guidebook 28th field conf., p. 193-197.
- Fellows, P.M. and Spears, D.A., 1978, The determination of feldspars in mudrocks using an x-ray powder diffraction method: Clays and Clay Minerals, v. 26 p. 231-236.
- Fischer, W.R., and Schwertmann, U., 1975, The Formation of hematite from amorphous iron(III) hydroxide: Clay and Clay Min., v. 23, p. 33-37.
- Fush-Parker, J.W., 1977, Alibi for a Mesaverde misfit-The La Ventana Formation Cretaceous delta, New Mexico: New Mex. Geol. Soc. Guidebook, 28th Field Conf., p. 199-206.
- Gardner, J.H., 1909, The coal field between Gallina and Raton Springs, New Mexico; in Coal fields of

- Colorado, New Mexico, Utah, Oregon, and Virginia:
U.S.G.S., Bull. 341-C, p. 335-351.
- Gardner, J.H., 1910, The coal field between San Mateo and
Cuba, New Mexico: U.S.G.S., Bull. 381-C,
p.461-473.
- Gibbs, R.J., 1965, Error due to segregation in quantitative
clay mineral x-ray diffraction mounting techniques:
Am. Min., v. 50, p. 741-751.
- Gibbs, R.J., 1968, Clay mineral mounting techniques for
x-ray diffraction analysis, a discussion: Jour.
Sed. Pet., v. 38, p. 242-244.
- Gibbs, R.J., 1975, Clay mineral segregation in the marine
environment: Jour. Sed. Pet., v. 47, p. 237-243.
- Gibbs, Ronald J., 1977, Clay mineral segregation in the
marine environment, J.S.P. Vol. 47, No. 1, p. 237-243.
- Gluskoter, H.J., 1965, Electronic low temperature ashing of
bituminous coal: Fuel, v. 44, p. 285-291.
- Gluskoter, H.J., 1967, Clay minerals in Illinois coals:
Jour. Sed. Pet., v. 37, p. 295-314.
- Grim, R.E., 1968, Clay mineralogy: McGraw-Hill, New York,
2nd ed., 596 p.
- Helgeson, H.C., and MacKenzie, F.T., 1970, Silicate-seawater
equilibrium in the ocean system: Deep Sea Res., v. 17,
p. 877-892.
- Heling, D., 1978, Diagenesis of illite in argillaceous
sediments of the Rhinegraben (southwest Germany):
Clay Min., v. 21, p. 463-472.
- Hinds, J.S., 1966, Geologic map of the Johnson Trading Post
Quadrangle, Sandoval County, New Mexico: U.S.G.S.,
Map GQ-591
- Hollenshead, C.T., and Pritchard, R.L., 1961, Geometry of
producing Mesaverde sandstones, San Juan Basin: in
"Geometry of sandstone bodies.", Peterson, J.A., and
Osmond, J.C., eds., A.A.P.G., Sumposium vol.,
p. 98-118.
- Holmes, W.H., 1877, Geologic report on the San Juan
District, Colorado: U.S. Geol. and Geog. Sur.,
Terr. 9th Ann. Rept., for 1875, p. 35.
- Hower, John, and Mowatt, T.C., 1966, The mineralogy of

illites and mixed-layer montmorillonites: Am. Min.
v. 51, p. 825-854.

Hower, John, 1974, Order of mixed-layering in illite/
montmorillonites: 15th Conf. on Clays and Clay
Minerals, p. 63-74.

Hower, John, Eslinger, E.V., Hower, M.E., and Perry, E.A., 1976,
Mechanism of burial metamorphism of argillaceous sediment:
1. Mineralogic and chemical evidence: G.S.A. Bull., v. 53,
p. 725-737.

Hunt, C.B., 1936, The Mount Taylor coal field: U.S.G.S.,
Bull. 860-B, p. 31-80.

Inoue, A., and Minato, H., 1979, Ca-K exchange reaction and
interstratification in montmorillonite: Clays and Clay
Min., v. 27, No. 6, P. 393-401.

Jenkins, Ron, 1976, An introduction to x-ray spectrometry:
Heyden and Son Ltd., London, 163 p.

Keller, W.D., 1970, Environmental aspects of clay
minerals: Jour. Sed. Pet., v. 40, p. 788-813.

Kinter, E.B., and Diamond, S., 1956, A new method for
preparation and treatment of oriented-aggregate
specimens of soil clays for x-ray diffraction
analysis: Soil Science, v. 81, no. 2, p. 111-120.

Krukowski, S.K., in prep., M.S. thesis on San Juan clays,
New Mexico Inst. of Mining and Tech.

van Langeveld, A.D., van der Gaast, S.J., and Eisma, D., 1977,
A comparison of the effectiveness of eight methods
for the removal of organic matter from clay: Clays
and Clay Minerals, v. 26, p. 361-364.

Lindsay, Everett H., 1982, Correlation of the San Juan Basin
magnetic polarity sequence with the magnetic polarity
time scale: Seminar-talk at N.M.I.M.T., March 4.

Lindsay, E.H., Butler, R.F., and Johnson, N.M., 1981,
Magnetic polarity zonation and biostratigraphy of
late Cretaceous and Paleocene continental deposits,
San Juan Basin, New Mexico: Am. Jour. Sci., v. 281
p. 390-435.

MacKenzie, F.T., and Garrels, R.M., 1966, Chemical mass
balance between rivers and oceans: Am. Jour. Sci.,
v. 264, p. 507-525.

Mannhard, G.W., 1976, Stratigraphy, sedimentology and

- paleoenvironments of the La Ventana Tongue (Cliff House Sandstone) and adjacent formations of the Mesaverde Group (Upper Cretaceous), southeastern San Juan Basin, New Mexico: Ph.D. thesis, University of New Mexico, 182 p.
- McBride, Murray B., 1979, An interpretation of cation selectivity variations in M⁺-M⁺ exchange on clays: *Clays and Clay Min.*, v. 27, No. 6, p. 417-422.
- Mills, J.G., and Zwarich, M.A., 1972, Recognition of interstratified clays: *Clay and Clay Minerals*, v. 20, p. 169-174.
- Molenaar, C.M., 1977, Stratigraphy and depositional history of the Upper Cretaceous rocks of the San Juan Basin area, New Mexico and Colorado: Guidebook 28th field conf., New Mex. Geol. Soc., p. 193-197.
- Norrish, K., and Hutton, J.T., 1969, An accurate x-ray spectrographic method for the analysis of a wide range of geologic samples: *Geoc. et Cosmo. Acta*, v. 33, p. 431-453.
- O'Brien, N.R., 1964, Origin of Pennsylvanian underclays in Illinois Basin: *G.S.A. Bull.*, v. 75, p. 823-832.
- Parham, Walter E., 1965, Lateral clay mineral variations in certain Pennsylvanian underclays: Twelfth National Conference on Clays and Clay Minerals, p.581-601.
- Pike, W.S., Jr., 1947, Intertonguing marine and nonmarine Upper Cretaceous deposits of New Mexico, Arizona, and southwestern Colorado: *G.S.A., Mem.* 24, 103 p.
- Reynolds, R.C., Jr., and Hower, John, 1970, The nature of interlayering in mixed-layer illite-montmorillonite: *Clay and Clay Minerals*, v. 18, p.25-36.
- Rhoton, F.E., and Smeck, N.E., 1981, Equilibration of clays in natural and simulated bottom-sediment environments: *Clays and Clay Min.*, v. 29, No. 1, p. 17-22.
- Sabins, F.F., Jr., 1964, Symmetry, stratigraphy and petrography of cyclic Cretaceous deposits in the San Juan Basin: *A.A.P.G., Bull.*, v. 48, p. 292-316.
- Schrader, F.C., 1906, The Durango-Gallup coal field of Colorado and New Mexico: *U.S.G.S., Bull.* 285-F, p. 241-258.
- Schultz, L.G., 1958, Petrology of underclays: *G.S.A. Bull.*, v. 69, p. 41-49.

- Schultz, L.G., 1964, Quantitative interpretation of mineralogic composition from x-ray and chemical data for the Pierre Shale: U.S.G.S. Prof. Paper 391-C, p. C1-C31.
- Sears, J.D., 1934, The coal field from Gallup eastward toward Mount Taylor: U.S.G.S., Bull. 860, p. 1-29.
- Sears, J.D., Hunt, C.B., and Hendricks, T.A., 1941, Transgressive and regressive Cretaceous deposits in southern San Juan Basin, New Mexico: U.S.G.S., Prof. Paper 193, p. 101-121.
- Shetiwy, M.M., 1978, Sedimentological and stratigraphic analysis of the Point Lookout Sandstone, southeast San Juan Basin, New Mexico: Ph.D. thesis, New Mex. Inst. of Mining and Tech., 262 p.
- Shieh, Yuch-Ning, and Suter, Terri G., 1979, Formation conditions of authigenic kaolinite and calcite in coals by stable isotope determinations: Clays and Clay Min., v. 27, No. 2, p. 154-156.
- Shomaker, J.W., Beaumont, E.C., and Kottowski, F.E., 1971, Strippable low-sulfur coal resources of the San Juan Basin in New Mexico: New Mexico Geol. Soc., Guidebook supplement, 28th field conf., p. 1-21.
- Shomaker, J.W., and Whyte, M.R., 1977, Geologic appraisal of deep coals, San Juan Basin, New Mexico: New Mex. Bur. Mines Min. Res., Circ. 155, 39 p.
- Shutor, V.D., 1969, On the mechanism of postsedimentary transition of montmorillonite into hydromica: Int. Clay Conf., 1969, p. 523-531.
- Siemers, C.T., and Wadell, J.S., 1977, Humate deposits of the Menefee Formation (Upper Cretaceous), northwestern New Mexico: New Mex. Geol. Soc., Guidebook supplement, 28th field conf., p. 1-21.
- Swanson, R.G., 1981, Sample examination manual: Shell Oil Company Exploration Training, A.A.P.G. Publication
- Tabet, D.E., and Frost, S.J., 1979, Environmental characteristics of Menefee coals in the Torreon Wash area, New Mexico: New Mex. Bur. Mines Min. Res., Open-file Rept. 102, 134 p.
- Tschudy, R.H., 1976, Palynology of Crevasse Canyon and Menefee Formation of San Juan Basin, New Mexico: N.M. Bur. Mines Min. Res., Circ. 154, p. 48-55.

- Weaver, C.E., 1956, The distribution and identification of mixed-layer clays in sedimentary rocks: *Am. Min.*, v. 41, p. 202.
- Weaver, C.E., 1967, Potassium, illite and the ocean: *Geochim. et Cosmochim. Acta*, v. 31, p. 2181-2196.
- Weaver, C.E., and Pollard, L.D., 1973, The chemistry of clay minerals: Elsevier, Amsterdam, 213 p.
- Whitehouse, G., and McCarter, R.S., 1958, Diagenetic modification of clay minerals in artificial sea water: *Clays and Clay Min.*, *Nat. Acad. Sci.*, *Nat. Res. Council Pub.* 566, p. 81-119.
- Woodward, L.A., and Callender, J.F., 1977, Tectonic framework of the San Juan Basin: *New Mex. Geol. Soc. Guidebook*, 28th Field Conf., p. 209-212.

APPENDIX

APPENDIX 1

PROCEDURE FOR CALCULATION OF RELATIVE ABUNDANCES OF CLAYS

- 1) Perform X-ray analysis on untreated, glycol, 350 degree centigrade, and 550 degree centigrade oriented clay mounts.
- 2) Measure the areas for the 7A glycol, the 10A glycol, and the 10A 350 degree peaks. Measure the heights of the 7A glycol, the 17A glycol, the 10A 350 degree, and the 14A 550 degree peaks.
- 3) Determine the corrected 7A peak area by dividing the 7A glycol peak by 1.4.
- 4) Calculate the relative abundance of chlorite plus kaolinite by dividing the corrected 7A peak area by the sum of the corrected 7A peak area and the 10A 350 degree peak area, and multiply by 100.
- 5) Find the relative abundance of chlorite in the sample by dividing the 14A 550 degree peak height by 1.5 times the 7A peak height and multiplying this number by the percent of chlorite plus kaolinite.
- 6) Determine the relative abundance of kaolinite by subtracting the percent of chlorite from the percent of chlorite plus kaolinite.
- 7) Calculate the relative abundance of illite by dividing the 10A peak area by the sum of the corrected 7A and 10A peak areas and multiplying by 100 percent.
- 8) Find the relative abundance of smectite by dividing the 17A peak height by 4.5 times the 10A 350 degree peak height, multiplying by 100, and subtracting the kaolinite plus chlorite value.
- 9) Determine the percent of mixed-layer illite-smectite by subtracting the relative abundances of all other clay minerals from 100 percent.

APPENDIX 2A

CLAY DATA FOR COMPUTER ANALYSIS

A R E A S (grams) H E I G H T S (mm)

Sample No.	Frac.	A R E A S (grams)			H E I G H T S (mm)			
		7A Glycol	10A Glycol	10A 350 C	7A Glycol	17A Glycol	10A 350 C	14A 550 C
TW-C1-50.2	<8	0.0319	0.0092	0.0517	70	28	64	0
B	<8R	0.0349	0.0081	0.0462	79	33	61	0
A	<1	0.0239	0.0077	0.0835	46	50	73	0
B	<1R	0.0276	0.0106	0.0834	48	48	77	0
B	<1SR	0.0251	0.0116	0.0878	49	50	78	0
B	<1SR	0.0238	0.0093	0.0824	47	50	76	0
C	<1R	0.0247	0.0083	0.0763	49	56	75	0
	<.25	0.0165	0.0083	0.0972	31	52	80	0
	<.1	0.0083	0.0000	0.0940	10	38	86	0
TW-C1-52.9	<1	0.0413	0.0175	0.1042	61	36	101	14
TW-C1-56.3	<1ED	0.0595	0.0199	0.1432	81	41	134	3
	<.25	0.0621	0.0189	0.1389	69	40	135	0
TW-C1-59.0	<2AE	0.0518	0.0094	0.0448	102	17	46	0
TW-C1-60.5	<1	0.0359	0.0194	0.1162	68	45	124	7
TW-C1-64.9	<1	0.0432	0.0171	0.1007	65	60	99	5
TW-C1-69.3	<1	0.0414	0.0132	0.1159	83	35	101	4
	<1SM	0.0527	0.0118	0.0484	99	16	44	0
TW-C1-153.4	<1	0.0231	0.0401	0.1076	50	21	117	12
TW-C1-165.0	<2AE	0.0428	0.0000	0.0000	223	0	0	4
TW-C1-169.6	<1	0.0223	0.0151	0.1051	46	98	107	0
TW-C2-115.5	<1	0.0419	0.0160	0.0900	62	48	80	5
TW-C2-119.2	<1	0.0303	0.0107	0.0519	59	36	52	0
TW-C2-122.3	<1	0.0707	0.0274	0.1255	153	33	130	20
TW-C3-10.4	<2	0.0105	0.0030	0.0296	34	19	36	0
TW-C3-18.3	<2	0.0187	0.0120	0.0573	43	57	77	9
TW-C3-20.2	<2	0.0145	0.0062	0.0198	38	38	24	0
TW-C3-21.7	<2	0.0300	0.0296	0.1002	49	115	104	0
	<.25	0.0405	0.0499	0.2327	42	155	234	0
TW-C3-23.8	<2	0.0882	0.0148	0.0854	120	59	72	0
TW-C3-29.8	<2	0.0191	0.0096	0.0411	31	135	50	8
	<.25	0.0095	0.0093	0.0801	15	112	78	0
TW-C3-34.5	<2	0.0262	0.0055	0.0512	40	85	53	13
TW-C3-38.5	<8	0.0746	0.0294	0.1189	94	82	113	0
	<2	0.0294	0.0136	0.1553	58	103	142	15
TW-C3-50.1	<2	0.0272	0.0077	0.1743	50	106	150	10
TW-C3-50.9	<2AE	0.1093	0.0061	0.0515	141	45	47	6
TW-C3-52.1	<2	0.0319	0.0051	0.0851	50	91	71	0
	<.25	0.0230	0.0124	0.0855	31	80	79	0
TW-C3-54.2	<8	0.0495	0.0175	0.0992	90	90	100	5
	<2	0.0240	0.0114	0.0921	42	98	85	9
TW-C3-57.4	<2ED	0.0431	0.0218	0.0919	81	61	105	1
	<2BF	0.0351	0.0184	0.0343	84	26	50	7
TW-C3-58.8	<8	0.0626	0.0328	0.1441	122	113	139	10
A	<2	0.0355	0.0126	0.0705	67	105	64	8
B	<2R	0.0357	0.0154	0.0708	68	111	65	7
C	<2R	0.0328	0.0142	0.0737	64	103	63	7
	<1	0.0349	0.0148	0.0839	70	99	80	5
	<1SM	0.0843	0.0261	0.1009	179	101	105	14
	<.5	0.0277	0.0119	0.0787	56	87	72	6
A	<.25	0.0198	0.0072	0.0790	36	84	72	0

CLAY DATA
A R E A S (grams) H E I G H T S (mm)

Sample No.	Frac.	A R E A S (grams)			H E I G H T S (mm)			
		7A Glycol	10A Glycol	10A 350 C	7A Glycol	17A Glycol	10A 350 C	14A 550 C
B	<.25	0.0188	0.0067	0.0774	34	80	72	0
C	<.25	0.0214	0.0078	0.0787	33	83	70	0
TW-C3-63.5	<2AE	0.0432	0.0000	0.0097	178	6	17	0
TW-C3-64.2	<2	0.1554	0.0089	0.2611	169	66	115	5
TW-C3-66.9	<1	0.0618	0.0187	0.1011	115	105	103	8
TW-C3-82.5	<2	0.1256	0.0241	0.1226	197	45	118	32
TW-C3-105.8	<2	0.0184	0.0128	0.0931	31	79	95	11
	<.25	0.0091	0.0172	0.1196	11	132	112	0
TW-C3-106.6	<2	0.0368	0.0091	0.1339	66	145	92	0
	<.25	0.0344	0.0059	0.1019	41	150	97	0
TW-C3-107.3	<2	0.0158	0.0055	0.0792	49	209	77	8
	<.25	0.0058	0.0020	0.0750	13	187	67	3
TW-C3-108.4	<2AE	0.0558	0.0000	0.0304	152	55	34	9
TW-C3-109.2	<2	0.0388	0.0068	0.0721	66	100	75	10
	<.25	0.0585	0.0155	0.0912	59	111	93	0
TW-C3-111.7	<8	0.0617	0.0152	0.1105	104	109	116	6
	<2	0.0269	0.0106	0.1592	40	113	142	6
	<1	0.0278	0.0075	0.1688	45	123	158	9
	<1SM	0.0798	0.0273	0.1104	138	96	116	12
	<.5	0.0211	0.0120	0.0667	35	77	62	0
	<.25	0.0127	0.0062	0.0655	22	87	62	0
	<.1	0.0074	0.0038	0.0624	8	83	53	0
TW-C3-114.5	<8	0.1323	0.0103	0.0730	167	70	81	0
A	<2	0.0800	0.0083	0.0694	88	72	61	0
B	<2R	0.0788	0.0087	0.0589	90	77	58	0
C	<2R	0.0789	0.0075	0.0615	86	82	58	0
	<1	0.0738	0.0092	0.0579	84	70	53	0
	<1SM	0.0887	0.0091	0.0354	112	46	38	0
	<.5	0.1183	0.0166	0.0886	133	99	86	4
A	<.25	0.0658	0.0074	0.0512	67	65	49	0
B	<.25	0.0665	0.0076	0.0541	64	60	51	0
C	<.25	0.0551	0.0065	0.0493	63	63	51	0
	<.1	0.0517	0.0037	0.0678	35	70	57	0
TW-C3-117.9	<1	0.0556	0.0129	0.1065	61	135	80	0
TW-C3-120.1	<2	0.0172	0.0092	0.0822	31	109	80	6
	<.25	0.0114	0.0170	0.0909	17	94	92	0
TW-C3-121.9	<1	0.0619	0.0146	0.0722	110	102	70	10
TW-C3-135.1	<1	0.0351	0.0152	0.1069	61	146	100	6
TW-C3-149.2	<1	0.0645	0.0140	0.1127	99	114	114	4
TW-C3-150.4	<1	0.0482	0.0045	0.0883	63	85	86	0
TW-C3-153.7	<2	0.0825	0.0092	0.0648	131	93	65	12
	<.25	0.0664	0.0111	0.0873	50	77	90	0
TW-C3-160.4	<2	0.0221	0.0051	0.0797	46	66	59	0
TW-C3-221.3	<2	0.1003	0.0142	0.1006	153	122	104	12
TW-C3-224.8	<1	0.0264	0.0010	0.0012	101	3	5	0
TW-C4-87.1	<1	0.0213	0.0132	0.1067	42	88	113	9
TW-C4-103.2	<1	0.0431	0.0185	0.1057	79	44	107	12
TW-C4-104.8	<1	0.0363	0.0135	0.0768	56	38	84	0
	<1SM	0.0798	0.0159	0.0686	112	48	70	0
TW-C4-119.5	<1	0.0402	0.0096	0.0883	57	60	103	0

CLAY DATA
A R E A S (grams) H E I G H T S (mm)

Sample No.	Frac.	A R E A S (grams)			H E I G H T S (mm)				
		7A Glycol	10A Glycol	10A 350 C	7A Glycol	17A Glycol	10A 350 C	14A 550 C	
TW-C4-120.4	<1SM	0.0936	0.0229	0.0739	120	48	85	0	
	<1	0.0651	0.0073	0.0727	85	60	78	0	
	<1SM	0.0745	0.0063	0.0469	122	34	49	0	
TW-C4-170.6	<1	0.0290	0.0119	0.0843	58	51	92	8	
TW-C4-172.8	<2AE	0.0628	0.0035	0.0224	139	20	20	19	
TW-C4-176.6	<1	0.0601	0.0143	0.1086	82	40	116	0	
TW-C5-13.3	<1	0.0096	0.0117	0.1678	20	80	186	10	
TW-C5-19.2	<1	0.0010	0.0000	0.0568	5	252	79	3	
	<.25	0.0000	0.0000	0.0202	0	127	31	0	
TW-C5-24.0	<1	0.0177	0.0216	0.1007	31	68	118	0	
	<1SM	0.0352	0.0207	0.1071	56	73	124	0	
TW-C5-37.5	<1	0.0204	0.0195	0.1192	38	89	122	12	
	<1SM	0.0199	0.0181	0.0667	39	72	82	6	
TW-C5-37.8	<2AE	0.0539	0.0188	0.0921	96	65	86	15	
TW-C5-38.6	<8	0.0559	0.0048	0.0647	144	61	72	21	
	A	<1	0.0537	0.0073	0.0564	68	82	58	0
	B	<1R	0.0538	0.0081	0.0642	73	92	57	0
	B	<1SR	0.0567	0.0063	0.0589	74	90	59	0
	B	<1SR	0.0506	0.0055	0.0605	71	92	55	0
	C	<1R	0.0496	0.0054	0.0584	65	88	57	0
	<.25	0.0508	0.0106	0.1142	56	95	93	0	
TW-C5-95.8	<1	0.0305	0.0352	0.1425	47	61	147	11	
TW-C5-96.9	<1	0.0293	0.0127	0.0656	31	67	68	0	
TW-C5-98.2	<2AE	0.0791	0.0049	0.0640	149	118	58	6	
TW-C5-100.4	<1	0.0800	0.0167	0.0658	78	58	69	6	
TW-C5-105.8	<1	0.0561	0.0217	0.1233	64	61	123	0	
TW-C5-122.5	<1	0.1006	0.0289	0.1147	180	76	108	15	
TW-C5-123.9	<1	0.0632	0.0411	0.1671	119	86	176	19	
TW-C5-125.3	<1	0.0480	0.0258	0.1370	64	64	142	0	
TW-C5-128.1	<1	0.1196	0.0124	0.0852	120	69	84	0	
AC-TW-1	<1AH	0.0283	0.0034	0.1494	65	16	94	0	
AC-TW-2	<2AE	0.0629	0.0205	0.0666	140	21	64	0	
AC-TW-3	<1	0.0266	0.0199	0.0898	57	12	53	0	
	<.25	0.0345	0.0158	0.1289	51	14	73	0	
AC-TW-4	<1	0.0289	0.0144	0.0832	63	20	51	0	
AC-TW-7	<1	0.0646	0.0184	0.1078	170	40	92	8	
	<.25	0.0534	0.0166	0.1718	110	68	151	8	
AC-TW-8	<1ED	0.0498	0.0542	0.1834	99	34	189	0	
	<.25	0.0184	0.0513	0.1907	28	29	186	0	
AC-TW-10	<1	0.0452	0.0189	0.1487	103	64	161	0	
AC-TW-12	<1	0.0260	0.0256	0.1234	63	32	114	5	
	<.25	0.0159	0.0272	0.1471	33	42	124	0	
AC-TW-17	<1ED	0.0834	0.0377	0.1958	135	59	192	0	
AC-TW-21	<1ED	0.0362	0.0398	0.1805	72	52	185	0	
	<1ER	0.0218	0.0173	0.1672	43	54	136	0	
	<.25	0.0344	0.0576	0.2696	53	84	252	0	
	<.10	0.0069	0.0371	0.1722	13	53	155	0	
AC-TW-24	<1	0.0331	0.0260	0.1021	63	42	104	4	
	<.25	0.0496	0.0449	0.2046	89	63	185	0	
AC-TW-25	<1	0.0500	0.0316	0.1588	105	45	113	0	

CLAY DATA

Sample No.	Frac.	A R E A S (grams)			H E I G H T S (mm)			
		7A	10A	10A	7A	17A	10A	14A
		Glycol	Glycol	350 C	Glycol	Glycol	350 C	550 C
	<.25	0.0307	0.0263	0.1422	52	43	103	0
AC-TW-26	<1ED	0.0659	0.0432	0.2417	99	84	240	0
AC-TW-27	<1ED	0.1064	0.0421	0.1992	171	51	204	0
	<.25	0.0743	0.0479	0.2031	103	43	202	0
	<.1	0.0289	0.0342	0.2921	34	42	255	0
AC-TW-28	<1ED	0.0737	0.0166	0.1093	108	33	108	5
AC-TW-29	<1ED	0.0177	0.0444	0.1419	42	50	166	7
AC-TW-32	<1ED	0.0585	0.0308	0.1802	87	76	193	0
AC-TW-34	<1ED	0.0627	0.0276	0.1872	123	100	176	0
	<.25	0.0479	0.0317	0.1986	81	71	189	0
	<.1	0.0121	0.0133	0.1528	11	80	114	0
AC-TW-35	<1	0.0302	0.0345	0.2055	61	61	165	9
AC-TW-36	<1	0.0249	0.0250	0.1267	49	42	115	5
AC-TW-38	<1ED	0.0611	0.0428	0.2007	99	88	138	5
	<.25	0.0421	0.0453	0.2651	72	112	249	0
	<.1	0.0097	0.0070	0.1837	11	88	154	0
AC-TW-40	<1ED	0.0281	0.0407	0.2336	52	102	204	0
AC-CM-56	<1	0.0359	0.0082	0.1271	62	103	121	0
	<.25	0.0205	0.0084	0.1221	34	120	128	0
AC-CM-57	<1	0.0464	0.0056	0.0840	72	86	79	0
AC-CM-58	<1	0.0681	0.0038	0.0611	92	75	58	6
2A	<1RS	0.1239	0.0021	0.0946	100	102	84	0
2B	<1R	0.1128	0.0008	0.1039	90	109	102	0
2C	<1R	0.1555	0.0026	0.1294	115	126	113	0
3	<1RS	0.1103	0.0043	0.0864	106	126	81	0
	<.25	0.0647	0.0053	0.1019	66	91	94	0
AC-CM-59	<1	0.0411	0.0274	0.1095	84	84	114	8
AC-CM-62	<1	0.0396	0.0146	0.0896	83	87	90	0
	<.25	0.0305	0.0118	0.1081	54	84	114	0
AC-CM-63	<1	0.0178	0.0196	0.1067	42	62	108	4
AC-UM-64	<1	0.0552	0.0289	0.1433	154	79	139	0
AC-UM-65	<1	0.0331	0.0078	0.1063	94	68	101	0
AC-UM-66	<1	0.0457	0.0129	0.1218	110	82	129	0
	<.25	0.0129	0.0051	0.0976	21	34	83	0
AC-UM-67	<1	0.0391	0.0178	0.1414	97	47	139	0
AC-FR-71	<1	0.0006	0.0000	0.1807	2	182	170	0
AC-FR-72	<1	0.0028	0.0107	0.1046	6	161	103	0
	<.25	0.0019	0.0114	0.2749	3	257	126	0
	<.1	0.0000	0.0032	0.1092	0	139	72	0
AC-FR-73	<1	0.0000	0.0000	0.0748	0	204	78	0
AC-FR-74	<1	0.0021	0.0000	0.1397	7	250	67	0
AC-FR-75	<1	0.0011	0.0000	0.0592	2	239	75	0
AC-FR-76	<1	0.0000	0.0000	0.0471	0	126	28	0
	<1RS	0.0000	0.0000	0.0482	0	166	37	0
AC-FR-77	<1	0.0000	0.0000	0.0424	0	118	40	0
AC-FR-78	<1	0.0060	0.0000	0.0898	8	177	53	0
AC-FR-79	<1	0.0112	0.0000	0.0695	22	127	51	2
	<.25	0.0287	0.0000	0.1553	41	157	82	5
AC-FR-80	<1AH	0.0066	0.0000	0.0719	17	65	57	0
AC-FR-82	<1	0.0051	0.0000	0.0998	7	201	60	0

APPENDIX 2B

RELATIVE ABUNDANCES OF CLAY MINERALS

Sample No.	Frac.	Formatn.	Chlort	Kaolnt	Illite	Smect	Mixed Ill/Smt
TW-C1-50.2	<8	Up.Men.	0	31	12	7	50
B	<8R		0	35	11	8	46
A	<1		0	17	8	13	62
B	<1R		0	19	10	11	60
B	<1SR		0	17	11	12	60
B	<1SR		0	17	9	12	62
C	<1R		0	19	9	13	59
	<.25		0	11	8	13	68
	<.1		0	6	0	9	85
TW-C1-52.9	<1	"	3	19	13	6	59
TW-C1-56.3	<1ED	"	1	22	11	5	61
	<.25		0	24	10	5	61
TW-C1-59.0	<2AE	"	0	45	11	5	39
TW-C1-60.5	<1	"	1	17	14	7	61
TW-C1-64.9	<1	"	1	22	13	10	54
TW-C1-69.3	<1	"	1	19	9	6	65
	<1SM		0	44	14	5	37
TW-C1-153.4	<1	"	2	11	32	3	52
TW-C1-165.0	<2AE	"	1	99	0	0	0
TW-C1-169.6	<1	"	0	13	12	18	57
TW-C2-115.5	<1	"	1	24	13	10	52
TW-C2-119.2	<1	"	0	29	15	11	45
TW-C2-122.3	<1	"	3	26	16	4	51
TW-C3-10.4	<2	Cleary	0	20	8	9	63
TW-C3-18.3	<2	"	3	16	17	13	51
TW-C3-20.2	<2	"	0	34	21	23	22
TW-C3-21.7	<2	"	0	18	24	20	38
	<.25		0	11	19	13	57
TW-C3-23.8	<2	"	0	42	10	11	37
TW-C3-29.8	<2	"	4	21	18	45	12
	<.25		0	8	11	29	52
TW-C3-34.5	<2	"	6	21	8	26	39
TW-C3-38.5	<8	"	0	31	17	11	41
	<2		2	10	8	14	66
TW-C3-50.1	<2	"	1	9	4	14	72
TW-C3-50.9	<2AE	"	2	58	5	9	26
TW-C3-52.1	<2	"	0	21	5	23	51
	<.25		0	16	12	19	53
TW-C3-54.2	<8	"	1	25	13	15	46
	<2		2	14	10	22	52
TW-C3-57.4	<2ED	"	0	25	18	10	47
	<2BF		2	40	31	7	20
TW-C3-58.8	<8	"	1	23	17	14	45
A	<2		2	24	13	27	34
B	<2R		2	24	16	28	30
C	<2R		2	22	15	28	33
	<1		1	22	14	21	42
	<1SM		2	35	16	13	34
	<.5		1	19	12	21	47
A	<.25		0	15	8	22	55

RELATIVE ABUNDANCES OF CLAY MINERALS

Sample No.	Frac.	Formatn.	Chlort	Kaolnt	Illite	Smect	Mixed Ill/Smt
B	<.25		0	15	7	21	57
C	<.25		0	16	8	22	54
TW-C3-63.5	<2AE	"	0	76	0	2	22
TW-C3-64.2	<2	"	1	29	2	9	59
TW-C3-66.9	<1	"	1	29	13	16	41
TW-C3-82.5	<2	Point Lk.	5	37	11	5	42
TW-C3-105.8	<2	Mancos	3	9	12	16	60
	<.25		0	5	14	25	56
TW-C3-106.6	<2	"	0	16	6	29	49
	<.25		0	19	5	28	48
TW-C3-107.3	<2	"	1	11	6	53	29
	<.25		1	4	3	59	33
TW-C3-108.4	<2AE	"	2	55	0	15	28
TW-C3-109.2	<2	"	3	25	7	21	44
	<.25		0	31	12	18	39
TW-C3-111.7	<8	"	1	28	10	15	46
	<2		1	10	6	16	67
	<1		1	10	4	15	70
	<1SM		2	32	16	12	38
	<.5		0	18	15	17	50
	<.25		0	12	8	27	53
	<.1		0	8	6	32	54
TW-C3-114.5	<8	"	0	56	6	8	30
A	<2		0	45	7	14	34
B	<2R		0	49	8	15	28
C	<2R		0	48	6	16	30
	<1		0	48	8	15	29
	<1SM		0	64	9	10	17
	<.5		1	48	10	13	28
A	<.25		0	48	8	15	29
B	<.25		0	47	7	14	32
C	<.25		0	44	7	15	34
	<.1		0	35	4	18	43
TW-C3-117.9	<1	"	0	27	9	27	37
TW-C3-120.1	<2	"	2	11	10	26	51
	<.25		0	8	17	21	54
TW-C3-121.9	<1	"	2	36	13	20	29
TW-C3-135.1	<1	"	1	18	12	26	43
TW-C3-149.2	<1	"	1	28	9	16	46
TW-C3-150.4	<1	"	0	28	4	16	52
TW-C3-153.7	<2	"	3	45	7	17	28
	<.25		0	35	8	12	45
TW-C3-160.4	<2	"	0	17	5	21	57
TW-C3-221.3	<2	"	2	40	8	15	35
TW-C3-224.8	<1	"	0	94	5	1	0
TW-C4-87.1	<1	Cleary	2	10	11	15	62
TW-C4-103.2	<1	"	2	21	14	7	56
TW-C4-104.8	<1	"	0	25	13	8	54
	<1SM		0	45	13	8	34
TW-C4-119.5	<1	"	0	25	8	10	57

RELATIVE ABUNDANCES OF CLAY MINERALS

Sample No.	Frac.	Formatn.	Chlort	Kaolnt	Illite	Smect	Mixed Ill/Smt
	<1SM		0	47	16	7	30
TW-C4-120.4	<1	"	0	39	6	10	45
	<1SM		0	53	6	7	34
TW-C4-170.6	<1	Mancos	2	18	11	10	59
TW-C4-172.8	<2AE	"	6	61	5	7	21
TW-C4-176.6	<1	"	0	28	9	6	57
TW-C5-13.3	<1	Cleary	1	3	7	9	80
TW-C5-19.2	<1	"	0	1	0	70	29
	<.25		0	0	0	91	9
TW-C5-24.0	<1	"	0	11	19	11	59
	<1SM		0	19	16	11	54
TW-C5-37.5	<1	"	2	9	15	14	60
	<1SM		2	16	22	16	44
TW-C5-37.8	<2AE	"	3	26	14	12	45
TW-C5-38.6	<8	"	4	34	5	12	45
A	<1		0	40	8	19	33
B	<1R		0	37	8	23	32
B	<1SR		0	41	6	20	33
B	<1SR		0	37	6	23	34
C	<1R		0	38	6	21	35
	<.25		0	24	7	17	52
TW-C5-95.8	<1	Mancos	2	11	21	8	58
TW-C5-96.9	<1	"	0	24	15	17	44
TW-C5-98.2	<2AE	"	1	46	4	24	25
TW-C5-100.4	<1	"	2	44	14	10	30
TW-C5-105.8	<1	"	0	25	13	8	54
TW-C5-122.5	<1	"	2	37	15	10	36
TW-C5-123.9	<1	"	2	19	19	9	51
TW-C5-125.3	<1	"	0	20	15	8	57
TW-C5-128.1	<1	"	0	50	7	9	34
AC-TW-1	<1AH	Up. Men.	0	12	2	3	83
AC-TW-2	<2AE	"	0	40	18	4	38
AC-TW-3	<1	"	0	17	18	4	61
	<.25		0	16	10	4	70
AC-TW-4	<1	"	0	20	14	7	59
AC-TW-7	<1	"	1	29	12	7	51
	<.25		1	17	8	8	66
AC-TW-8	<1ED	"	0	16	25	3	56
	<.25		0	6	25	3	66
AC-TW-10	<1	"	0	18	10	7	65
AC-TW-12	<1	"	1	12	18	5	64
	<.25		0	7	17	7	69
AC-TW-17	<1ED	"	0	23	15	5	57
AC-TW-21	<1ED	"	0	13	19	5	63
	<1ER		0	9	9	8	74
	<.25		0	8	20	7	65
	<.10		0	3	21	7	69
AC-TW-24	<1	"	1	18	21	7	53
	<.25		0	15	19	6	60
AC-TW-25	<1	"	0	18	16	7	59

RELATIVE ABUNDANCES OF CLAY MINERALS

Sample No.	Frac.	Formatn.	Chlort	Kaolnt	Illite	Smect	Mixed Ill/Smt
	<.25		0	13	16	8	63
AC-TW-26	<1ED	Up.Men.	0	16	15	7	62
AC-TW-27	<1ED	"	0	28	15	4	53
	<.25		0	21	19	4	56
	<.1		0	7	11	3	79
AC-TW-28	<1ED	"	1	32	10	5	52
AC-TW-29	<1ED	"	1	7	29	6	57
AC-TW-32	<1ED	"	0	19	14	7	60
AC-TW-34	<1ED	"	0	19	12	10	59
	<.25		0	15	14	7	64
	<.1		0	5	8	15	72
AC-TW-35	<1	"	1	8	15	7	69
AC-TW-36	<1	"	1	11	17	7	64
AC-TW-38	<1ED	"	1	17	18	12	52
	<.25		0	10	15	9	66
	<.1		0	4	4	12	80
AC-TW-40	<1ED	"	0	8	16	10	66
AC-CM-56	<1	Cleary	0	17	5	16	62
	<.25		0	11	6	19	64
AC-CM-57	<1	"	0	28	5	17	50
AC-CM-58	<1	"	2	42	3	16	37
2A	<1RS		0	48	1	14	37
2B	<1R		0	44	0	13	43
2C	<1R		0	46	1	13	40
3	<1RS		0	48	3	18	31
	<.25		0	31	4	15	50
AC-CM-59	<1	"	1	20	20	13	46
AC-CM-62	<1	"	0	24	12	16	48
	<.25		0	17	9	14	60
AC-CM-63	<1	"	1	10	16	11	62
AC-UM-64	<1	Up.Men.	0	22	16	10	52
AC-UM-65	<1	"	0	18	6	12	64
AC-UM-66	<1	"	0	21	8	11	60
	<.25		0	9	5	8	78
AC-UM-67	<1	"	0	16	11	6	67
AC-FR-71	<1	Fruitland	0	0	0	24	76
AC-FR-72	<1	"	0	2	10	34	54
	<.25		0	0	4	45	51
	<.1		0	0	3	43	54
AC-FR-73	<1	"	0	0	0	58	42
AC-FR-74	<1	"	0	1	0	82	17
AC-FR-75	<1	"	0	1	0	70	29
AC-FR-76	<1	"	0	0	0	100	0
	<1RS		0	0	0	100	0
AC-FR-77	<1	"	0	0	0	66	34
AC-FR-78	<1	"	0	5	0	71	24
AC-FR-79	<1	"	1	9	0	50	40
	<.25		1	11	0	37	51
AC-FR-80	<1AH	"	0	6	0	24	70
AC-FR-82	<1	"	0	4	0	71	25

EXPLANATION OF FRAC. (FRACTION) NOTATIONS

<8 = LESS THAN 8 MICRON CLAY FRACTION
<2 = " " 2 " " "
<1 = " " 1 " " "
<.5 = " " 0.5 " " "
<.25 = " " 0.25 " " "
<.1 = " " 0.1 " " "
AH = UNTREATED COAL ASH SAMPLE
AE = COAL ASH SAMPLE TREATED WITH EDTA BEFORE
CLAY MINERALOGY COULD BE DETERMINED
BF = SAMPLE ANALYZED BEFORE EDTA WAS ADDED BUT
SUBSEQUENTLY TREATED WITH EDTA
ED = SAMPLE TREATED WITH EDTA AND ANALYZED FOR
CLAYS IN THE USUAL WAY
ER = REANALYSIS OF THE SAME SAMPLE FROM SCRATCH
USING EDTA FOR BOTH
R = REANALYSIS OF A SAMPLE USING DIFFERENT
SLIDES PREPARED FROM THE SAME CLAY SUSPENSION
RS = REANALYSIS OF THE SAME SAMPLE FROM SCRATCH
SR = REANALYSIS USING THE SAME SLIDES
SM = REANALYSIS USING THE SMEAR SLIDE TECHNIQUE

WHOLE ROCK DATA FOR COMPUTER ANALYSIS

Sample No.	Micro-			Ortho- class	Calcite	Calcite	
	Quartz	cline	Albite			Mixed	Gypsm
TW-C1-50.2	2550	100	100	0	0	0	0
TW-C1-52.9	3650	200	150	0	0	0	0
TW-C1-56.3	4750	25	750	0	0	0	0
TW-C1-60.5	2850	100	150	0	0	0	0
TW-C1-64.9	4100	300	500	0	0	0	0
TW-C1-69.3	4750	25	750	0	0	0	0
TW-C1-153.4	4050	200	400	0	0	0	0
TW-C1-169.6	5600	1200	100	0	0	0	0
TW-C2-115.5	4750	700	200	0	0	0	50
TW-C2-119.2	7000	400	150	0	0	0	0
TW-C2-122.3	5600	1200	100	0	0	0	0
TW-C3-10.4	3750	600	1300	0	0	125	0
TW-C3-18.3	2750	150	450	0	0	100	0
TW-C3-20.2	1650	100	300	0	0	125	0
TW-C3-21.7	2700	100	50	0	0	0	100
TW-C3-23.8	4950	350	0	0	0	0	0
TW-C3-29.8	2700	100	350	0	0	100	0
TW-C3-34.5	5150	600	400	0	0	100	0
TW-C3-38.5	3250	200	100	0	0	0	0
TW-C3-50.1	3950	100	0	0	0	0	0
TW-C3-52.1	4750	300	0	600	0	0	0
TW-C3-54.2	3550	150	350	0	0	100	0
TW-C3-57.4	1200	0	150	0	2100	0	0
TW-C3-58.8	3400	150	500	0	0	100	0
TW-C3-64.2	4950	250	0	0	0	0	0
TW-C3-66.9	3050	500	500	300	0	100	0
TW-C3-82.5	4500	800	1500	0	0	125	0
TW-C3-105.8	2950	100	350	0	0	0	0
TW-C3-106.6	2750	100	400	0	0	0	0
TW-C3-107.3	2550	350	550	0	0	0	0
TW-C3-109.2	5200	350	200	0	0	100	0
TW-C3-111.7	3350	150	450	0	0	0	0
TW-C3-114.5	4300	300	0	0	0	0	0
TW-C3-117.9	2400	100	150	0	0	0	0
TW-C3-120.1	3850	300	700	0	0	0	0
TW-C3-121.9	4700	800	1850	0	0	0	0
TW-C3-135.1	2500	100	250	0	0	0	0
TW-C3-149.2	3500	100	250	0	0	0	0
TW-C3-150.4	3250	100	300	0	0	0	0
TW-C3-153.7	2700	100	200	0	0	0	0
TW-C3-160.4	5100	550	1050	0	0	125	0
TW-C3-221.3	3500	300	400	0	0	0	0
TW-C3-224.8	15250	0	0	0	0	0	0
TW-C4-87.1	2900	100	150	0	0	0	0
TW-C4-103.2	2700	200	300	0	0	0	0
TW-C4-104.8	3550	450	50	0	0	0	75
TW-C4-119.5	3000	50	0	0	0	0	0
TW-C4-120.4	4500	100	0	0	0	0	50
TW-C4-170.6	3150	250	500	0	0	0	0
TW-C4-176.6	3500	250	150	0	0	0	0
TW-C5-13.3	3100	100	450	0	0	100	0
TW-C5-19.2	2300	600	900	0	0	0	0
TW-C5-24.0	3150	50	0	0	0	0	0

WHOLE ROCK DATA

Sample No.	Quartz	Micro- cline	Albite	Ortho- clase	Calcite	Calcite Mixed	Gypsm
TW-C5-37.5	1350	0	100	0	0	0	0
TW-C5-38.6	2100	50	200	0	0	0	0
TW-C5-95.8	2200	100	150	0	0	0	0
TW-C5-96.9	3300	350	250	0	0	0	0
TW-C5-100.4	3450	150	50	0	0	0	75
TW-C5-105.8	2850	150	50	0	0	0	0
TW-C5-122.5	3100	200	700	0	0	100	0
TW-C5-123.9	2600	100	400	0	0	0	0
TW-C5-125.3	2850	50	100	0	0	0	0
TW-C5-128.1	4500	50	0	0	0	0	0
AC-TW-3	3750	50	100	0	0	0	0
AC-TW-4	3850	200	0	0	0	0	0
AC-TW-7	5200	450	400	0	0	0	0
AC-TW-8	4750	200	0	0	0	0	0
AC-TW-10	5600	550	600	0	0	0	0
AC-TW-12	3650	250	500	0	0	0	0
AC-TW-17	4250	300	350	0	0	0	0
AC-TW-21	3100	150	200	0	0	0	0
AC-TW-24	3700	200	400	0	0	0	0
AC-TW-25	4950	350	550	0	0	0	0
AC-TW-26	3250	100	150	0	0	0	0
AC-TW-27	3800	250	350	0	0	0	0
AC-TW-28	6300	200	150	0	0	0	0
AC-TW-29	4150	200	200	0	0	0	0
AC-TW-32	4300	200	450	0	0	0	0
AC-TW-34	6500	450	1200	0	0	0	0
AC-TW-35	3500	150	300	0	0	0	0
AC-TW-36	3750	200	450	0	0	0	0
AC-TW-38	4950	400	1150	0	0	0	0
AC-TW-40	4150	250	300	0	0	0	0
AC-CM-56	3300	200	450	0	0	0	0
AC-CM-57	3300	800	800	0	0	0	0
AC-CM-58	6300	250	50	0	0	0	75
AC-CM-59	2200	200	250	0	0	0	50
AC-CM-62	2450	100	300	0	0	0	0
AC-CM-63	2700	100	175	0	0	0	0
AC-CM-64	3400	300	950	0	0	0	0
AC-UM-65	3950	300	900	0	0	0	0
AC-UM-66	3250	150	100	0	0	0	75
AC-UM-67	2950	200	350	0	0	0	0
AC-FR-71	3700	250	800	0	0	100	0
AC-FR-72	2500	100	300	0	0	100	0
AC-FR-73	0	0	100	0	0	0	0
AC-FR-74	1150	0	0	0	0	0	0
AC-FR-75	150	0	0	0	0	0	0
AC-FR-76	3900	450	1050	0	0	0	0
AC-FR-77	2500	100	250	0	0	0	0
AC-FR-78	3550	150	200	0	0	0	50
AC-FR-79	3700	150	200	0	0	0	100
AC-FR-82	2350	100	300	0	0	0	0

WHOLE ROCK PERCENTS

Sample No.	Ortz	Micro cline	Albte	Ortho clase	Calct	Calct Mixed	Gypsm	Clay
TW-C1-50.2	17	1	1	0	0	0	0	81
TW-C1-52.9	21	2	2	0	0	0	0	75
TW-C1-56.3	20	2	1	0	28	0	0	49
TW-C1-60.5	17	1	2	0	0	0	0	80
TW-C1-64.9	24	4	6	0	0	0	0	66
TW-C1-69.3	28	0	9	0	0	0	0	63
TW-C1-153.4	24	2	5	0	0	0	0	69
TW-C1-169.6	21	1	0	0	0	0	0	78
TW-C2-115.5	28	8	2	0	0	0	0	62
TW-C2-119.2	41	5	2	0	0	0	0	52
TW-C2-122.3	33	14	1	0	0	0	0	52
TW-C3-10.4	22	7	15	0	0	3	0	53
TW-C3-18.3	16	2	5	0	0	2	0	75
TW-C3-20.2	10	1	4	0	0	3	0	82
TW-C3-21.7	16	1	1	0	0	0	1	81
TW-C3-23.8	29	4	0	0	0	0	0	67
TW-C3-29.8	16	1	4	0	0	2	0	77
TW-C3-34.5	30	7	5	0	0	2	0	56
TW-C3-38.5	19	2	1	0	0	0	0	78
TW-C3-50.1	23	1	0	0	0	0	0	76
TW-C3-52.1	28	4	0	7	0	0	0	61
TW-C3-54.2	21	2	4	0	0	2	0	71
TW-C3-57.4	7	0	2	0	25	0	0	66
TW-C3-58.8	20	2	6	0	0	2	0	70
TW-C3-64.2	29	3	0	0	0	0	0	68
TW-C3-66.9	18	6	6	4	0	2	0	64
TW-C3-82.5	26	9	18	0	0	3	0	44
TW-C3-105.8	17	1	4	0	0	0	0	78
TW-C3-106.6	16	1	5	0	0	0	0	78
TW-C3-107.3	15	4	6	0	0	0	0	75
TW-C3-109.2	31	4	2	0	0	2	0	61
TW-C3-111.7	20	2	5	0	0	0	0	73
TW-C3-114.5	25	4	0	0	0	0	0	71
TW-C3-117.9	14	1	2	0	0	0	0	83
TW-C3-120.1	23	4	8	0	0	0	0	65
TW-C3-121.9	28	9	22	0	0	0	0	41
TW-C3-135.1	15	1	3	0	0	0	0	81
TW-C3-149.2	21	1	3	0	0	0	0	75
TW-C3-150.4	19	1	4	0	0	0	0	76
TW-C3-153.7	16	1	2	0	0	0	0	81
TW-C3-160.4	30	6	12	0	0	3	0	49
TW-C3-221.3	21	4	5	0	0	0	0	70
TW-C3-224.8	90	0	0	0	0	0	0	10
TW-C4-87.1	17	1	2	0	0	0	0	80
TW-C4-103.2	16	2	4	0	0	0	0	78
TW-C4-104.8	21	5	1	0	0	0	1	72
TW-C4-119.5	18	1	0	0	0	0	0	81
TW-C4-120.4	26	1	0	0	0	0	0	73
TW-C4-170.6	19	3	6	0	0	0	0	72
TW-C4-176.6	21	3	2	0	0	0	0	74
TW-C5-13.3	18	1	5	0	0	2	0	74
TW-C5-19.2	14	7	11	0	0	0	0	68

WHOLE ROCK PERCENTS

Sample No.	Qrtz	Micro cline	Albte	Ortho clase	Calct	Calct Mixed	Gypsm	Clay
TW-C5-24.0	19	1	0	0	0	0	0	80
TW-C5-37.5	8	0	1	0	0	0	0	91
TW-C5-38.6	12	1	2	0	0	0	0	85
TW-C5-95.8	13	1	2	0	0	0	0	84
TW-C5-96.9	19	4	3	0	0	0	0	74
TW-C5-100.4	20	2	1	0	0	0	1	76
TW-C5-105.8	17	2	1	0	0	0	0	80
TW-C5-122.5	18	2	8	0	0	2	0	70
TW-C5-123.9	15	1	5	0	0	0	0	79
TW-C5-125.3	17	1	1	0	0	0	0	81
TW-C5-128.1	26	1	0	0	0	0	0	73
AC-TW-3	22	1	1	0	0	0	0	76
AC-TW-4	23	2	0	0	0	0	0	75
AC-TW-7	31	5	5	0	0	0	0	59
AC-TW-8	28	2	0	0	0	0	0	70
AC-TW-10	33	6	7	0	0	0	0	54
AC-TW-12	21	3	6	0	0	0	0	70
AC-TW-17	25	4	4	0	0	0	0	67
AC-TW-21	18	2	2	0	0	0	0	78
AC-TW-24	22	2	5	0	0	0	0	71
AC-TW-25	29	4	6	0	0	0	0	61
AC-TW-26	19	1	2	0	0	0	0	78
AC-TW-27	22	3	4	0	0	0	0	71
AC-TW-28	37	2	2	0	0	0	0	59
AC-TW-29	24	2	2	0	0	0	0	72
AC-TW-32	25	2	5	0	0	0	0	68
AC-TW-34	38	5	14	0	0	0	0	43
AC-TW-35	21	2	4	0	0	0	0	73
AC-TW-36	22	2	5	0	0	0	0	71
AC-TW-38	29	5	14	0	0	0	0	52
AC-TW-40	24	3	4	0	0	0	0	69
AC-CM-56	19	2	5	0	0	0	0	74
AC-CM-57	19	9	9	0	0	0	0	63
AC-CM-58	37	3	1	0	0	0	1	58
AC-CM-59	13	2	3	0	0	0	0	82
AC-CM-62	14	1	4	0	0	0	0	81
AC-CM-63	16	1	2	0	0	0	0	81
AC-CM-64	20	4	11	0	0	0	0	65
AC-UM-65	23	4	11	0	0	0	0	62
AC-UM-66	19	2	1	0	0	0	1	77
AC-UM-67	17	2	4	0	0	0	0	77
AC-FR-71	22	3	9	0	0	2	0	64
AC-FR-72	15	1	4	0	0	2	0	78
AC-FR-73	0	0	1	0	0	0	0	99
AC-FR-74	7	0	0	0	0	0	0	93
AC-FR-75	1	0	0	0	0	0	0	99
AC-FR-76	23	5	12	0	0	0	0	60
AC-FR-77	15	1	3	0	0	0	0	81
AC-FR-78	21	2	2	0	0	0	0	75
AC-FR-79	22	2	2	0	0	0	1	73
AC-FR-82	14	1	4	0	0	0	0	81

APPENDIX 3A

CHEMICAL COMPOSITIONS-WEIGHT PERCENTS OF OXIDE CONSTITUENTS

WHOLE ROCK SAMPLES

NO.	SiO ₂	Al ₂ O ₃	Fe ₂ O ₃	K ₂ O	Na ₂ O	CaO	MgO	MnO	TiO ₂	P ₂ O ₅	LOI	TOTAL
1	60.54	16.98	3.37	2.43	1.24	0.27	1.09	0.01	0.69	0.08	13.99	100.69
2	69.75	16.39	1.84	2.44	1.17	0.16	1.23	0.01	0.76	0.02	7.20	100.97
3	62.54	16.95	2.52	3.14	1.19	0.54	1.42	0.02	0.78	0.12	10.18	99.40
4	60.77	18.01	4.72	2.90	1.58	0.31	1.79	0.03	0.76	0.16	9.86	100.89
R	60.31	17.82	4.70	2.95	1.84	0.32	1.78	0.02	0.78	0.15	9.86	100.53
5	69.16	15.05	4.73	2.33	1.19	0.11	1.06	0.02	0.69	0.01	6.43	100.78
6	69.91	14.34	4.22	2.74	1.96	0.20	1.13	0.01	0.83	0.07	4.74	100.15
7	57.78	14.97	8.86	2.75	1.60	0.69	1.88	0.24	0.63	0.16	11.24	100.80
8	56.07	19.76	2.51	2.11	1.74	0.12	1.18	0.01	0.50	0.02	16.09	100.11
9	58.84	19.36	5.23	2.76	1.46	0.09	1.73	0.02	0.71	0.02	10.15	100.37
R	58.80	19.31	5.27	2.80	1.74	0.10	1.70	0.02	0.74	0.03	10.15	100.66
10	56.38	17.72	4.64	1.92	1.32	0.08	0.97	0.01	0.83	0.02	16.19	100.08
R	56.10	17.56	4.64	1.93	1.55	0.14	0.96	0.01	0.87	0.03	16.19	99.98
11	65.66	17.10	2.56	1.56	0.51	0.06	0.81	0.01	0.89	0.01	11.71	100.88
R	65.36	16.89	2.55	1.52	0.75	0.07	0.80	0.01	0.93	0.02	11.71	100.61
12	63.23	17.70	3.22	2.16	2.06	0.50	1.63	0.02	0.64	0.13	9.22	100.51
13	57.99	12.87	2.34	2.08	0.15	0.02	1.00	0.01	0.70	0.02	22.54	99.72
14	59.70	17.81	5.09	2.83	0.66	0.07	2.09	0.12	0.71	0.12	11.23	100.43
15	67.09	15.11	2.80	2.68	1.16	0.11	1.49	0.02	0.70	0.11	8.41	99.68
16	61.84	16.30	2.55	2.63	0.80	0.05	1.97	0.01	0.72	0.05	13.83	100.75
17	64.70	17.13	4.23	2.58	1.35	0.15	1.20	0.01	0.81	0.05	8.20	100.41
R	64.36	16.99	4.18	2.62	1.52	0.15	1.19	0.01	0.84	0.06	8.20	100.12
18	51.76	20.62	8.23	0.16	2.00	0.68	1.30	0.03	0.56	0.04	13.92	99.30
19	67.89	13.79	3.17	0.98	2.37	1.00	1.01	0.01	0.48	0.03	9.86	100.59
20	54.54	16.34	2.22	0.49	1.55	0.67	0.63	0.01	0.61	0.03	23.27	100.36

COAL ASH SAMPLES (WHOLE ASH)

21	44.02	10.73	9.63	1.03	1.77	0.01	0.38	0.00	0.45	0.01	31.72	99.75
22	47.92	15.26	4.21	0.70	1.07	0.63	0.88	0.01	0.78	0.01	28.55	100.02

IRONSTONE CONCRETION

23	3.81	1.54	65.34	0.11	0.11	3.86	2.38	2.32	0.08	0.85	15.99	96.39
----	------	------	-------	------	------	------	------	------	------	------	-------	-------

KEY TO SAMPLE NUMBERS

1) TW-C1-64.9	9) TW-C3-135.1	17) AC-CM-56	R = Reanalysis of same sample
2) TW-C1-69.3	10) TW-C3-153.7	18) AC-FR-73	
3) TW-C1-153.4	11) TW-C4-120.4	19) AC-FR-76	
4) TW-C3-29.8	12) TW-C5-19.2	20) AC-FR-79	
5) TW-C3-34.5	13) AC-TW-8	21) TW-C1-59.0	
6) TW-C3-82.5	14) AC-TW-21	22) TW-C5-98.2	
7) TW-C3-105.8	15) AC-TW-38	23) AC-FE-20	
8) TW-C3-107.3	16) AC-TW-40	(Inner)	

APPENDIX 3A

CHEMICAL COMPOSITIONS--WEIGHT PERCENTS OF OXIDE CONSTITUENTS

<2 MICRON SAMPLES

NO.	SiO2	Al2O3	Fe2O3	K2O	Na2O	CaO	MgO	MnO	TiO2	P2O5	LOI	TOTAL
1	50.63	22.60	2.93	2.87	1.12	0.27	2.35	0.02	0.68	0.10	13.63	97.20
2	50.24	24.10	6.82	1.92	1.08	0.16	1.81	0.01	0.73	0.01	13.62	100.50
3	47.04	24.70	8.43	3.15	0.83	0.13	2.22	0.01	1.24	0.03	12.74	100.52
4	53.53	20.58	6.06	3.00	1.07	0.45	2.33	0.08	0.59	0.13	13.02	100.84
5	50.21	23.46	3.92	1.83	1.45	0.09	1.83	0.01	0.38	0.02	17.69	100.89
6	47.40	24.99	5.97	2.00	1.04	0.08	1.50	0.01	0.95	0.02	16.80	100.76

<1 MICRON CLAY FRACTION

7	50.00	24.25	4.10	2.66	0.99	0.31	1.94	0.01	0.64	0.05	16.03	100.98
8	49.60	25.51	3.59	2.66	0.78	0.24	1.56	0.01	0.85	0.02	13.88	98.70
9	53.09	23.40	3.92	4.23	0.78	0.46	2.11	0.02	0.76	0.09	12.16	101.02
10	48.76	24.08	5.83	3.03	0.24	0.47	2.55	0.02	0.38	0.07	16.36	101.80
11	49.20	27.34	3.52	2.12	0.33	0.15	1.59	0.01	0.82	0.03	15.56	100.65
12	50.60	22.93	6.20	2.47	1.38	0.08	2.02	0.01	0.75	0.03	13.67	100.14
13	48.88	26.38	4.37	2.05	1.05	0.10	1.49	0.01	0.86	0.01	15.70	100.90
14	54.42	21.21	3.88	0.83	1.50	0.54	2.35	0.01	0.79	0.03	15.43	100.99
15	49.08	25.82	5.76	2.32	0.60	0.38	1.67	0.01	0.82	0.02	14.01	100.49
16	51.26	24.60	4.63	3.01	0.53	0.42	1.71	0.01	0.71	0.01	13.51	100.40
17	53.62	23.13	3.39	3.41	1.35	0.03	1.65	0.01	1.07	0.02	13.65	101.33
RP	53.62	23.02	3.37	3.39	1.43	0.01	1.56	0.01	1.12	0.03	13.65	101.21
18	51.91	26.56	3.48	2.94	1.29	0.00	1.67	0.01	0.81	0.02	12.75	101.44
19	49.36	23.17	7.47	3.38	1.36	0.02	2.10	0.05	0.63	0.06	12.84	100.44
20	49.75	23.71	5.48	2.96	0.04	0.22	2.53	0.03	0.68	0.10	15.99	101.49
21	49.25	24.20	5.05	2.90	1.29	0.01	1.89	0.01	0.84	0.04	12.88	98.36
22	50.76	23.69	4.54	3.31	1.53	0.01	1.84	0.01	0.75	0.03	13.80	100.27
23	49.16	24.07	6.17	2.38	1.20	0.12	1.88	0.01	0.63	0.03	14.59	100.24
24	50.45	20.27	7.48	0.09	2.14	0.46	1.15	0.03	0.58	0.00	17.68	100.33
25	54.39	18.95	5.04	0.32	1.59	0.81	1.80	0.02	0.46	0.02	16.68	100.08
26	47.35	24.37	3.58	0.25	1.68	0.63	0.93	0.01	0.57	0.05	20.77	100.19

Key to sample numbers at end of next page

APPENDIX 3A

CHEMICAL COMPOSITIONS-WEIGHT PERCENTS OF OXIDE CONSTITUENTS

<0.25 MICRON FRACTION

No.	SiO ₂	Al ₂ O ₃	Fe ₂ O ₃	K ₂ O	Na ₂ O	CaO	MgO	MnO	TiO ₂	P ₂ O ₅	LOI	TOTAL
27	48.12	25.85	3.70	2.65	1.43	0.01	1.56	0.01	0.40	0.01	15.35	99.08
28	50.66	22.35	6.67	3.03	0.20	0.45	2.37	0.02	0.53	0.09	13.88	100.26
29	49.72	23.43	5.41	2.61	1.07	0.24	2.45	0.01	0.44	0.07	15.44	100.89
30	47.20	25.88	5.90	2.14	1.09	0.08	1.68	0.01	0.70	0.02	15.78	100.48
31	54.45	20.92	3.64	0.48	1.94	0.51	2.48	0.00	0.31	0.00	15.36	100.09
32	49.21	25.13	4.95	3.24	1.51	0.04	2.30	0.01	0.67	0.03	13.51	100.60
33	44.38	24.28	3.25	0.15	1.55	0.51	0.98	0.02	1.08	0.03	21.51	97.74

<0.1 MICRON FRACTION

34	50.94	25.41	3.93	3.21	1.57	0.02	1.94	0.01	0.48	0.03	13.79	101.32
35	49.39	23.55	4.62	2.96	2.13	0.01	2.08	0.01	0.30	0.03	15.39	100.47

KEY TO SAMPLE NUMBERS

1) TW-C3-29.8	12) TW-C3-135.1	23) AC-CM-56	34) AC-TW-27
2) TW-C3-34.5	13) TW-C4-120.4	24) AC-FR-73	35) AC-TW-38
3) TW-C3-82.5	14) TW-C5-19.2	25) AC-FR-76	
4) TW-C3-105.8	15) TW-C5-100.4	26) AC-FR-79	
5) TW-C3-107.3	16) TW-C5-125.3	27) TW-C1-56.3	
6) TW-C3-153.7	17) AC-TW-8	28) TW-C3-21.7	
7) TW-C1-64.9	18) AC-TW-17	29) TW-C3-29.8	
8) TW-C1-69.3	19) AC-TW-21	30) TW-C3-153.7	
9) TW-C1-153.4	20) AC-TW-36	31) TW-C5-19.2	
10) TW-C3-21.7	21) AC-TW-38	32) AC-TW-38	
11) TW-C3-23.8	22) AC-TW-40	33) AC-FR-79	

RP = Reanalysis using same pellet

CHEMICAL COMPOSITIONS-MOLE PERCENTS OF OXIDE CONSTITUENTS *

Samp. #	Frac.	SiO ₂	Al ₂ O ₃	Fe ₂ O ₃	K ₂ O	Na ₂ O	CaO	MgO	MnO	TiO ₂	P ₂ O ₅
TW-C1-64.9	WR	78.54	12.98	1.64	2.01	1.56	0.38	2.11	0.01	0.67	0.10
TW-C1-69.3	WR	81.68	11.31	0.81	1.82	1.33	0.20	2.15	0.01	0.67	0.02
TW-C1-153.4	WR	78.13	12.48	1.18	2.50	1.44	0.72	2.64	0.02	0.73	0.15
TW-C3-29.8	WR	75.69	13.22	2.21	2.30	1.91	0.41	3.32	0.03	0.71	0.19
TW-C3-34.5	WR	81.66	10.47	2.10	1.75	1.36	0.14	1.87	0.02	0.61	0.01
TW-C3-82.5	WR	81.11	9.80	1.84	2.03	2.20	0.25	1.95	0.01	0.72	0.08
TW-C3-105.8	WR	74.45	11.37	4.30	2.26	2.00	0.95	3.61	0.26	0.61	0.20
TW-C3-107.3	WR	75.79	15.74	1.28	1.82	2.28	0.17	2.38	0.01	0.51	0.03
TW-C3-135.1	WR	74.82	14.51	2.50	2.24	1.80	0.12	3.28	0.02	0.68	0.02
TW-C3-153.7	WR	76.96	14.25	2.38	1.67	1.75	0.12	1.97	0.01	0.85	0.03
TW-C4-120.4	WR	81.92	12.57	1.20	1.24	0.62	0.08	1.51	0.01	0.84	0.01
TW-C5-19.2	WR	77.26	12.75	1.48	1.68	2.44	0.65	2.97	0.02	0.59	0.15
AC-TW-8	WR	82.85	10.84	1.26	1.90	0.21	0.03	2.13	0.01	0.75	0.03
AC-TW-21	WR	76.05	13.37	2.44	2.30	0.82	0.10	3.97	0.13	0.68	0.15
AC-TW-38	WR	80.96	10.74	1.27	2.06	1.36	0.14	2.68	0.02	0.64	0.13
AC-TW-40	WR	78.83	12.24	1.22	2.14	0.99	0.07	3.74	0.01	0.69	0.06
AC-CM-56	WR	78.94	12.32	1.94	2.01	1.60	0.20	2.18	0.01	0.74	0.06
AC-FR-73	WR	71.69	16.83	4.29	0.14	2.69	1.01	2.68	0.04	0.58	0.05
AC-FR-76	WR	81.69	9.78	1.44	0.75	2.76	1.29	1.81	0.01	0.43	0.04
AC-FR-79	WR	79.07	13.96	1.21	0.45	2.18	1.04	1.36	0.01	0.67	0.04
TW-C1-59.0	ASH	76.87	11.04	6.33	1.15	3.00	0.02	0.99	0.00	0.59	0.02
TW-C5-98.2	ASH	76.58	14.37	2.53	0.71	1.66	1.08	2.10	0.01	0.94	0.02
AC-FE-20	CONCR	9.52	2.27	61.44	0.18	0.27	10.34	8.87	4.91	0.15	2.06
TW-C3-29.8	<2	69.95	18.40	1.52	2.53	1.50	0.40	4.84	0.02	0.71	0.13
TW-C3-34.5	<2	69.09	19.53	3.53	1.68	1.44	0.24	3.71	0.01	0.75	0.01
TW-C3-82.5	<2	65.33	20.22	4.41	2.79	1.12	0.19	4.60	0.01	1.30	0.04
TW-C3-105.8	<2	70.92	16.02	3.02	2.54	1.37	0.64	4.60	0.09	0.59	0.17
TW-C3-107.3	<2	70.50	19.41	2.07	1.64	1.97	0.14	3.83	0.01	0.40	0.03
TW-C3-153.7	<2	67.99	21.12	3.22	1.83	1.45	0.12	3.21	0.01	1.02	0.03
TW-C1-64.9	<1	69.20	19.78	2.14	2.35	1.33	0.46	4.00	0.01	0.67	0.07
TW-C1-69.3	<1	69.19	20.97	1.88	2.37	1.05	0.36	3.24	0.01	0.89	0.03
TW-C1-153.4	<1	69.74	18.11	1.94	3.54	0.99	0.65	4.13	0.02	0.75	0.11
TW-C3-21.7	<1	67.74	19.71	3.05	2.68	0.32	0.70	5.28	0.02	0.40	0.09
TW-C3-23.8	<1	68.82	22.54	1.85	1.89	0.45	0.22	3.31	0.01	0.86	0.04
TW-C3-135.1	<1	69.26	18.50	3.19	2.16	1.83	0.12	4.12	0.01	0.77	0.04
TW-C4-120.4	<1	68.47	21.78	2.30	1.83	1.43	0.15	3.11	0.01	0.91	0.01
TW-C5-19.2	<1	72.49	16.65	1.94	0.71	1.94	0.77	4.67	0.01	0.79	0.04
TW-C5-100.4	<1	68.11	21.11	3.01	2.05	0.81	0.56	3.45	0.01	0.86	0.03
TW-C5-125.3	<1	69.76	19.73	2.37	2.61	0.70	0.61	3.47	0.01	0.73	0.01
AC-TW-8	<1	71.18	18.09	1.69	2.89	1.74	0.04	3.26	0.01	1.07	0.03
AC-TW-17	<1	69.10	20.83	1.74	2.50	1.66	0.00	3.31	0.01	0.81	0.03
AC-TW-21	<1	67.59	18.70	3.85	2.95	1.81	0.03	4.29	0.06	0.65	0.08
AC-TW-36	<1	68.76	19.31	2.85	2.61	0.05	0.33	5.21	0.04	0.71	0.13
AC-TW-38	<1	68.39	19.80	2.64	2.57	1.74	0.01	3.91	0.01	0.88	0.05
AC-TW-40	<1	69.18	19.03	2.33	2.88	2.02	0.01	3.74	0.01	0.77	0.04
AC-CM-56	<1	68.48	19.76	3.23	2.11	1.62	0.18	3.90	0.01	0.66	0.04
AC-FR-73	<1	72.06	17.06	4.02	0.08	2.96	0.70	2.45	0.04	0.62	0.00
AC-FR-76	<1	74.37	15.27	2.59	0.28	2.11	1.19	3.67	0.02	0.47	0.03
AC-FR-79	<1	70.26	21.31	2.00	0.24	2.42	1.00	2.06	0.01	0.64	0.07
TW-C1-56.3	<.2	68.28	21.61	1.98	2.40	1.97	0.02	3.30	0.01	0.43	0.01

* (Recast from Weight Percents-Water Content Disregarded)

APPENDIX 3B

CHEMICAL COMPOSITIONS—MOLE PERCENTS OF OXIDE CONSTITUENTS

Samp. #	Frac.	SiO ₂	Al ₂ O ₃	Fe ₂ O ₃	K ₂ O	Na ₂ O	CaO	MgO	MnO	TiO ₂	P ₂ O ₅
TW-C3-21.7	<.25	69.41	18.05	3.44	2.65	0.27	0.66	4.84	0.02	0.55	0.12
TW-C3-29.8	<.25	68.50	19.02	2.80	2.29	1.43	0.35	5.03	0.01	0.46	0.09
TW-C3-153.7	<.25	67.20	21.71	3.16	1.94	1.50	0.12	3.57	0.01	0.75	0.03
TW-C5-19.2	<.25	72.78	16.48	1.83	0.41	2.51	0.73	4.94	0.00	0.31	0.00
AC-TW-38	<.25	67.02	20.17	2.54	2.81	1.99	0.06	4.67	0.01	0.69	0.04
AC-FR-79	<.25	68.94	22.23	1.90	0.15	2.33	0.85	2.27	0.03	1.26	0.05
AC-TW-27	<.1	68.58	20.16	1.99	2.76	2.05	0.03	3.89	0.01	0.49	0.04
AC-TW-38	<.1	68.28	19.19	2.40	2.61	2.85	0.01	4.29	0.01	0.31	0.04

KEY

WR = WHOLE ROCK
 ASH = COAL ASH SAMPLES (WHOLE ASH)
 CON = IRONSTONE CONCRETION
 <2 = <2 MICRON FRACTION
 <1 = <1 " "
 <.25 = <0.25 " "
 <.1 = <0.1 " "

APPENDIX 4

COAL ASH RESULTS

AVERAGE WEIGHT LOSS VS. TIME ASHED DATA

SAMPLE NO.	LOSS	HRS	LOSS	HRS	LOSS	HRS	LOSS	HRS	LOSS	HRS
AC-TW-1 CS	3.43	6	4.17	12	4.12	22	4.54	32	4.58	42
AC-TW-2* CS	4.95	10	5.99	25	6.88	45	7.09	65		
AC-FR-80 CS	8.18	10	8.96	20	9.60	30	10.30	50	10.62	60
"	10.91	70	11.08	80	11.16	90				
TW-C1-59.0*	29.41	10	36.47	20	41.51	40	48.93	60	50.76	80
"	55.61	90								
TW-C1-165.0	80.51	10	96.88	20	96.95	30				
TW-C3-50.9	53.14	10	66.54	20	69.98	30	71.00	40	71.51	50
"	71.87	60	71.95	70						
TW-C3-63.5	47.14	5	80.33	15	82.13	25	82.19	35		
TW-C3-108.4	64.33	10	94.98	21	95.97	31	96.02	41		
TW-C4-172.8	66.58	10	92.89	20	94.33	30	94.46	40	94.51	50
TW-C5-37.8	43.39	10	49.98	20	51.90	30	52.75	40	53.19	50
"	53.58	60	53.67	70						
TW-C5-98.2	59.48	10	87.27	20	92.29	31	92.63	41	92.66	51

EXPLANATION

LOSS = CUMULATIVE PERCENT WEIGHT LOST AFTER INDICATED
NUMBER OF HOURS
HRS = HOURS OF TIME ASHED
* = SAMPLE REMOVED BEFORE COMPLETELY ASHED
CS = CARBONACEOUS SHALE

APPENDIX 5A

SMECTITE+MIXED LAYER ILLITE-SMECTITE+ILLITE (001) D-SPACINGS

SAMPLE NUMBER	FORMATION	FRACTION (MICRONS)	D-SPACING (001) PEAKS	RELATIVE ABUND.	
				MIXED	SMECTITE
TW-C1-50.2	UM	<1	11.79	61	12
TW-C1-52.9	UM	<1	11.33	59	6
TW-C1-56.3	UM	<1	11.41	61	5
		<.25	11.05	61	5
TW-C1-60.5	UM	<1	11.94	61	7
TW-C1-64.9	UM	<1	11.95	54	10
TW-C1-69.3	UM	<1	11.33	65	6
TW-C1-153.4	UM	<1	11.33	52	3
TW-C1-169.6	UM	<1	12.28	57	18
TW-C2-115.5	UM	<1	14.73+11.48	52	10
TW-C2-119.2	UM	<1	14.73+11.95	45	11
TW-C2-122.3	UM	<1	14.26+12.11	51	4
TW-C3-10.4	CM	<2	14.03	63	9
TW-C3-18.3	CM	<2	14.25	51	13
TW-C3-20.2	CM	<2	14.37	22	23
TW-C3-21.7	CM	<2	14.31	38	20
		<.25	14.26	57	13
TW-C3-23.8	CM	<2	13.39	37	11
TW-C3-29.8	CM	<2	12.45	12	45
		<.25	12.19	52	29
TW-C3-34.5	CM	<2	12.45	39	26
TW-C3-38.5	CM	<2	12.31	66	14
TW-C3-50.1	CM	<2	12.10	72	14
TW-C3-52.1	CM	<2	12.28	51	23
		<.25	12.11	53	19
TW-C3-54.2	CM	<2	12.45	52	22
TW-C3-57.4	CM	<2	12.54	47	10
TW-C3-58.8	CM	<2	12.28	32	28
TW-C3-64.2	CM	<2	12.28	59	9
TW-C3-66.9	CM	<1	12.28	41	16
TW-C3-82.5	PL	<2	11.19	42	5
TW-C3-105.8	MN	<2	12.38	60	16
		<.25	12.28	56	25
TW-C3-106.6	MN	<2	12.63	49	29
		<.25	12.45	48	28
TW-C3-107.3	MN	<2	12.45	29	53
		<.25	12.28	33	59
TW-C3-109.2	MN	<2	12.63	44	21
		<.25	12.11	39	18
TW-C3-111.7	MN	<1	12.45	70	15
TW-C3-114.5	MN	<1	12.63	29	15
TW-C3-117.9	MN	<1	12.28	37	27
TW-C3-120.1	MN	<2	12.45	51	26
		<.25	12.28	54	21
TW-C3-121.9	MN	<1	12.63	29	20
TW-C3-135.1	MN	<1	12.28	43	26
TW-C3-149.2	MN	<1	11.95	46	16
TW-C3-150.4	MN	<1	12.28	52	16
TW-C3-153.7	MN	<2	12.38	28	17
TW-C3-153.7	MN	<.25	11.79	45	12
TW-C3-160.4	MN	<2	12.28	57	21

APPENDIX 5A

SMECTITE+MIXED LAYER ILLITE-SMECTITE+ILLITE (001) D-SPACINGS

SAMPLE NUMBER	FORMATION	FRACTION (MICRONS)	D-SPACING (001) PEAKS	RELATIVE ABUND.	
				MIXED	SMECTITE
TW-C3-221.3	MN	<2	12.11	35	15
TW-C4-87.1	CM	<1	11.94	62	15
TW-C4-103.2	CM	<1	11.63	56	7
TW-C4-104.8	CM	<1	11.79	54	8
TW-C4-119.5	CM	<1	11.79	57	10
TW-C4-120.4	CM	<1	11.95	45	10
TW-C4-170.6	MN	<1	12.11	59	10
TW-C4-176.6	MN	<1	12.11	57	6
TW-C5-13.3	CM	<1	14.26+12.81	80	9
TW-C5-19.2	CM	<1	12.63+15.24	29	70
		<.25	12.45	9	91
TW-C5-24.0	CM	<1	12.11	59	11
TW-C5-37.5	CM	<1	12.11	60	14
TW-C5-38.6	CM	<1	12.28	33	21
TW-C5-95.8	MN	<1	11.33	58	8
TW-C5-96.9	MN	<1	12.63	44	17
TW-C5-100.4	MN	<1	14.03	30	10
TW-C5-105.8	MN	<1	12.63	54	8
TW-C5-122.5	MN	<1	12.63	36	10
TW-C5-123.9	MN	<1	14.26	51	9
TW-C5-125.3	MN	<1	13.19	57	8
TW-C5-128.1	MN	<1	12.63	34	9
AC-TW-3	UM	<1	11.95	61	4
		<.25	12.45	70	4
AC-TW-4	UM	<1	12.28	59	7
AC-TW-7	UM	<1	12.63	66	8
AC-TW-8	UM	<1	11.19	56	3
		<.25	9.94	66	3
AC-TW-10	UM	<1	11.33+16.07	65	7
AC-TW-12	UM	<1	12.63	64	5
		<.25	14.49	69	7
AC-TW-17	UM	<1	11.48	57	5
AC-TW-21	UM	<1	11.63	63	5
		<.25	11.48	65	7
		<.1	11.33	69	7
AC-TW-24	UM	<1	14.26	53	7
		<.25	14.26	60	6
AC-TW-25	UM	<1	13.00	59	7
		<.25	11.63+14.03	63	8
AC-TW-26	UM	<1	11.19	62	7
AC-TW-27	UM	<1	11.05	53	4
		<.25	11.33	56	4
		<.1	11.05	79	3
AC-TW-28	UM	<1	11.48	52	5
AC-TW-29	UM	<1	11.48	57	6
AC-TW-32	UM	<1	11.33	60	7
AC-TW-34	UM	<1	11.95	59	10
		<.25	11.63	64	7
		<.1	11.63	72	15
AC-TW-35	UM	<1	12.63	69	7
AC-TW-36	UM	<1	14.37	64	7

APPENDIX 5A

SMECTITE+MIXED LAYER ILLITE-SMECTITE+ILLITE (001) D-SPACINGS

SAMPLE NUMBER	FORMATION	FRACTION (MICRONS)	D-SPACING (001) PEAKS	RELATIVE ABUND.	
				MIXED	SMECTITE
AC-TW-38	UM	<1	12.11	52	12
		<.25	11.91	66	9
		<.1	11.79	72	15
AC-TW-40	UM	<1	11.63	66	10
AC-CM-56	CM	<1	12.28	62	16
		<.25	11.95	64	19
		<1	12.11	50	17
AC-CM-57	CM	<1	12.11	50	17
AC-CM-58	CM	<1	12.28	37	16
		<.25	12.11	50	15
		<1	12.11	46	13
AC-CM-59	CM	<1	12.11	46	13
AC-CM-62	CM	<1	12.45	48	16
		<.25	12.28	60	14
		<1	11.95	62	11
AC-UM-64	CM	<1	11.95+16.37	52	10
AC-UM-65	UM	<1	11.95	64	12
AC-UM-66	UM	<1	12.11	60	11
		<.25	11.79+16.07	78	8
		<1	11.79	67	6
AC-UM-67	UM	<1	11.79	67	6
AC-FR-71	FR	<1	12.45	76	24
AC-FR-72	FR	<1	12.45	54	34
		<.25	12.28	51	45
		<.1	12.28	54	43
AC-FR-73	FR	<1	12.63	42	58
AC-FR-74	FR	<1	12.63	17	82
AC-FR-75	FR	<1	12.63	29	70
AC-FR-76	FR	<1	12.63	0	100
AC-FR-77	FR	<1	12.81	34	66
AC-FR-78	FR	<1	12.63	24	71
AC-FR-79	FR	<1	13.00	40	50
		<.25	12.81	51	37
		<1	12.63	25	71
AC-FR-82	FR	<1	12.63	25	71

KEY TO FORMATION NAMES

UM = UPPER MENEFE
 CM = CLEARLY MEMBER OF THE MENEFE
 MN = MANCOS SHALE
 PL = POINT LOOKOUT SANDSTONE
 FR = FRUITLAND FORMATION

STATISTICAL INFORMATION FOR UNTREATED (001) SMECTITE-MIXED LAYER-ILLITE D-SPACINGS

FORMATION OR MEMBER	NUMBER OF SAMPLES	AVERAGE (001) D'S	STANDARD DEVIATION	RANGE OF (001) D'S
UPPER MENEFE	34	11.988	.7228	11.05-14.26
CLEARLY MEMBER	32	12.545	.7980	11.63-14.37
MANCOS SHALE	25	12.555	.6198	11.33-14.26
FRUITLAND	10	12.380	.8274	9.94-13.00

APPENDIX 5B

PERCENT EXPANDABLE LAYERS IN MIXED-LAYER ILLITE-SMECTITE

SAMPLE NUMBER	FORM- ATION	(001)10/(002)17 D-SPACING(A)		%EXP.	(002)10/(003)17 D-SPACING(A)		%EXP.
		20			20		
AC-TW-3	UM	9.75	9.1	53%	16.2	5.47	58%
AC-TW-10	UM	9.45	9.35	41	----		
AC-TW-25	UM	9.4	9.4	39	----		
AC-TW-28	UM	9.6	9.2	47	----		
AC-TW-32	UM	9.2	9.6	32	----		
AC-TW-34	UM	9.9	8.95	66	16.15	5.48	62
AC-TW-36	UM	9.8	9.0	56	16.3	5.44	55
AC-TW-38	UM	9.3	9.5	35	----		
AC-CM-56	CM	9.9	8.9	60	----		
AC-CM-57	CM	9.9	8.9	60	16.2	5.47	58
AC-CM-58	CM	9.8	9.0	56	16.3	5.44	55
AC-CM-59	CM	9.7	9.1	51	16.6	5.35	42
AC-CM-62	CM	10.2	8.7	79	----		
AC-UM-65	UM	10.1	8.75	73	----		
AC-UM-67	UM	9.3	9.5	35	16.6	5.85	42
TW-C1-52.9	UM	9.3	9.5	35	16.5	5.37	45
TW-C1-64.9	UM	9.7	9.1	51	16.3	5.44	54
TW-C1-169.6	UM	9.9	8.9	60	16.2	5.47	59
TW-C2-119.2	UM	9.9	8.9	60	----		
TW-C2-122.3	UM	9.6	9.2	47	----		
TW-C3-23.8	CM	10.0	8.85	66	----		
TW-C3-29.8	CM	10.1	8.75	73	----		
TW-C3-38.5	CM	10.2	8.7	79	----		
TW-C3-50.1	CM	9.9	8.9	60	16.2	5.47	59
TW-C3-52.1	CM	10.25	8.65	84	----		
TW-C3-54.2	CM	10.0	8.85	66	----		
TW-C3-57.4	CM	9.2	9.6	31	----		
TW-C3-58.8	CM	10.0	8.85	66	----		
TW-C3-66.9	CM	9.7	9.1	51	16.4	5.40	49
TW-C3-82.5	PL	9.5	9.3	43	16.7	5.31	37
TW-C3-105.8	MN	10.0	8.85	66	----		
TW-C3-106.6	MN	10.0	8.85	66	16.2	5.47	59
TW-C3-107.3	MN	10.25	8.65	84	----		
TW-C3-109.2	MN	10.2	8.7	79	----		
TW-C3-111.7	MN	9.85	9.0	56	----		
TW-C3-114.5	MN	9.7	9.1	51	----		
TW-C3-117.9	MN	9.7	9.1	51	16.2	5.47	59
TW-C3-120.1	MN	9.6	9.2	47	16.3	5.44	54
TW-C3-121.9	MN	10.2	8.7	79	----		
TW-C3-135.1	MN	9.9	8.95	59	16.3	5.44	54
TW-C3-149.2	MN	9.9	8.95	59	16.4	5.40	49
TW-C3-150.4	MN	9.5	9.3	43	16.6	5.85	42
TW-C3-153.7	MN	9.6	9.2	47	----		
TW-C3-160.4	MN	10.0	8.85	66	16.0	5.54	73
TW-C3-221.3	MN	9.6	9.2	47	16.5	5.37	45
TW-C4-176.6	MN	9.8	9.0	56	16.4	5.40	49
TW-C4-104.8	CM	9.5	9.3	43	----		
TW-C4-119.5	CM	9.6	9.2	47	----		
TW-C4-9.45	CM	9.45	9.25	45	----		

APPENDIX 5B

PERCENT EXPANDABLE LAYERS IN MIXED-LAYER ILLITE-SMECTITE

SAMPLE NUMBER	FORM- ATION	(001)10/(002)17		%EXP.	(002)10/(003)17		%EXP.
		20	D-SPACING(A)		20	D-SPACING(A)	
TW-C5-19.2	CM	10.4	8.5	100	15.7	5.65	100
TW-C5-37.5	CM	9.9	8.95	59	-----		
TW-C5-100.4	MN	9.4	9.4	39	16.6	5.85	42
TW-C5-105.8	MN	9.6	9.2	47	16.6	5.85	42
TW-C5-122.5	MN	9.4	9.4	39	16.4	5.40	49
TW-C5-123.9	MN	9.4	9.4	39	-----		
TW-C5-125.3	MN	9.4	9.4	39	16.4	5.40	49
TW-C5-128.1	MN	10.1	8.75	73	-----		

FORMATION KEY

UM=UPPER COAL-BEARING UNIT OF THE MENEFEE FORMATION

CM=CLEARY MEMBER OF THE MENEFEE

MN=MANCOS SHALE

PL=POINT LOOKOUT SANDSTONE

STATISTICAL INFORMATION USING (001)10/(002)17 PEAKS

FORMATION NAME	NUMBER OF SAMPLES	RANGE (IN %)	AVERAGE % EXPANDABLE LAYERS	STANDARD DEVIATION
UPPER MENEFEE	15	32-73	48.67	12.15
CLEARY MEMBER	19	31-100	61.89	15.89
MANCOS SHALE	22	39-84	56.00	13.73
POINT LOOKOUT	1	43	43.00	0.00

APPENDIX 5C

LOW INTENSITY CLAY PEAKS

GROUP 1 - REGULAR MIXED LAYER ILLITE-SMECTITE

SAMPLE #	FORMATION & SIZE FRACTION (IN MICRONS)		D-SPACINGS (IN ANGSTROMS)		
			UNTREATED	GLYCOL	350
TW-C3-105.8	MN	<.25	22.08	-----	-----
TW-C3-107.3	MN	<2	24.54	27.61	-----
TW-C5-13.3	CM	<1	26.77	28.50	20.08
TW-C5-19.2	CM	<1	25.99	33.98	19.21
AC-FR-73	FR	<1	24.54	33.98?	-----
AC-FR-74	FR	<1	25.24	33.98	22.08
AC-FR-76	FR	<1	25.24	35.34	22.08
AC-FR-77	FR	<1	25.24	35.34	-----
AC-FR-82	FR	<1	25.24	-----	-----

GROUP 2 - SMECTITES WITH ORGANICS IN THE INTERLAYER POSITION

TW-C1-52.9	UM	<1	15.78		
TW-C1-60.5	UM	<1	17.33		
TW-C1-64.9	UM	<1	19.21		
TW-C5-95.8	MN	<1	16.99		
AC-TW-10	UM	<1	16.07		
AC-CM-64	CM	<1	16.37		

FORMATION KEY: SAME AS PREVIOUS TABLE

APPENDIX 6A

AVERAGE MINERALOGIC COMPOSITIONS FOR CARBONACEOUS

 VS. NON-CARBONACEOUS STRATA

FORM.	LITH.	NO.	QUARTZ	FELD.	CHLOR.	KAOL.	ILLT.	SMECT.	MIXED
FRUIT.	CARB.	5	17.4	6.0	0.2	3.8	0.0	74.8	21.2
*			6.1	5.8	0.0	3.1	0.0	16.3	13.0
	BARREN	5	10.6	4.4	0.0	0.6	2.0	50.4	47.0
*			8.6	4.2	0.0	0.5	0.0	18.2	16.8
UP.MEN.	CARB.	15	24.1	4.1	0.5	20.0	13.3	7.9	58.2
*			6.7	2.6	0.6	4.8	4.0	3.7	4.7
	INT.	6	26.5	8.8	0.7	14.5	17.0	7.3	60.5
*			3.9	2.4	0.4	5.9	7.0	2.3	6.7
	BARREN	13	25.0	10.0	0.7	18.2	16.1	6.9	58.1
*			5.9	5.1	0.6	6.5	5.3	2.5	5.5
CLEARY	CARB.	12	21.4	4.3	1.1	22.9	9.9	13.8	52.3
*			7.0	3.6	1.6	11.5	5.1	5.9	11.0
	INT.	3	18.0	4.7	2.7	15.0	13.0	27.3	42.0
*			2.2	1.0	0.6	4.6	3.6	12.8	21.6
	BARREN	14	17.7	7.5	0.7	23.9	12.6	15.8	47.0
*			6.6	6.2	0.7	8.5	6.5	5.0	12.2
MANCOS	CARB.	11	20.1	5.0	1.1	30.9	9.5	20.0	38.6
*			5.0	2.7	1.0	13.7	3.5	12.2	9.0
	INT.	8	19.3	6.6	1.0	19.5	10.4	17.3	51.9
*			5.1	5.1	1.1	7.8	4.9	6.7	6.9
	BARREN	6	20.2	11.3	1.5	24.7	11.8	11.7	50.3
*			3.9	8.9	0.6	9.9	4.7	4.5	13.9

KEY

* = STANDARD DEVIATION

FORM. = FORMATION NAME FRUIT. = FRUITLAND FORMATION

UP.MEN. = UPPER COAL-BEARING MEMBER OF THE
 MENELEE

CLEARY = CLEARY COAL MEMBER OF THE MENELEE
 MANCOS = MANCOS SHALE

LITH. = LITHOLOGY CARB. = CARBONACEOUS SHALES OR (LESS OFTEN)
 MUDSTONES

INT. = INTERMEDIATE, SLIGHTLY CARBONACEOUS
 STRATA

BARREN = BARREN MUDSTONES OR SHALES

NO. = NUMBER OF SAMPLES AVERAGED (ODD OR SANDY SAMPLES OMITTED)

QUARTZ = AVERAGE QUARTZ CONTENT

FELD. = " TOTAL FELDSPAR (MICROCLINE + ALBITE + ORTHOCLASE)

CHLOR. = " CHLORITE CONTENT OF <2 OR <1 MICRON FRACTIONS

KAOL. = " KAOLINITE " " " " "

ILLT. = " ILLITE " " " " "

SMECT. = " SMECTITE " " " " "

MIXED = " RANDOM ILLITE/SMECTITE MIXED-LAYER CONTENT OF
 <2 OR <1 MICRON FRACTIONS

APPENDIX 6B

FORMATIONAL AVERAGES FOR CLAY MINERALS

 (EXCLUDING SANDY, COAL ASH, AND BENTONITE SAMPLES)

FORM.	NO.	QTZ	FELD	CHLORITE	KAOLINITE	ILLITE	SMECTITE	MIXED
FRUITLAND	10	14.0	5.2	0.1	2.2	1.0	62.6	34.1
*				0.0	2.7	3.0	21.1	19.8
UPPER MEN.	34	24.9	7.2	0.7	18.3	15.6	7.2	58.1
*				0.6	6.2	5.2	3.1	5.4
CLEARY	32	21.3	5.9	1.0	21.2	11.2	17.4	49.2
*				1.2	10.4	6.0	12.0	14.3
MANCOS	25	19.9	6.9	1.2	25.8	10.4	17.2	45.5
*				0.0	2.7	3.0	21.1	19.8

NO. = NUMBER OF SAMPLES AVERAGED

* = STANDARD DEVIATION

APPENDIX 6C

AVERAGE CLAY MINERALOGY FOR VARIOUS CLAY FRACTIONS

CLAY FRACTION	NUMBER OF SAMPLES	AVERAGE CHLORITE	AVERAGE KAOLINITE	AVERAGE ILLITE	AVERAGE SMECTITE	AVERAGE MIXED
OVERALL						
<8	7	1.0	32.9	11.4	11.7	43.0
<1, <2	5, 2	0.9	23.1	8.7	16.9	50.4
<2	3	1.0	26.7	9.3	19.7	43.3
<1	3	0.7	26.7	8.7	17.0	47.0
UPPER MENELEE						
<1	13	0.4	18.9	15.2	7.3	58.2
<.25	13	0.1	13.2	14.3	6.8	65.5
CLEARY						
<1	8	0.6	26.0	10.9	22.1	40.4
<.25	8	0.0	16.6	9.5	18.5	55.4
MANCOS						
<1	8	1.6	21.9	7.5	24.0	45.0
<.25	8	0.1	20.0	9.3	25.6	45.0
FRUITLAND						
<1	2	0.5	5.5	5.0	42.0	47.0
<.25	2	0.5	5.5	2.0	41.0	51.0
OVERALL						
<1	3	0.7	26.7	8.7	17.0	47.0
<.5	3	0.7	28.3	12.3	17.0	41.7
<1	8	0.3	19.1	11.3	13.8	55.6
<.1	8	0.0	8.5	7.1	17.4	67.0

NOTE : THE SAME SAMPLES, BUT DIFFERENT CLAY FRACTIONS WERE USED IN X-RAY ANALYSIS AND AVERAGING. UNLESS SPECIFIED, NUMBERS REPRESENT AVERAGES FROM THE MENELEE AND MANCOS SAMPLES IN GENERAL.

* TWO OF THREE SAMPLES FROM THE MANCOS SHALE

APPENDIX 6D

AVERAGE MINERALOGIC COMPOSITIONS OF SAMPLES

 TAKEN ABOVE AND BELOW COALS

FORM.	NO.	POSI.	QUARTZ	FELD.	CHLOR.	KAOL.	ILLT.	SMECT.	MIXED
UP.MEN. *	7	ABOVE	24.6	6.9	1.4	19.1	17.6	6.7	55.1
			3.5	2.9	0.5	7.1	8.2	2.2	3.5
*	9	BELOW	25.4	5.1	0.7	20.4	13.8	7.4	57.7
			6.4	4.3	0.8	5.4	4.6	4.4	4.1
CLEARY *	5	ABOVE	17.6	4.6	2.2	17.2	12.2	13.6	54.8
			7.1	4.0	2.0	6.4	3.4	6.5	8.2
*	10	BELOW	20.8	3.7	0.6	21.6	8.7	14.1	55.0
			5.4	2.8	0.5	10.6	4.8	4.7	10.5
MANCOS *	6	ABOVE	16.8	6.0	1.5	13.2	11.8	18.5	55.0
			2.3	2.9	0.8	4.2	5.2	15.8	12.1
*	6	BELOW	23.2	4.2	0.8	35.0	8.3	15.0	40.8
			4.8	1.7	0.9	12.7	2.6	7.9	9.8
FRUIT.	1	ABOVE	7	0	0	1	0	82	17
	1	BELOW	15	5	0	2	10	34	54

KEY

SAME AS PREVIOUS PAGE EXCEPT:

POSI. = SAMPLE POSITION, EITHER (<1.5 FEET) ABOVE OR BELOW A COAL

* LINE REPRESENTS STANDARD DEVIATIONS

APPENDIX 7

RECASTING A CLAY ANALYSIS

1) Choose a sample that you believe to be relatively pure as far as the clay mineralogy is concerned. In order to do this the sample should be x-rayed first and all of the peaks should be catalogued. Bear in mind that many illite and smectite structures are actually mixed-layer clays, so that the recast values obtained may be an average of several populations.

2) Perform an accurate chemical analysis of the sample.

3) Guess what type of clay structure you are dealing with based on the diffraction data. The number of oxygens in the structure plus half the number of hydroxides determines the number of anions the oxide percents will be normalized to.

4) Divide the oxide percents by associated cation's atomic weight. This yields the mole percent (per gram) for each element.

5) Total the mole percents and divide this number into the number of anions to be normalized to.

6) Multiply the resulting number by their respective mole percents for each element. This yields the number of anions bound to each cation.

7) Convert this number to number of cations by multiplying by cation per anion in the original oxides.

8) The recast cation values tell you the number of each cation within the structural formula. These can then be used to reconstruct the structural formulas, given knowledge as to what ions substitute where. Examples of recasting clays into their structural formulas are given in the second part of this appendix.

This thesis is accepted on behalf of the faculty
of the Institute by the following committee:

Walter B. ...

Adviser

Donald B. ...

Date